Temporal Bone, Posterior Skull Base, Posterior Fossa, and Cranial Nerves

TEMPORAL BONE, POSTERIOR SKULL BASE, POSTERIOR FOSSA, AND CRANIAL NERVES

ANTHONY A. MANCUSO, BERIT M. VERBIST, AND PATRICK J. ANTONELLI

TECHNICAL ASPECTS

In general, computed tomography (CT) and magnetic resonance imaging (MRI) in this anatomic region almost always require the highest possible spatial resolution, sometimes needing to balance that against required low-contrast resolution. These issues are discussed in detail in conjunction with general CT and MRI parameters in Chapters 1 through 3. General imaging parameters used in this region of interest are presented in Appendixes A and B. More refined protocols are presented when appropriate in the disease- and anatomy-specific discussions.

Ultrasound is essentially not used in this anatomic area of interest.

General applications of radionuclide and related techniques are discussed in Chapter 5.

Pros and Cons
Relative Indications for Computed Tomography and Magnetic Resonance Imaging

Patients with sensorineural and conductive hearing loss make up the bulk of temporal bone study referrals. Other common indications for CT and MRI of the temporal bone and related posterior fossa structures include facial nerve dysfunction, vertigo, tinnitus, otitis media, mass lesions in and about the temporal bone, and patients with unexplained otalgia. These general indications and others are outlined in Table 104.1, where they are keyed to the likely preferred primary study. Given different practice preferences or mitigating clinical circumstances, either CT or MRI can be an appropriate starting place for some of these indications.

CT should be the primary examination for indications that require bone detail. MRI becomes the adjunctive study where bone detail is of primary interest. As a secondary study, MRI may help characterize the nature or extent of a mass—for instance, petrous apex cholesterolosis versus phlegmon. MRI may also provide adjunctive information about the membranous labyrinth (Table 104.1).

MRI becomes the more likely primary examination when a complete evaluation of the brain stem, cerebellopontine angle (CPA), and intracanalicular course of cranial nerve (CN) VIII is necessary. The most common use of MRI is in patients with sensorineural hearing loss (SNHL) and vestibular signs and symptoms. Screening for lesions producing such dysfunction should include use of paramagnetic contrast and three-dimensional (3D) steady state images. Contrast enhancement is sometimes nonspecific. A combination of morphologic features, associated findings, and clinical settings needs to determine the next best course of action when abnormal enhancement of the membranous labyrinth, nerves, meninges, or a mass is present.

Facial nerve dysfunction may require clinical triage to determine whether CT and/or MRI are indicated at all. The clinical situation may also guide the sequencing of CT and MRI.

Patients with pulse synchronous tinnitus or a mass of possible vascular origin will often come to diagnostic imaging. These studies may establish the precise etiology of the mass or identify the cause of objective or subjective pulse synchronous tinnitus. More often, they are negative and therefore only exclusionary diagnostic efforts. However, such imaging triage can help avoid clinical misadventures—for instance, biopsy of a highly vascular mass such as a paraganglioma or injury to an important normal vessel such as the internal carotid. The primary study for this indication depends on whether there is a mass visible behind the tympanic membrane. If a mass is visible, then non–contrast-enhanced CT is done. If a mass is not visible, then a more complex contrast-enhanced CT with CT angiography and CT venography approach is necessary (Appendix A). MRI and magnetic resonance (MR) angiography are usually secondary studies for these indications as directed by non–contrast-enhanced CT or contrast-enhanced CT results and the clinical situation (Appendix B). If CT angiography and CT venography can be performed on multidetector CT, then only a single imaging study is necessary to depict middle ear, arterial, and venous causes of pulsatile tinnitus.1 Mistaking inner ear–related nonpulsatile tinnitus for pulse synchronous tinnitus is a common error in ordering of imaging studies on patients with tinnitus. The approach to these problems is very different, and this distinction must be made by the requesting physician to assure that the proper imaging approach is used.

The relative indications for CT and MRI in patients with parapharyngeal space and nasopharyngeal masses potentially involving the temporal bone is discussed in conjunction with those anatomic sites of origin of pathology.

Radionuclide studies are used primarily and sparingly for diagnosis and following treatment for skull base osteomyelitis and necrotizing otitis externa. They may also be used in the evaluation of cerebrospinal fluid (CSF) leaks (Chapter 5).

TABLE 104.1. GENERAL INDICATIONS FOR TEMPORAL BONE COMPUTED TOMOGRAPHY AND MAGNETIC RESONANCE IMAGINGa

Sensorineural hearing loss, nonpulse synchronous tinnitus, vertigo (MRI)
Cochlear implant preoperative evaluation (MRI)[b]
Conductive hearing loss (CT)
Acquired and congenital cholesteatoma
Inflammatory middle ear disease
Middle ear mass[b]
Congenital malformation (CT)
Otosclerosis (CT)
Trauma (CT)
Mass of the external auditory canal, pinna, extratemporal bone (CT)
Mass of the petrous apex (MRI)[b]
Malignant tumor—Extent of temporal bone involvement (CT)
Aggressive inflammatory disease—for example, necrotizing otitis externa (CT)
Pulse synchronous tinnitus, either objective or subjective (CT)[b]
Peripheral facial nerve dysfunction, weakness, spasticity (usually MRI—see algorithm)[b]
Trauma (CT)
Acute onset (MRI if nonresolving in 4 to 6 weeks or progressive)
Slow onset (MRI)
Jugular fossa syndrome (MRI)[b]

MRI, magnetic resonance imaging; CT, computed tomography.
[a]The study in parentheses should usually be done first. Supplemental study is necessary in some cases.
[b]Both studies frequently are necessary.

There is essentially no role for ultrasound in these anatomic areas of interest.

Controversies

Computed Tomography Versus Magnetic Resonance for Precochlear Implant Evaluation––One Test or Both?

CT and MRI render complementary information in the preoperative assessment of cochlear implant candidates. The surgeon needs to be informed about the patency of the cochlea, cochlear and vestibular anomalies, bone dysplasias, retrocochlear disease, and anatomic variations, especially those of the facial nerve that might alter the surgical approach. CT provides information about the bony labyrinth, the vestibular aqueduct, and anatomic variants of the mastoid and vascular structures. MRI will identify cochlear and retrocochlear soft tissue abnormalities, such as cochlear fibrosis in labyrinthitis, absence or extreme atrophy of the cochlear nerve, and brain pathology along the auditory pathways. The abnormalities detected with MRI, such as cochlear patency and along the auditory neural pathway, are more likely to influence the selection of candidates and the selection of preferred side of surgery than the findings on CT.

CT and MRI should be considered especially for prelingual deafness or complex pathology. If a group prefers only CT, a routine MRI should at least be added in all cases of previously documented meningitis or prelingual deafness to establish the presence of a normal cochlear nerve. These relative values and roles of CT are currently under study, and the safest course of action seems to be doing both studies when there is a reasonable need for both.[2–4]

Can One Reasonably Screen SNHL Patients or those with other CN VIII Symptoms with Three-Dimensional Fourier Transform (3DFT) Steady State Sequences (CSF bright) such as CISS and FIESTA and not use Intravenous Gadolinium Enhancement?

In SNHL, the entire acoustic pathway should be carefully scrutinized to rule out cochlear and retrocochlear disease. T2-weighted imaging of the brain allows for evaluation of the brain stem, acoustic pathway, and auditory cortex. For evaluation of the CPA, the internal auditory canal (IAC), and the cochlea, both T1-weighted images before and after contrast and very thin fast spin echo T2-weighted images or a 3D gradient echo steady state sequence, such as CISS and FIESTA of the temporal bone, are mandatory.

The use of contrast will clearly increase the yield of MRI, albeit in a small but unpredictable number of cases, by demonstrating inflammatory and neoplastic labyrinthine lesions and meningeal pathology in the IAC and CPA. Although potentially visible on all sequences, contrast-enhanced T1-weighted imaging is considered the best sequence to detect CPA or IAC tumors. Middle ear and inner ear diseases such as complicated cholesteatoma and otosclerosis may cause enhancement. To diagnose acute labyrinthitis and exclude neoplastic disease, both sequences yield complementary information. In chronic labyrinthitis, fibrosis may only be depicted on T2-weighted images or 3DFT gradient echo sequences in the steady state.[5]

What is the Utility of Measurements Such as Bony Island Within the Lateral Semicircular Canal (LSCC) and Cochlear Height for Detecting Subtle Developmental Inner Ear Abnormalities?

Over the decades since the start (1960s and 1970s) of detailed sectional temporal bone imaging with multidimensional x-ray tomography, several measurements have been advocated in the evaluation of SNHL:

1. The width of the IAC, measured on CT, is correlated with hearing loss. A narrow IAC (≤2 mm) reflects the risk of cochlear nerve aplasia. However, in cases of cochlear nerve hypoplasia, the development of the IAC is normal. MRI provides a means to visualize CN VIII directly.
2. An enlarged vestibular aqueduct defines a population at risk for sudden or progressive hearing loss. The size of the vestibular aqueduct should not exceed 1.5 mm at its midportion. As a "screening" observation, the diameter should clearly appear to exceed the diameter of the adjacent semicircular canal, and any vestibular aqueduct exceeding that screening observation should be measured.
3. Measurements of the cochlear and vestibular systems contribute to the detection of cochlear and/or vestibular dysplasia. Whereas gross inner ear abnormalities are detected by visual inspection only, milder dysplasias can be overlooked. Thus, the latter are often missed, although they are more prevalent. To increase sensitivity, radiographic measurements of the cochlear height on coronal images and of the LSCC bony island width should be performed. The height of a normal cochlea ranges from 4.4 to 5.9 mm. Cochlear hypoplasia (<4.4 mm) is associated with SNHL. Dimensions of the bony island of the LSCC <2.6 mm are consistent with dysplasia. There is no consistent correlation between LSCC abnormalities and SNHL (Fig. 104.1). Measurements above the range of normal for these structures may have no practical benefit in identifying inner ear dysplasias.[6]

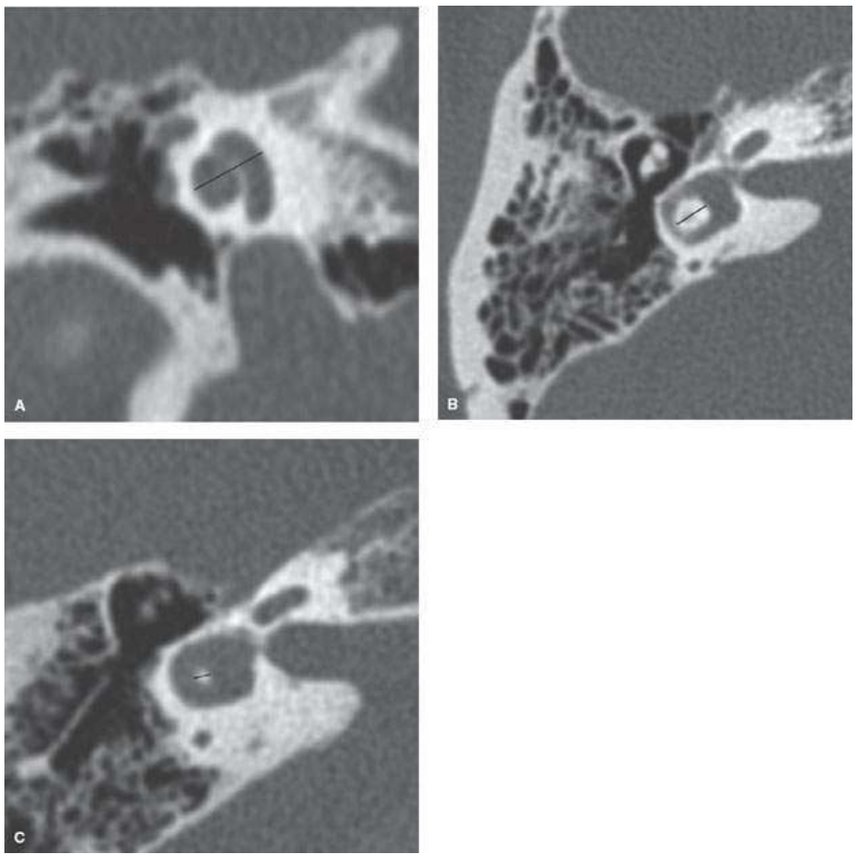

FIGURE 104.1. A, **B:** Standardized measurements of the inner ear on temporal bone computed tomography. The cochlear height is measured in a coronal section at an oblique angle (line). The lateral semicircular bony island width is measured on an axial image on a line connecting the apex of the canal's turn to the midpoint of the communication between the canal and the vestibule (line). **C:** Dysplasia of the lateral semicircular canal. The bony island measures 1.3 mm.

Modern imaging is constantly improving. Anatomic abnormalities such as incomplete cochlear partition, modiolar deficiency, and/or an abnormal cochlear nerve aperture to the cochlear base may be observed independent of an abnormal measurement such as the cochlear height. A small cochlear aperture at the base of the modiolus may identify a hypoplastic CN VIII. Normal measurements do not exclude dysplasia; they are only another tool in a multifactor risk assessment for dysplasia. A complete assessment for inner ear dysplasia should use a limited number of measurements in addition to observations for subtle dysmorphic features such as those just mentioned. With such a system, anatomic imaging will provide a reasonable but still imperfect means for such screening until better tools such as genetic screening take over or augment anatomic observations at some point.

Is There Any Real Value of MRI in Middle Ear Acquired Cholesteatoma Versus Other Erosive Disease?

The value of MRI in the evaluation of chronic ear disease, in particular cholesteatoma, is still a matter of debate. CT remains the first line technique in the pre- and postoperative assessment of suspected or residual/recurrent cholesteatomas. MRI has an additional role in the preoperative evaluation in cases of cholesteatoma-caused complications, such as labyrinthitis, encephalocele, facial palsy, sinus thrombosis, otitic hydrocephalus, brain abscess, and iatrogenic injuries. Reports on its role in uncomplicated cholesteatoma are sparse. Diffusion-weighted imaging (DWI) has been shown to be useful in the differentiation of acute otitis and cholesteatoma, but data on DWI in chronic otitis is not available.7

In the case of complete opacification of the tympanomastoid cavities on postoperative CT, it is not possible to differentiate residual/recurrent cholesteatoma from scar tissue. There is growing evidence in the literature that delayed contrast-enhanced T1-weighted imaging (30 to 45 minutes after contrast injection8) and echo planar imaging or fast spin echo DWI enable the depiction of residual/recurrent cholesteatoma. The high signal intensity on DWI and lack of enhancement differentiates cholesteatoma from granulomatous/noncholesteatomatous tissue. Disease <5 mm, however, may be missed.9–11

Is There a Useful and Reliable Correlation Between Vascular Loops in the ICA as Seen on Imaging and Unilateral Auditory Symptoms?

Unexplained unilateral hearing loss, tinnitus, vertigo, and Ménière disease have been attributed to neurovascular compression of CN VIII by a loop of the anterior inferior cerebellar artery (AICA) within the IAC. Anatomic studies12 and radiologic studies13 have not been able to confirm a correlation between the presence of an AICA loop within the IAC and auditory symptoms and have considered it a normal anatomic variation. On the other hand, several reports14,15 of successful surgical neurovascular decompressions support the existence of the AICA syndrome.

The reason for this discrepancy might be the variability of the depth of extension into the IAC. Loops may be identified on MRI and classified based on their depth into the IAC. A significant association has been found with AICA loops extending up to 50% and particularly beyond 50% of the IAC and unilateral hearing loss, whereas loops confined to the CPA showed no significant association.16 In case of unexplained unilateral hearing loss, attention should be paid to the course of the AICA; however, the diagnosis of a neurovascular causation of CN VIII symptoms should not be made on imaging alone (Fig. 104.2).

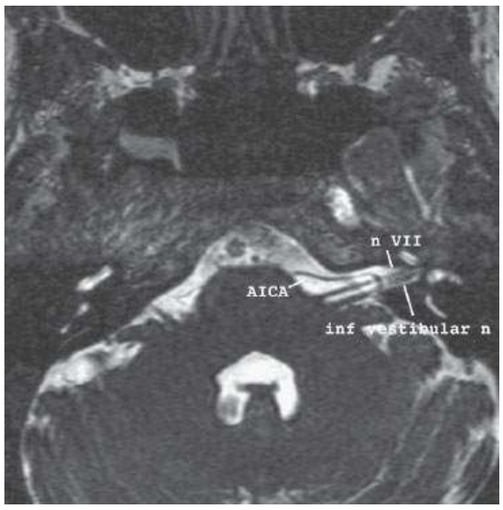

FIGURE 104.2. Possible neurovascular compression in a patient with unilateral sensorineural hearing loss. Axial magnetic resonance image (CISS) at the level of the internal auditory canal (IAC) shows the anterior inferior cerebellar artery extending deep into the IAC.

Is Imaging Necessary in Cases of Acute Facial Nerve Palsy?

The first step in evaluating patients with acute facial nerve paralysis is to determine whether the paralysis is central or peripheral. In case of central weakness, brain MRI is recommended to evaluate for ischemia and infectious or inflammatory disease. In most cases of peripheral weakness, no cause will be found; this is Bell palsy, and immediate imaging is not indicated unless other CN deficits develop indicating more widespread disease, a facial twitching or spasticity preceded or accompanying the palsy indicating continuous facial nerve irritation suggestive of a tumor, there is no recovery 3 to 6 weeks after the onset of symptoms, or the palsy recurs after partial or complete resolution. All of these atypical features suggest the possibility of a more serious cause, such as a benign or malignant neoplasm rather than the usual viral neuritis.

There are contradictory reports on the value of quantitative contrast-enhanced MR in an early phase as a predictive factor for the outcome.[17,18] Although MRI can be performed earlier than electrodiagnostic studies, clinically the extent and rate of nerve degeneration measured by electroneurography are used as predictive factors.[19]

NORMAL ANATOMY

Parts of the Temporal Bone

The temporal bone is composed of several parts and one joint surface (Fig. 104.3A,B). The osseous parts include the mastoid portion, the petrous portion housing the inner ear, the tympanic portion forming much of the external auditory canal (EAC), the styloid process, and the squamous portion. The petrous forms the lateral floor/wall of the posterior fossa and together with the squamous forms the posterior inferior and lateral surfaces of the middle cranial fossa (Fig. 104.3C). Each petrous ridge serves as an attachment for the leaves of the tentorium cerebelli. The rigidity of the mastoid and petrous bones serves an important protective function for the senses of hearing and balance. Significant external and internal temporal bone anatomy and relevant spatial relationships will be discussed in the following sections. At the outset, it is useful to have a basic frame of reference for the temporal bone anatomy as suggested in Figures (140.3C–F).

Mastoid

The mastoid is a confluence of the petrous and squamous portions and as such is interposed between the petrous, tympanic, and squamous portions of the temporal bone and the occipital bone. Junctional sutures include the occipitomastoid and the tympanomastoid. The sutures are often asymmetrically fused, and wormian bones may be present in this location; these variations can simulate fractures of the skull base both on plain radiographs and CT. The posterolateral aspect of the mastoid abuts the sigmoid sinus; the bone separating the sigmoid sinus from mastoid air cells is called the sigmoid plate. Rarely, broad dehiscence of the sigmoid plate is seen as a normal anatomic variation (Fig. 104.4). Smaller focal dehiscence is also very uncommon as a normal variant. When imaged in a sagittal plane, the anteroposterior width or sagittal dimension of the mastoid is determined by the distance between the sigmoid plate posteriorly and either the tympanomastoid suture more superficially or the vertical portion of the facial canal more mesially. Normally, this sagittal mastoid dimension measures over 1 cm, unless there is underdevelopment of the mastoid air cells. This distance is used to define anterior displacement of the sigmoid sinus (Fig. 104.5A,B).

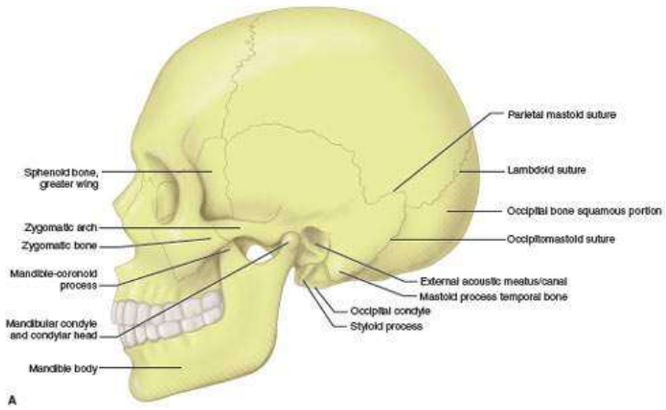
Parietal mastoid suture
Sphenoid bone, greater wing
Lambdoid suture
Occipital bone squamous portion
Zygomatic arch
Zygomatic bone
Occipitomastoid suture
Mandible-coronoid process
External acoustic meatus/canal
Mastoid process temporal bone
Occipital condyle
Mandibular condyle and condylar head
Styloid process
Mandible body
A

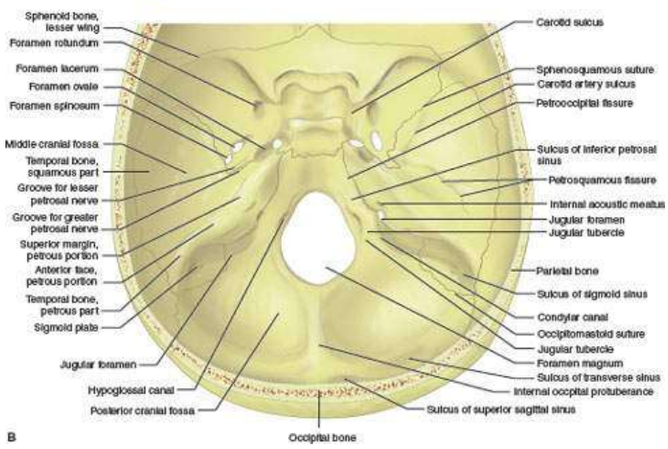
Sphenoid bone, lesser wing
Carotid sulcus
Foramen rotundum
Sphenosquamous suture
Foramen lacerum
Carotid artery sulcus
Foramen ovale
Petrooccipital fissure
Foramen spinosum
Middle cranial fossa
Sulcus of inferior petrosal sinus
Temporal bone, squamous part
Petrosquamous fissure
Groove for lesser petrosal nerve
Internal acoustic meatus
Groove for greater petrosal nerve
Jugular foramen
Jugular tubercle
Superior margin, petrous portion
Anterior face, petrous portion
Parietal bone
Temporal bone, petrous part
Sulcus of sigmoid sinus
Sigmoid plate
Condylar canal
Occipitomastoid suture
Jugular foramen
Jugular tubercle
Foramen magnum
Sulcus of transverse sinus
Hypoglossal canal
Internal occipital protuberance
Posterior cranial fossa
Sulcus of superior sagittal sinus
Occipital bone
B

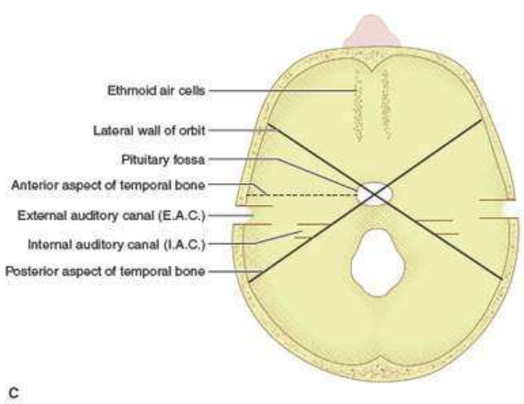
Ethmoid air cells
Lateral wall of orbit
Pituitary fossa
Anterior aspect of temporal bone
External auditory canal (E.A.C.)
Internal auditory canal (I.A.C.)
Posterior aspect of temporal bone
C

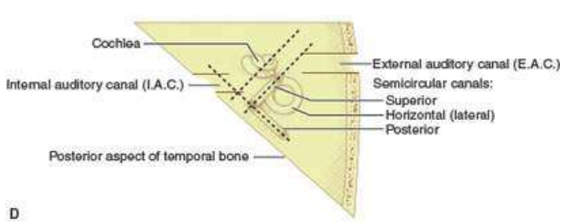
Cochlea
External auditory canal (E.A.C.)
Internal auditory canal (I.A.C.)
Semicircular canals:
Superior
Horizontal (lateral)
Posterior
Posterior aspect of temporal bone
D

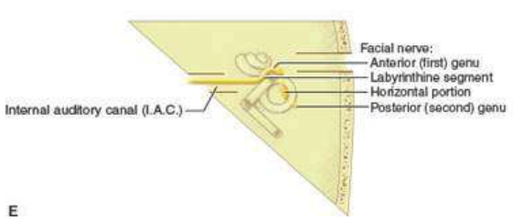
Facial nerve:
Anterior (first) genu
Labyrinthine segment
Horizontal portion
Internal auditory canal (I.A.C.)
Posterior (second) genu
E

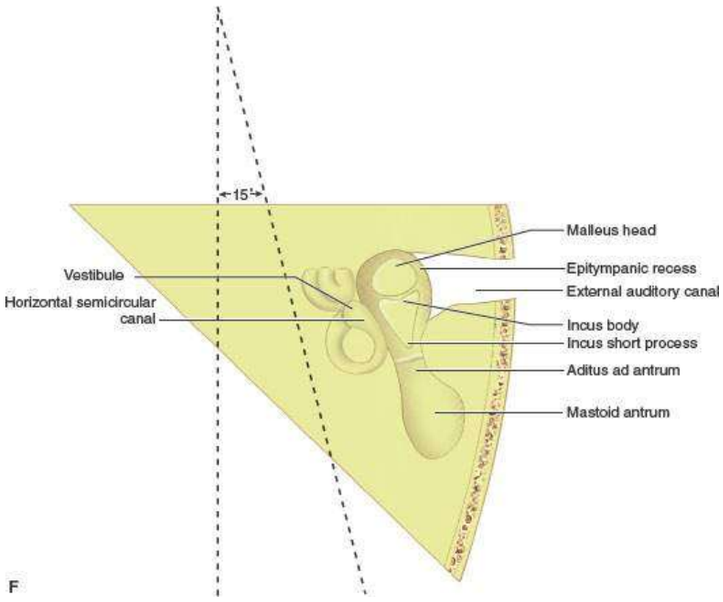

FIGURE 104.3. A, **B:** Gross osteology perspectives of perspectives of the temporal bone relative to the skull base and calvarium. **C:** Basic relationship of the temporal bone to the skull base considered schematically with an "X" drawn through the sella at the center and the temporal bone wedge basic relationship to the rest of the skull established as labeled. **D–F:** General schematic internal organization of the temporal bone to establish the basis of the relative positions of its major anatomic components, including the relationships of inner ear **(D)**, facial nerve **(E)**, and middle ear structures **(F)** to what is basically a triangular wedge of bone within the central and posterior skull base.

The superior surface of the mastoid partially forms the floor of the middle cranial fossa. Beneath this portion of the mastoid are the attic (epitympanic recess of the middle ear cavity) and the mastoid antrum (Fig. 104.6A,B). This bony roof covering the mastoid antrum and epitympanic recess is often very thin and frequently appears incomplete or dehiscent. The slope of the tegmen is variable. A low-lying tegmen— defined as one that encroaches on or falls caudal to the tympanic ring, especially along the lateral aspect of the tegmen—will narrow the surgical field in mastoid approaches (Fig. 104.7A,B). The dura beneath the temporal lobe lies just above the thin roof of the middle ear or tegmen tympani and roof of the mastoid or tegmen mastoideum. The vein of Labbé is an important venous pathway that courses above the roof of the middle ear and mastoid as it drains toward the transverse sinus. This spatial relationship helps explain the possibility of temporal lobe venous infarction secondary to mastoid inflammatory disease in cases where thrombus in the transverse sinus propagates into the vein of Labbé.

Moving from lateral to medial, important landmarks along the inferior mastoid include the mastoid process or tip, the digastric groove, and the stylomastoid foramen. The sternocleidomastoid muscle attaches to the tip of the mastoid process. Medial to the mastoid tip is a groove where the posterior belly of the digastric muscle attaches. The stylomastoid foramen, the exit foramen for the facial nerve, lies just medial to the digastric groove. The posterior belly of the digastric muscle is one of the surgical landmarks for identifying the course of the facial nerve. There is a fat pad filling the space between the digastric muscle laterally and the petrous bone through which the CN VII will pass before entering the parotid gland. This stylomastoid fat pad is an excellent CT and MRI landmark for localizing the facial nerve following its exit from the skull base (Fig. 104.8A–I).

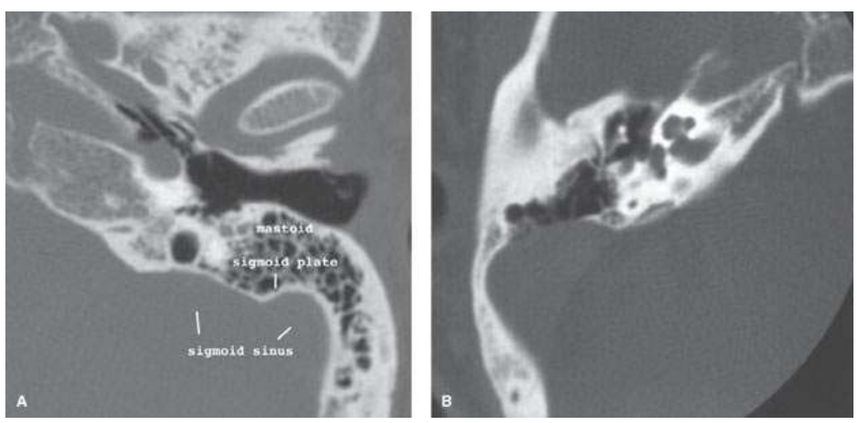

FIGURE 104.4. A: Computed tomography showing the close relationship between the mastoid and the sigmoid sinus. **B:** Rarely, dehiscence of the sigmoid plate can be seen as an anatomic variant.

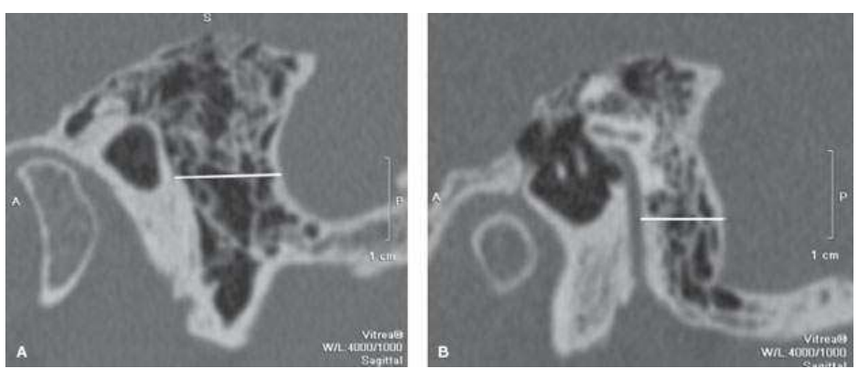

FIGURE 104.5. Anterior position of the sigmoid sinus as examined on sagittal computed tomography images. The anteroposterior width between the sigmoid plate and either the tympanomastoid suture **(A)** or the descending portion of the facial nerve **(B)** is measured (*white line*). Normal values are $1 cm.

Mastoid air cell development and middle ear anatomy are discussed in a following section.

Petrous Bone

The petrous bone is pyramidal in shape with an anterior, posterior, and inferior surface. Its base converges with the squamous bone to form with the mastoid bone, and its apex abuts the sphenoid and the basiocciput at the petroclival fissure or junction. Because of these relationships, the petrous portion of the temporal bone may be considered part of the "central skull base"; such alternate designations reflect the particular focus of pathoanatomic discussion. The petrous bone joins the mastoid without an apparent fusion line. Air cells of the mastoid are confluent with those of the petrous apex. The anterosuperior surface of the petrous bone is supratentorial, while its posterior surface is infratentorial. The anterior petrous surface joins with the anterior surface of the mastoid and with the greater wing of the sphenoid to form the floor of the middle cranial fossa. The posterior petrous surface forms the anterolateral aspect of the posterior fossa (Figs. 104.3 and 104.4). At the junction between the petrous apex and the clivus, called the petroclival fissure, there is a groove formed by the inferior petrosal sinus as it drains from the posterior aspect of the cavernous sinus to the jugular vein (Fig. 104.9).

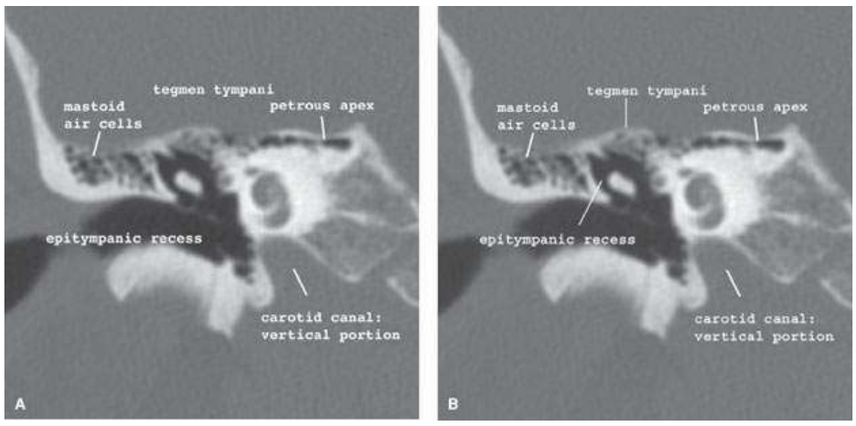

FIGURE 104.6. Coronal computed tomography images from anterior **(A)** to posterior **(B).** The bony roof of the mastoid consists of the tegmen tympani and the tegmen mastoideum. It is part of the middle cranial fossa and separates the middle ear and antrum from the temporal fossa.

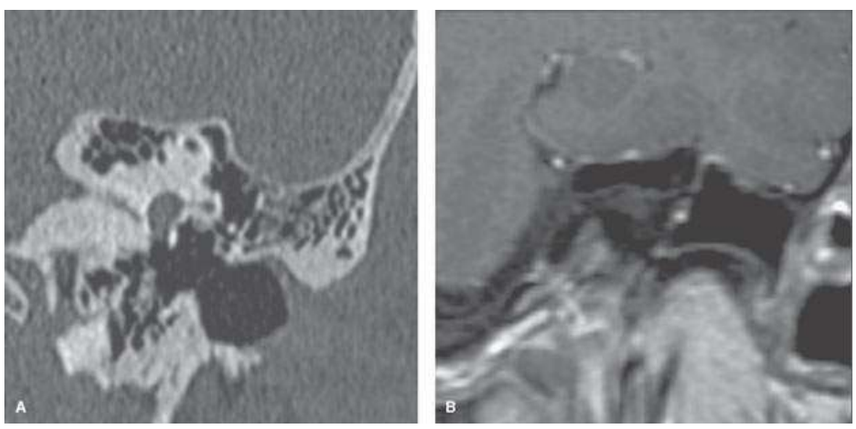

FIGURE 104.7. Coronal computed tomography image **(A)** and T1-weighted magnetic resonance image **(B)** through the mastoid. A low-lying tegmen mastoideum causes overhanging temporal dura, making surgical access more difficult.

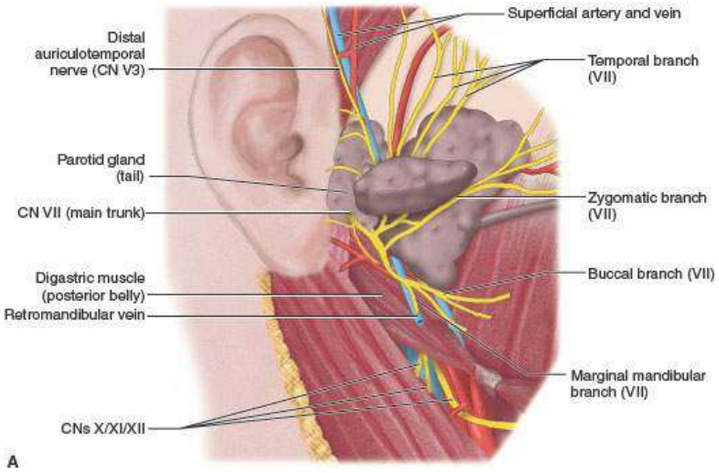

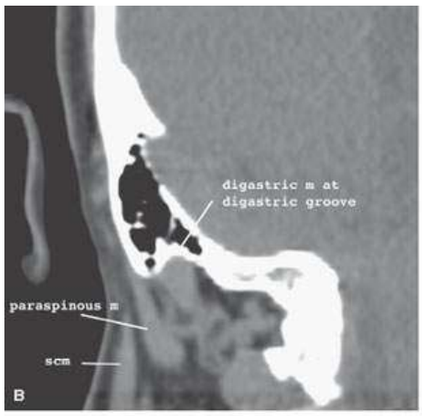
digastric m at
digastric groove
paraspinous m
scm
B

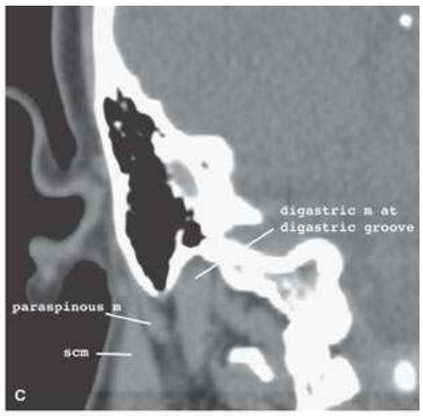
digastric m at
digastric groove
paraspinous m
scm
C

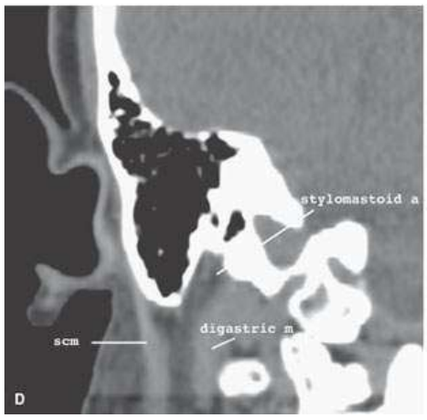
stylomastoid a
scm
digastric m
D

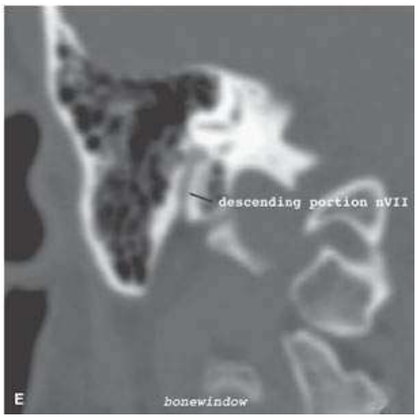
descending portion nVII
E
bonewindow

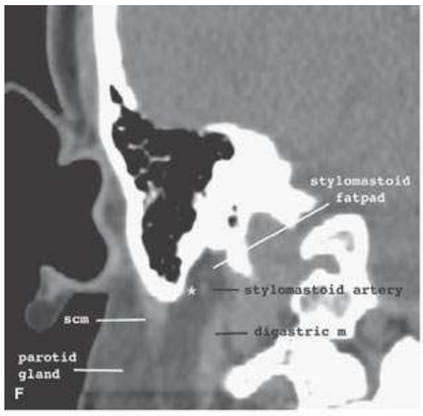
stylomastoid
fatpad
stylomastoid artery
scm
digastric m
parotid
gland
F

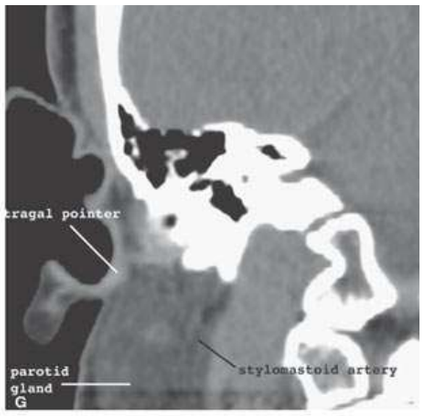
tragal pointer
parotid
gland
stylomastoid artery
G

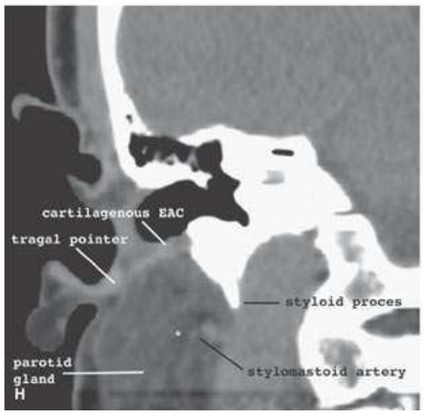
cartilagenous EAC
tragal pointer
styloid proces
parotid
gland
stylomastoid artery
H

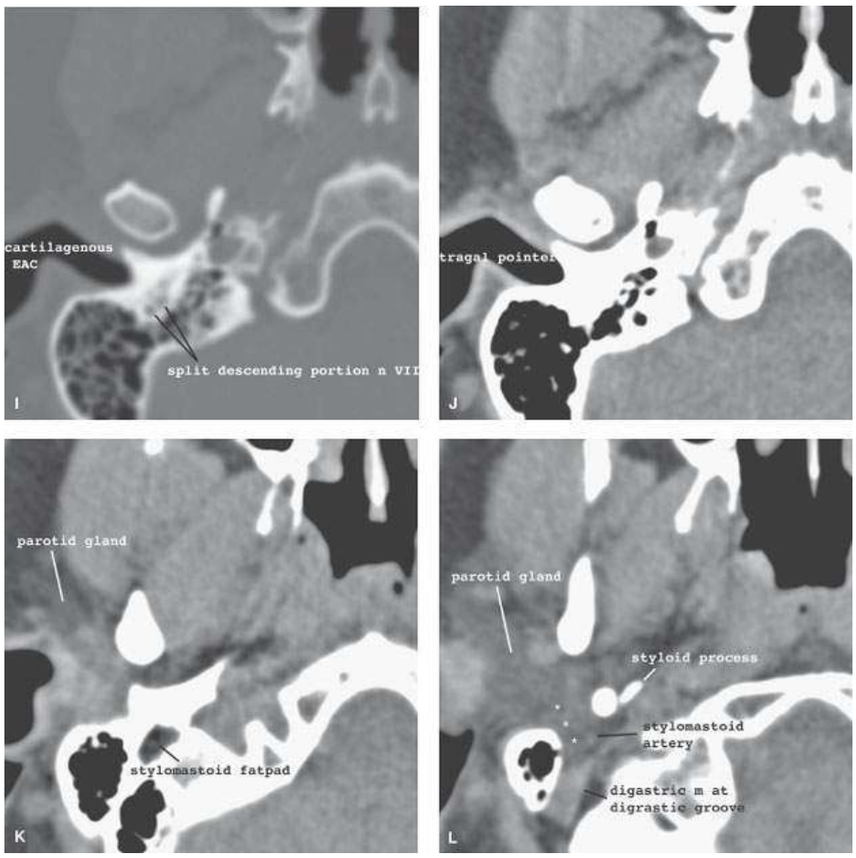

FIGURE 104.8. Anatomic drawing **(A)** and coronal **(B–H)** and axial **(I–L)** computed tomography images illustrating important landmarks identifying the course of the facial nerve related in part to how it is localized at surgery. Images **(B)** through **(E)** move posterior to the descending facial canal, while **(G)** and **(H)** are anterior. Images in **(I)** through **(L)** proceed from the stylomastoid foramen inferiorly. Cranial nerve VII (the asterisk shows its expected position as discussed in the text) runs through the stylomastoid fat pad, and its extracranial divisions show a close relationship to the mastoid tip and the attached muscles.

The inferior surface of the petrous bone contains a foramen for the internal carotid artery. Posterior and slightly more lateral to the carotid foramen is the jugular foramen, a cleft separating the petrous bone and the occipital bones. The jugular foramen or fossa actually has two parts separated incompletely by an osseous jugular spur or spine. The more medial and smaller of the two compartments contains the terminus of the inferior petrosal sinus and the glossopharyngeal nerve (CN IX). The more lateral of the two is larger and contains the jugular bulb, vagus nerve, and spinal accessory nerve. The tiny inferior tympanic canaliculus lies between the jugular fossa and vertical segment of the carotid canal; it contains the Jacobson nerve, which is a branch of the glossopharyngeal nerve. The internal carotid artery traverses the petrous bone within the carotid canal. This canal has a proximal vertical segment, a genu, and a distal horizontal segment. The internal carotid artery exits the petrous apex by turning superiorly as it passes above the cartilage that fills the foramen lacerum. The carotid canal lies just superior and medial to the proximal bony and cartilaginous portions of the auditory tube (Fig. 104.10).

The infratentorial surface of the petrous bone has several openings, the most prominent of which is the IAC. Others include openings for the cochlear and vestibular aqueducts and the subarcuate artery. The opening for the cochlear aqueduct lies just inferior to the IAC and that for the vestibular aqueduct is seen as a slitlike structure just lateral to the IAC.

The IAC contains neurovascular structures, CSF, and meninges. CSF within the IAC connects directly with fluid within the CPA cistern (Fig. 104.11). The cranial aspect of the IAC has a smooth wall. However, at the fundus (its more lateral aspect), the canal is partially subdivided by a curvilinear horizontal bone plate, the crista transversalis or falciformis, along its anterior wall. The anterosuperior compartment contains the facial nerve and nervus intermedius; the facial nerve then continues its course through the petrous bone by entering the labyrinthine segment of the facial canal. The Bill bar is a prominent ridge of bone and surgical landmark along the superolateral aspect of the IAC, identifying the transition of the facial nerve from its canalicular to labyrinthine segments (Fig. 104.12). The posterosuperior compartment of the IAC contains the superior vestibular nerve, while the inferior compartment contains both the cochlear nerve anteriorly, beneath the facial nerve and inferior vestibular nerve posteriorly, beneath the superior vestibular nerve. The facial nerve and the superior vestibular nerve show a parallel course within the IAC, whereas the cochlear nerve and inferior vestibular nerve are V shaped (Fig. 104.13). The cochlear nerve enters the cochlea and winds around the modiolus. The superior and inferior vestibular nerves continue on to the vestibule; a branch of the inferior vestibular nerve, the singular nerve, travels in a slitlike canal to reach the ampulla at the posterior semicircular canal. Details of the middle ear, the inner ear, and the course of the facial nerve will be presented in following sections. The shape and course of the IAC is variable without only uncommon relationships to hearing loss (Fig. 104.14).

There are other common variations of the anatomy of the petrous bone that can lead to interpretive difficulties, especially on MRI. These include the following:

1. Variations in aeration, fatty marrow content, and venous lakes within the petrous apex. These variations can lead to a markedly asymmetric appearance of the petrous apices and mistaken diagnoses of mass lesions or other pathologies such as cholesterolosis, epidermoid tumors, and petrous “apicitis” (Figs. 104.15A–C and 104.16A,B).
2. Arachnoid granulations that may produce areas of remodeling along the temporal bone surfaces that can be mistaken for erosive lesions (Fig. 104.17A–D). These can be a source of CSF leakage into adjacent aerated portions of the temporal bone.
3. Variations in the size of the jugular fossa. The jugular fossae (Fig. 104.18A–G) are, as a rule, asymmetric and usually high, or large jugular fossa may be mistakenly interpreted as evidence of a jugular fossa tumor. A high jugular bulb is more frequently seen on the right side. This may possibly be related to the amount of blood flow difference due to drainage dominance between the right and left transverse sinuses and jugular veins.

In radiologic and anatomic studies, several definitions for a high jugular bulb are given. A jugular bulb has been referred to as high if it is lying above the level of the tympanic annulus,20 if it abuts the round window niche, or when it extends superior to the internal acoustic canal. Due to this, reported incidences of high jugular bulb vary considerably. Its importance depends on the chosen surgical approach. If the jugular bulb projects into the middle ear, the vein can be injured during middle ear surgery (e.g., cholesteatoma removal from hypotympanic retrofacial air cells) and during elevation of a tympanomeatal flap or myringotomy. As soon as the jugular bulb reaches the level of the internal acoustic canal, it will block the access to the IAC for translabyrinthine or suboccipital removal of vestibular schwannoma.

If the bony plate covering the jugular bulb is even partially absent, it is referred to as a dehiscent jugular bulb, posing more risk to preoperative injury. Rarely, a jugular diverticulum can be seen.

1. Variations in signal intensity in the jugular bulb because of flow-related artifacts. This problem is compounded by the injection of paramagnetic contrast that emphasizes flow-related artifacts in these regions of complex, relatively slow flow (Fig. 104.19).

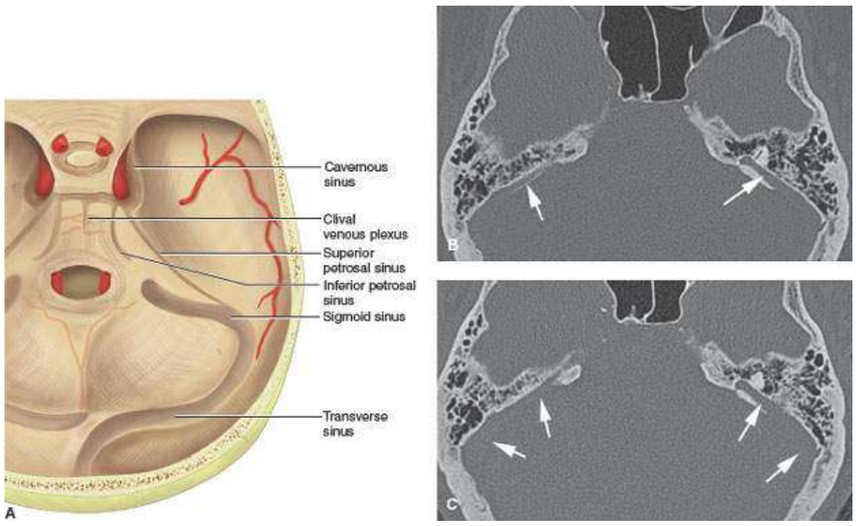

FIGURE 104.9. On the anatomic drawing **(A)**, the venous drainage of the cavernous sinus by the superior and inferior petrosal veins to the jugular vein is shown**.** Both the superior and inferior petrosal veins can cause a groove in the roof of the petrous bone and at the petroclival fissure, the former seen on axial CT images **(B)** and **(C).**

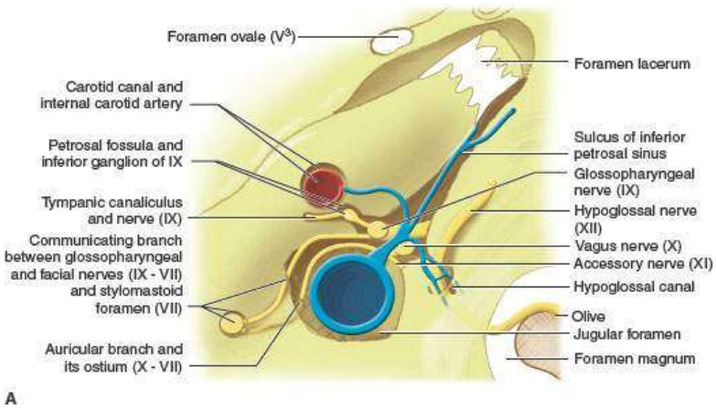

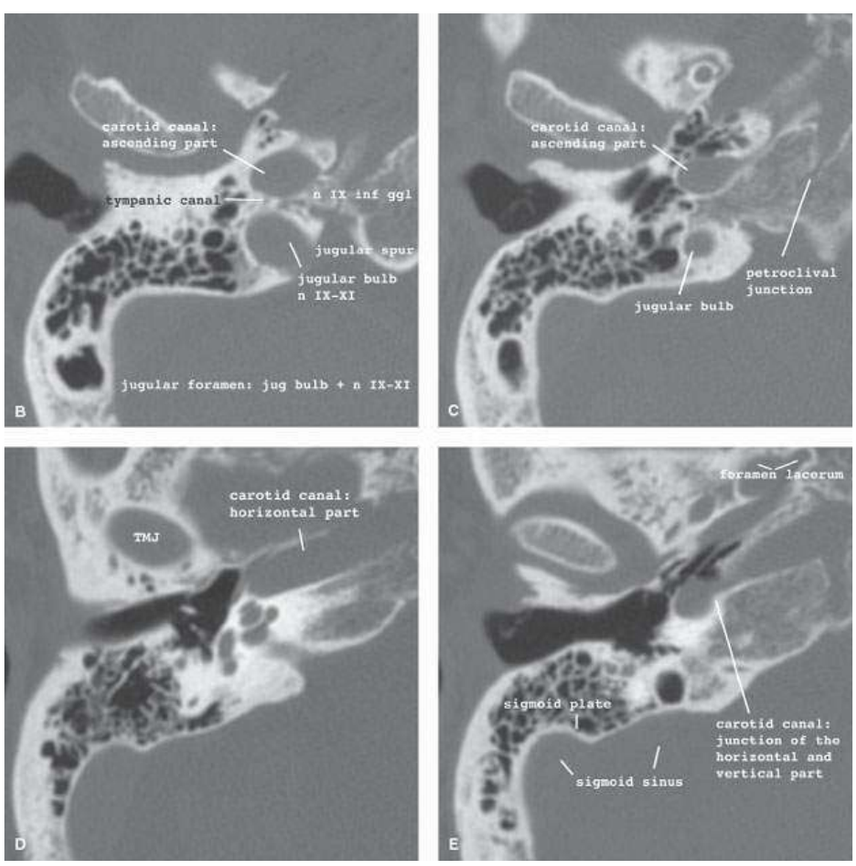

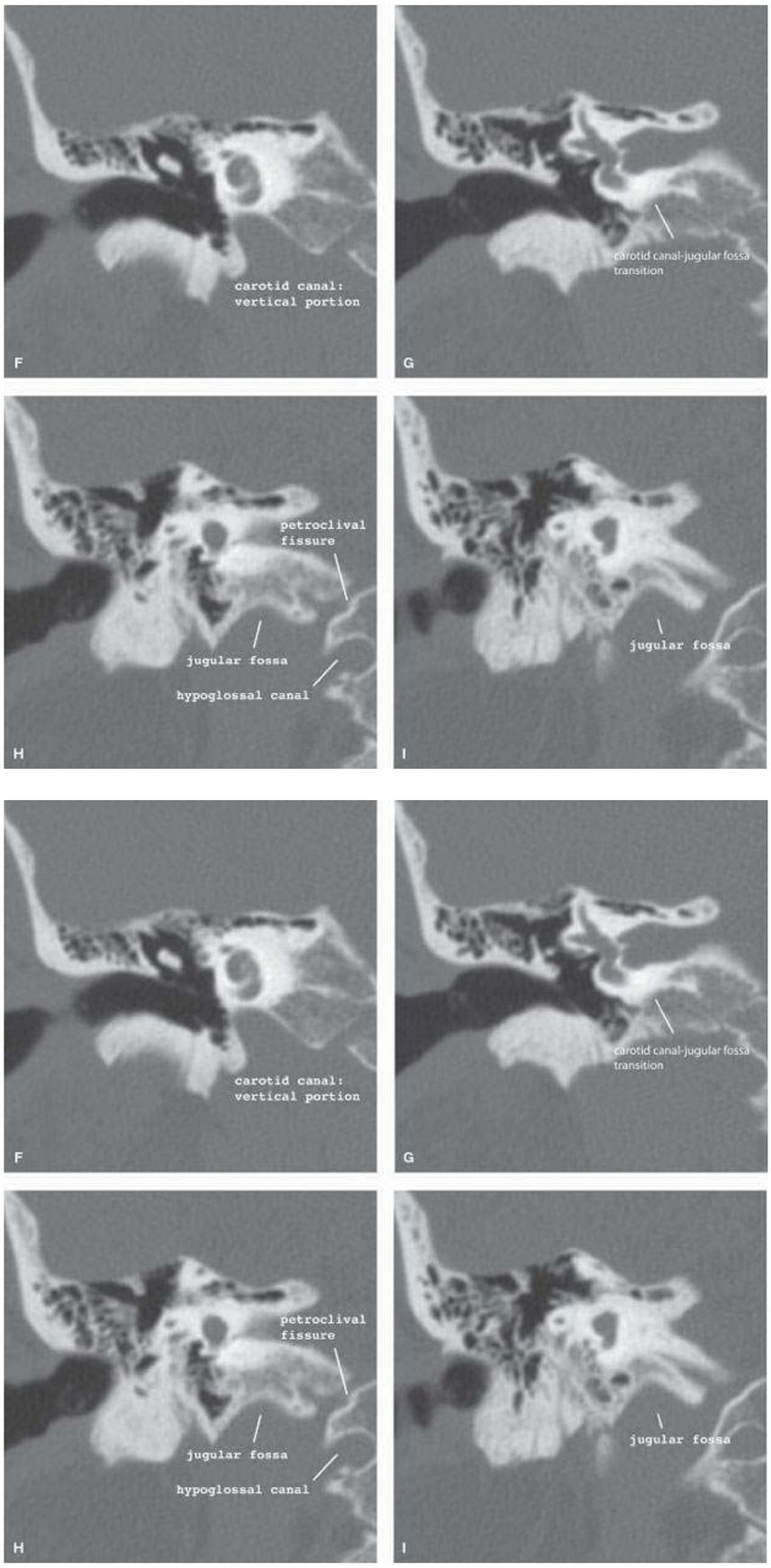

FIGURE 104.10. A: Diagram showing the rather complex neurovascular relationships within and around the carotid canal and jugular fossa. **B–I:** Axial computed tomography images from inferior to superior **(B–E)** and coronal images from anterior to posterior **(E–I)** through the internal carotid artery and internal jugular vein and their respective canals.

Zygomatic and Squamous Bones

The zygomatic process of the temporal bone projects anteriorly from its base toward the zygomatic process. The two combine to form the zygomatic arch (Fig. 104.3). The soft tissue space between the zygomatic arch and the lateral skull/lateral orbit is the (superficial) temporal fossa. The relatively wide base of the zygomatic portion of the temporal bone forms the main buttress for the zygomatic arch. The temporomandibular joint (TMJ) is located along the base of the zygomatic part of the temporal bone. The details of TMJ anatomy are discussed in Chapter 4.

The squamous portion of the temporal bone forms much of the lateral wall of the middle cranial fossa. External to this bone is the superficial temporal fossa; the temporalis muscle and fat fill the superficial temporal fossa. A vertical linear groove in the outer table of the squamous part of the temporal bone is created by the course of the anterior deep temporal artery. This groove may be misinterpreted as a fracture on lateral skull radiographs. The inner table of the squamous portion of the temporal bone contains a groove for the posterior division of the middle meningeal artery.

Tympanic Bone and External Auditory Canal

The EAC is essentially a 2.5-cm–long cylinder formed by tympanic bone medially and cartilage laterally (Fig. 104.20). The cartilaginous anterior wall is normally pierced by two or three vertical fissures (of Santorini); these are a potential route for spread of pathology between the EAC and parotid gland but are not routinely visible on CT or MRI. The EAC joins the mastoid and petrous portions of the temporal bone at the tympanomastoid suture and petrotympanic fissure,

respectively. The mesial aspect of the tympanic bone is separated from the middle ear cavity by the tympanic membrane. The forward angulation of the tympanic membrane results in the anterior EAC wall being about 6 mm longer than the posterior wall. The insertion of the tympanic membrane annulus around the mesial aspect of the tympanic bone is sometimes called the tympanic sulcus (Fig. 104.21). The pinna and cartilages of the external ear surround the ostium or meatus for the EAC. The central part of the external ear is formed by the tragal cartilage. On imaging studies, the deeper aspect of the tragal cartilage, at its junction with the cartilaginous part of the EAC, can be identified; this part has been nicknamed the "tragal pointer" by surgeons. The tragal pointer is a surgical landmark used to identify the main trunk of the facial nerve; the trunk is usually approximately 1 cm inferior and medial to the tragal pointer. On CT and MRI, the tragal pointer is seen as an angulated segment of the cartilaginous EAC about 1 cm from the bony cartilaginous junction (Fig. 104.8).

Slight irregularities of the tympanic bone are commonly seen on CT at the bony-cartilaginous junction of the EAC. In well-aerated temporal bones, the posterior wall of the canal may normally appear thin or dehiscent. A small gap in the anteroinferior portion of the tympanic bone is a common normal variant called the persistent foramen tympanicum or foramen of Huschke21 (Fig. 104.22). Fat and other portions of the TMJ capsule can rarely herniate into this and present as an external canal mass. A great variability in the configuration of the EAC is seen (Fig. 104.23).

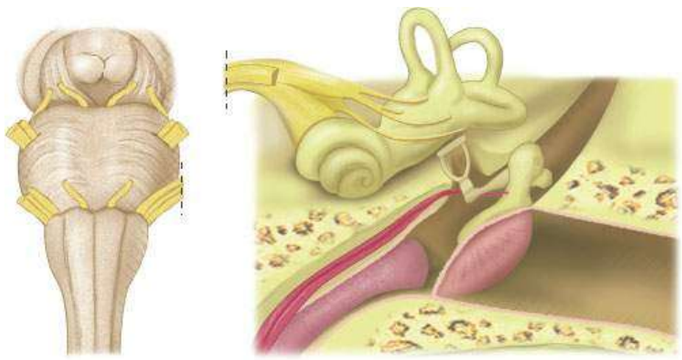

FIGURE 104.11. Drawing showing contents of the internal auditory canal and their relationship to the inner ear and brain stem. The appreciation of the location of cranial nerve nuclei in the brain stem and then the peripheral course of the nerve through its related cistern and exit foramen to its end point of innervation is a fundamental concept in evaluating any cranial neuropathy.

Middle Ear or Tympanic Cavity

The tympanic cavity is divided, somewhat arbitrarily, into three intercommunicating parts: the epitympanum, the mesotympanum, and the hypotympanum, corresponding, respectively, to the superior, middle, and inferior levels of the middle ear cavity (Figs. 104.24 and 104.25).

The epitympanum communicates anteriorly and superiorly with the anterior epitympanic recess; the floor of the recess forms the roof of the epitympanum. More posteriorly, the roof of the middle ear cavity (tegmen tympani) is simply the roof of the epitympanum. The mesotympanum is bounded medially by the otic capsule and laterally by the tympanic membrane. The hypotympanum is bounded inferiorly by the floor of the tympanic cavity that overlies the jugular fossa posteriorly and the lateral aspect of the carotid canal anteriorly. The hypotympanum opens anteriorly, forming the bony portion of the auditory tube; the more distal, cartilaginous portion, of the tube eventually connects the middle ear to the nasopharynx. This portion is only visible if containing air (Figs. 104.25 and 104.26). The middle ear cavity is about 1.5 cm in its vertical and anteroposterior dimensions. From a central constriction of about 2 to 3 mm in the mesotympanum, it expands to a transverse dimension of 6 mm in the epitympanum and 4 mm in the hypotympanum.

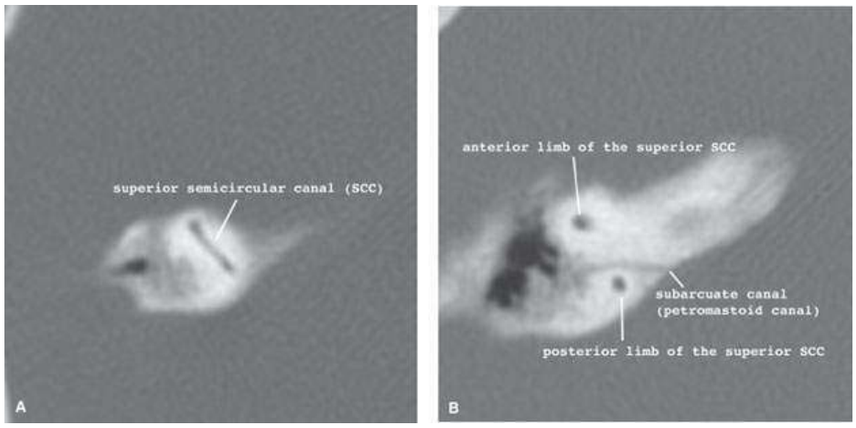


ampulla superior SCC
common crus superior and posterior SCC
posterior SCC
C

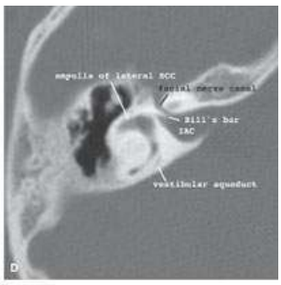
ampulla of lateral SCC
facial nerve canal
Bill's bar
IAC
vestibular aqueduct
D

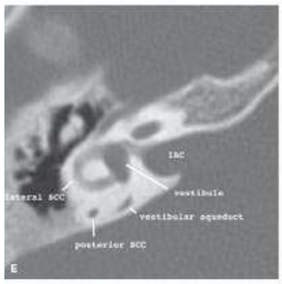
IAC
lateral SCC
vestibule
vestibular aqueduct
posterior SCC
E

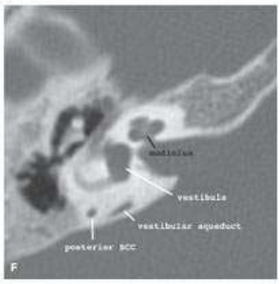
modiolus
vestibule
vestibular aqueduct
posterior SCC
F

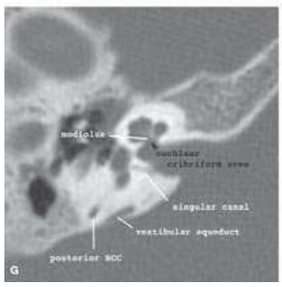
modiolus
cochlear cribriform area
singular canal
vestibular aqueduct
posterior SCC
G

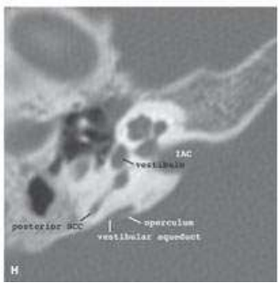
IAC
vestibule
posterior SCC
operculum
vestibular aqueduct
H

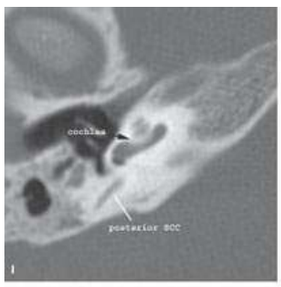
cochlea
posterior SCC
I


basal turn of the cochlea
cochlear aqueduct
J

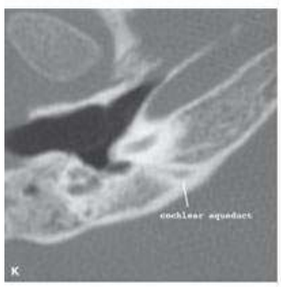
cochlear aqueduct
K

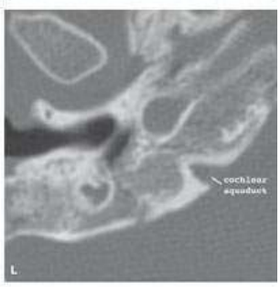
cochlear aqueduct
L

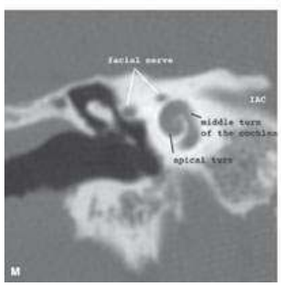
facial nerve
IAC
middle turn of the cochlea
apical turn
M

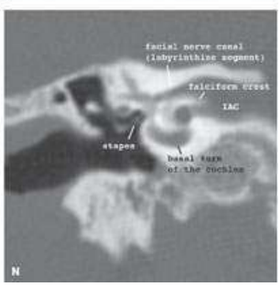
facial nerve canal (labyrinthine segment)
falciform crest
IAC
stapes
basal turn of the cochlea
N

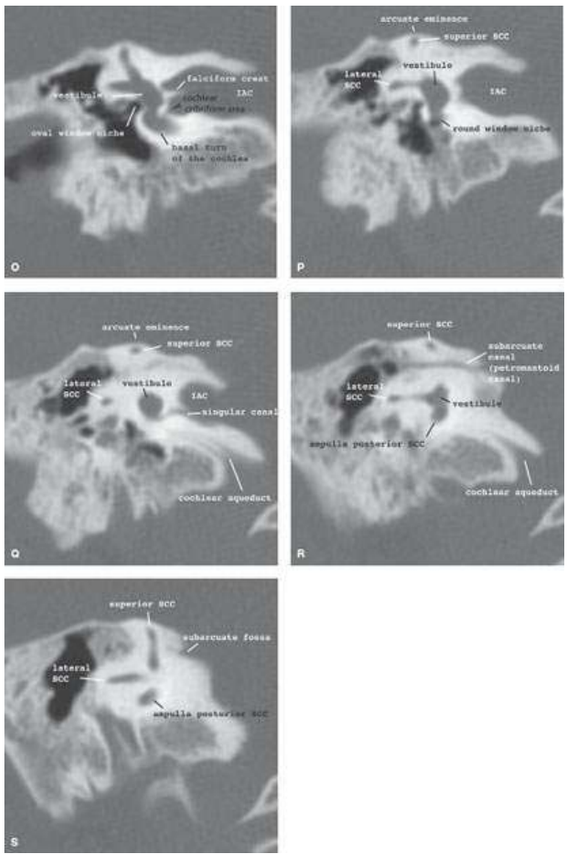

FIGURE 104.12. Normal axial **(A–L)** and coronal **(M–S)** computed tomography anatomy of the internal auditory canal, vestibular aqueduct, cochlear aqueduct, subarcuate canal, and singular canal.

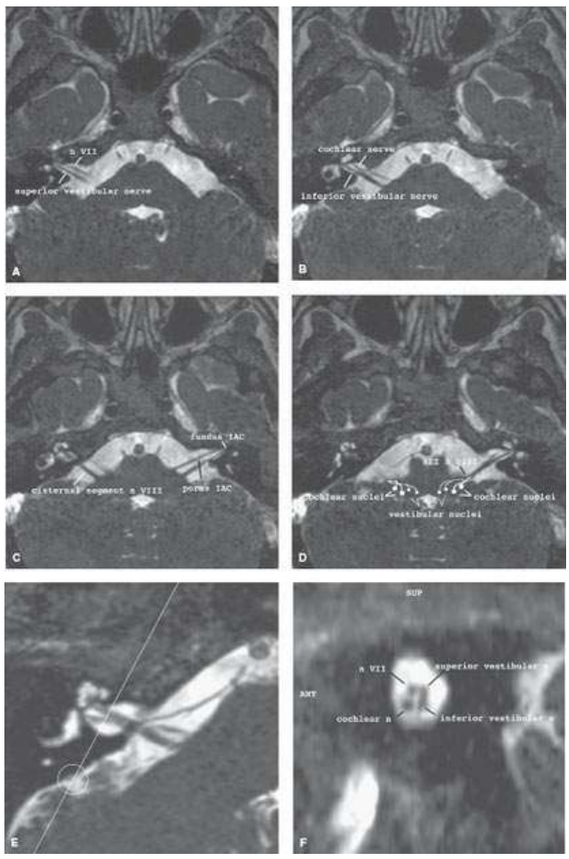

FIGURE 104.13. Normal magnetic resonance imaging anatomy of the internal auditory canal. On axial heavy T2-weighted images (CISS), the course of cranial nerves VII and VIII can be discerned**. A–D:** Oblique reformatted images **(E, F)** show the relation between the four nerves within the internal auditory canal.

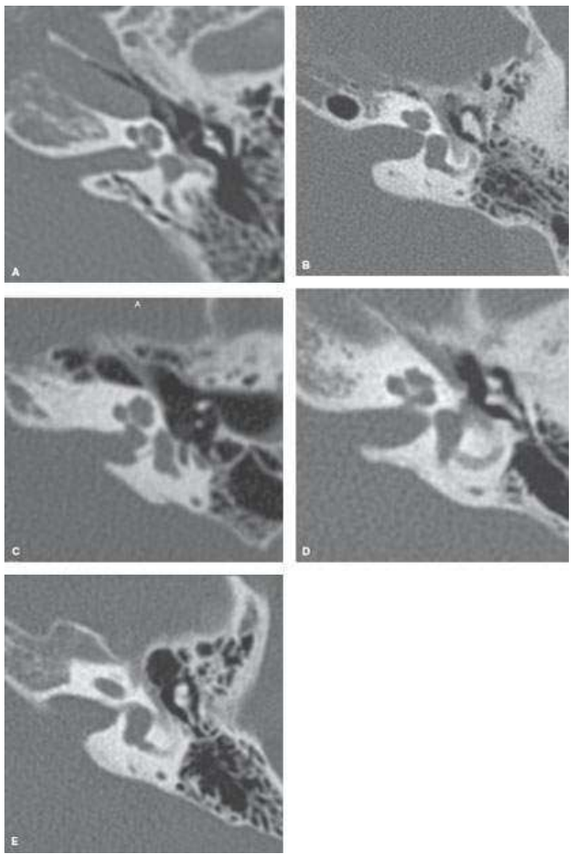

FIGURE 104.14. A–E: Normal variations in the size of the internal auditory canal.

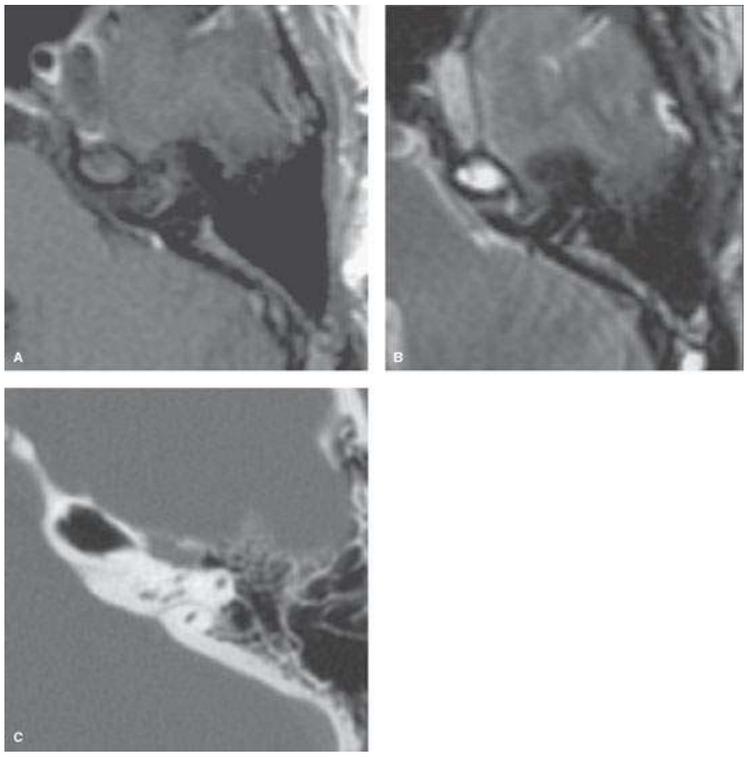

FIGURE 104.15. Variations of the petrous apex. **A**, **B**: T1- and T2-weighted images showing abnormal signal intensity in the left petrous apex, consistent with fluid. **C**: Computed tomography image taken a few weeks earlier showing a well-pneumatized petrous apex, confirming fluid and ruling out a mass lesion.

The normal mucosa of the middle ear cavity is normally not visible on CT or MRI. The ossicles, related muscles and tendons, portions of the facial nerve, and occasionally the suspensory ligaments of the ossicles are the only normal structures visible within the middle ear on CT.22 Only the facial nerve and tensor tympani muscle are consistently visible on MR.

Mesotympanum

The mesotympanum lies medial to the tympanic membrane. Its superolateral boundary is at the level of the scutum. The scutum is a layer of bone from the temporal squama that forms the lateral wall of the epitympanum as it fuses with the upper tympanic ring (annulus). The lower margin of the tympanic ring is the inferolateral boundary of the mesotympanum. Surgeons sometimes refer to an area anterior to a frontal plane placed through the anterior margin of the tympanic ring as the protympanum. For this discussion, the protympanum is included in the mesotympanum. Structures within the mesotympanum include the manubrium of the malleus, the tensor tympani muscle and tendon, the stapedius muscle, the long process of the incus, the stapes, and the tympanic segment of the facial nerve.

The Prussak space is the area between the malleus, the lateral malleal ligament, and the tympanic membrane. It is mainly medial to the pars flaccida and in the mesotympanum, but its superior aspect projects to the epitympanum between the scutum and malleal head. It is a common site of early cholesteatoma (Fig. 104.27).

Erosion of the scutum is a hallmark of such a pars flaccida cholesteatoma. To be able to recognize erosion, one must be familiar with the variable appearance of

the scutum; it can be thin or broad, long or short, but it is always pointed (Fig. 104.28). A blunt scutum is the result of erosion from disease or surgery.

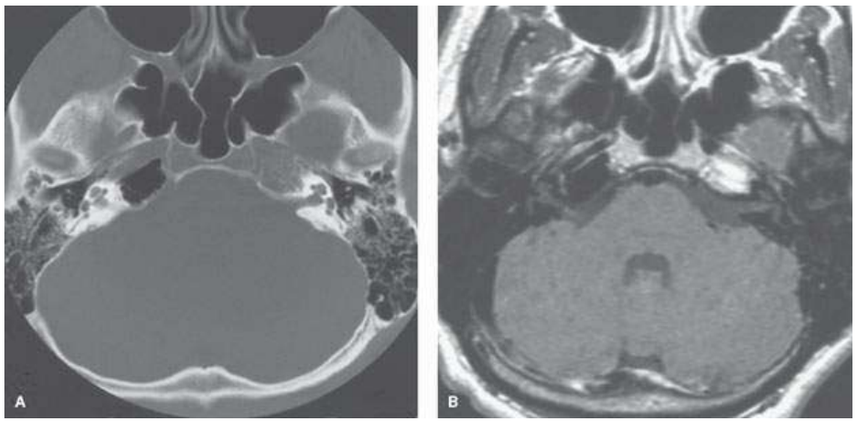

FIGURE 104.16. Normal variations of the petrous apex. Asymmetric appearance of the petrous apex due to variations in pneumatization. Computed tomography **(A)** and magnetic resonance **(B)** images show fatty marrow in the left petrous apex, whereas the right is well pneumatized.

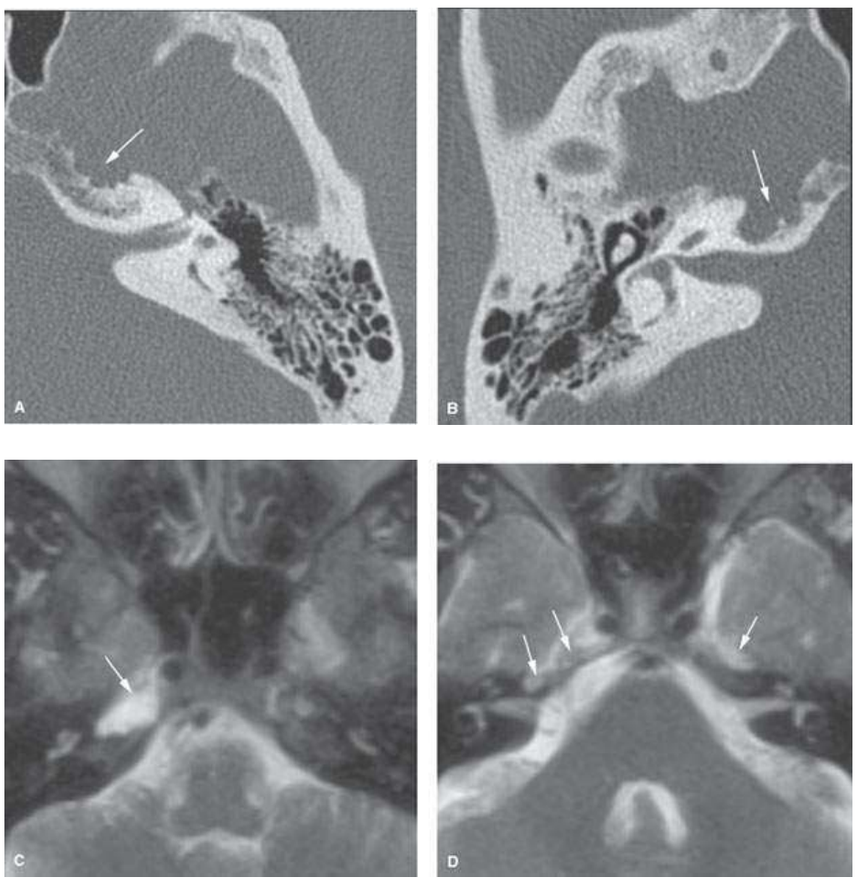

FIGURE 104.17. Arachnoid granulations at the petrous apex. On computed tomography **(A, B)**, lobular, smoothly marginated defects along the anterior surface of the petrous apex are seen bilaterally (*arrows*). On T2-weighted magnetic resonance images **(C, D)**, signal intensity of cerebrospinal fluid is seen at this level, confirming that the remodeling is due to arachnoid granulations (*arrows*).

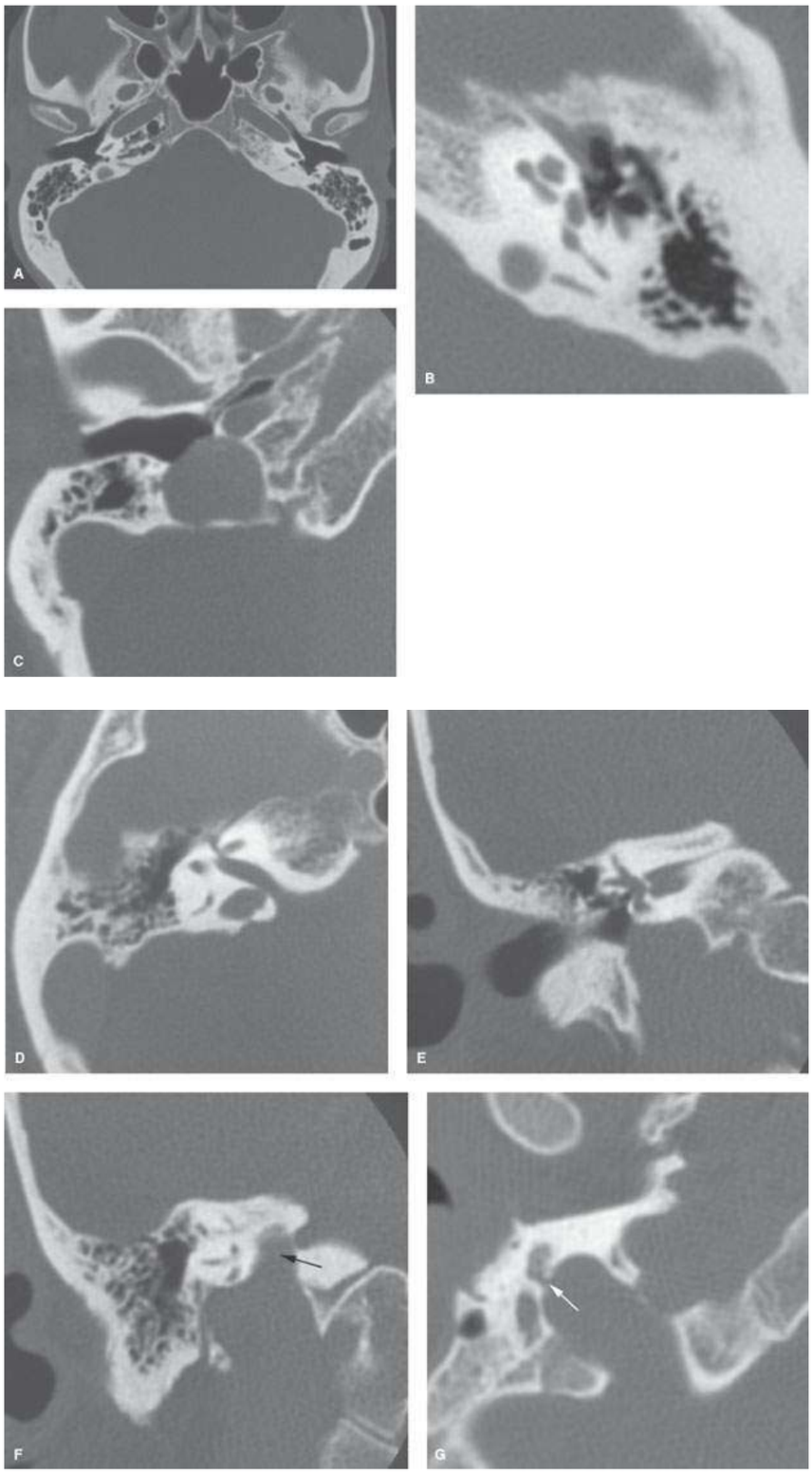

FIGURE 104.18. Anatomic variations of the jugular bulb. **A**: Jugular fossae are usually asymmetric and higher on the right. Various definitions are used for the term high-riding jugular bulb. **B**: Most commonly, the round window niche is used as a reference. **C–E**: In the case of translabyrinthine surgery, a high-riding bulb is significant if it is higher than the internal auditory canal. Dehiscence of the bony covering between the jugular bulb and the middle ear cavity is seen. **F, G**: Rarely, a jugular diverticulum (*arrow*) is present **(F, G)**.

The medial wall of the mesotympanum undulates because of several recesses and bulges created by the deeper structures related to the inner ear. The bone covering the basal turn of the cochlea is called the promontory. Just above the promontory, there is a shallow depression created by the oval window niche. The stapes lies within the oval window niche; its thin foot plate covers the oval window. The oval window niche is bounded superiorly by the facial nerve and its canal as they lie immediately beneath the LSCC. The facial canal may be partially or totally dehiscent and the nerve prolapsed as it transmits the tympanic segment of the nerve from the anterior to the posterior genu. The semicanal for the tensor tympani muscle lies just inferior to the facial canal. The tensor tympani muscle originates from a bony canal, the auditory tube, and an adjacent portion of the sphenoid bone. Its canal appears incomplete laterally. The muscle turns sharply laterally around the processus cochleariformis to insert on the upper manubrium or neck of the malleus. The muscle is always visible on CT and MRI. The region of fissula ante fenestram is located between the cochleariform process and the oval window (Fig. 104.29). The cochleariform process and subjacent fissula ante fenestram can be identified consistently on high-quality CT done with contiguous 1 mm sections or less sections in many children and some young adults (Fig. 104.30). In the vast majority of adults, the fissula ante fenestram is not visible, with this perilymphatic appendage having been obliterated by bone and/or fibrosis.23 It is the anticipated location of the fissula that is studied for subtle osteolytic change as evidence of early otosclerosis in the adult population (Fig. 104.31).

The round window niche is another depression in the medial wall of the mesotympanum; it lies posterior and slightly inferior to the oval window niche. The hypotympanum bounds the round window niche inferiorly, and the promontory bounds it superiorly. A third depression on the medial wall of the posterior hypotympanum is the tympanic sinus, which is also known as the sinus tympani; it is separated from the round window niche by a thin ridge of bone named the subiculum. The tympanic sinus is bounded superiorly by the LSCC and ponticulus, posteriorly by the posterior semicircular canal, and inferiorly by the subiculum and the jugular fossa wall. The bony labyrinth is the medial boundary of the sinus tympani. The pyramidal eminence and facial nerve form its lateral boundary. The dimensions of the sinus tympani vary considerably between patients but tend to be roughly symmetric in any one patient, assuming mastoid air cell development is roughly equivalent. A deep tympanic sinus may extend well posterior to the pyramidal eminence and facial nerve (Fig. 104.32). If a

cholesteatoma extends into a deep tympanic sinus, it will be out of direct sight and possibly out of reach for the surgeon. An extremely deep tympanic sinus may be reached via a transmastoid retrofacial approach.

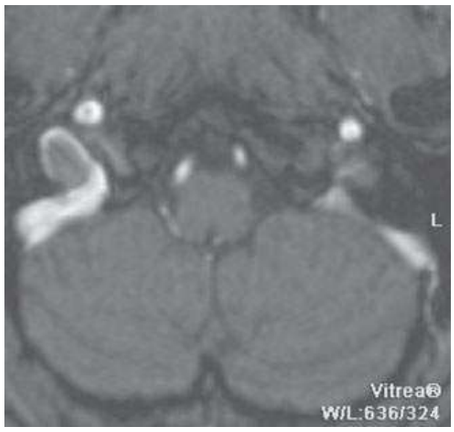

FIGURE 104.19. Flow artifacts in the jugular fossa may be mistaken for a mass. Time of flight magnetic resonance angiography shows a filling defect in the right jugular bulb due to flow-related artifact.

Like the medial wall of the mesotympanum, its posterior wall is marked by ridges and depressions. The pyramidal eminence, a major ridge, is located centrally on the posterior wall; it separates the facial recess and sinus tympani. The descending facial canal usually lies just lateral to the pyramidal eminence and posterior to both it and the facial recess. The facial recess ends superiorly at the incudal fossa that contains the short process of the incus. The incudal fossa marks the approximate level of the second (posterior) genu of the facial nerve, where the tympanic segment turns inferiorly to continue as the descending portion of the facial nerve (Fig. 104.33).

The anterior wall of the mesotympanum is the bony covering of the carotid artery. This wall may contain air cells or be focally dehiscent (Fig. 104.34).

Epitympanum

The epitympanic recess or attic is the middle ear space, projecting superior to a horizontal plane drawn through the most superior aspect of the tympanic membrane. More conveniently for imaging, a line may be drawn between the inferior tip of the scutum and the tympanic portion of the facial nerve (Fig. 104.24). The epitympanum is about 5 mm in height or roughly one third the total vertical dimension of the middle ear. Its roof is a thin plate of bone called the tegmen tympani, which is found on the temporal fossa side of the petrous bone. The epitympanum communicates with the mastoid antrum via the aditus and antrum. An anterior epitympanic recess of variable size may be partially separated from the epitympanum by a bony septum (Fig. 104.35). The head of the malleus and incus are suspended within the epitympanum by ligaments attached to its walls.

The roof of the tympanic cavity and mastoid antrum frequently appear very thin or dehiscent on CT (Fig. 104.35E). Focal arachnoid granulations can project into these apparent defects as a normal variant. Rarely, these defects and/or arachnoid granulations are sites of spontaneous CSF leakage.

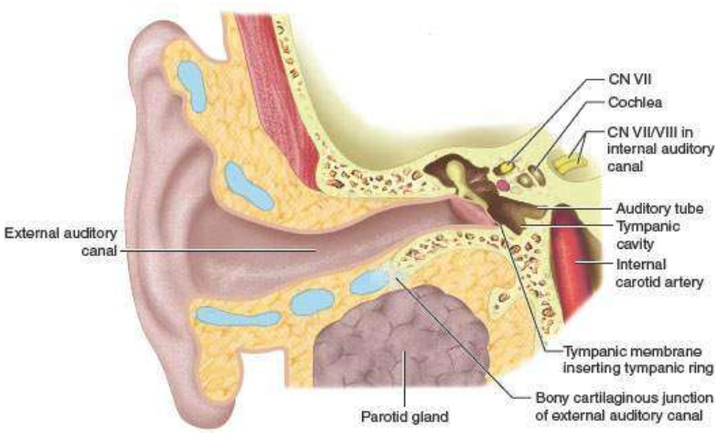

FIGURE 104.20. Drawing of the pinna and external auditory canal as they relate to the rest of the temporal bone.

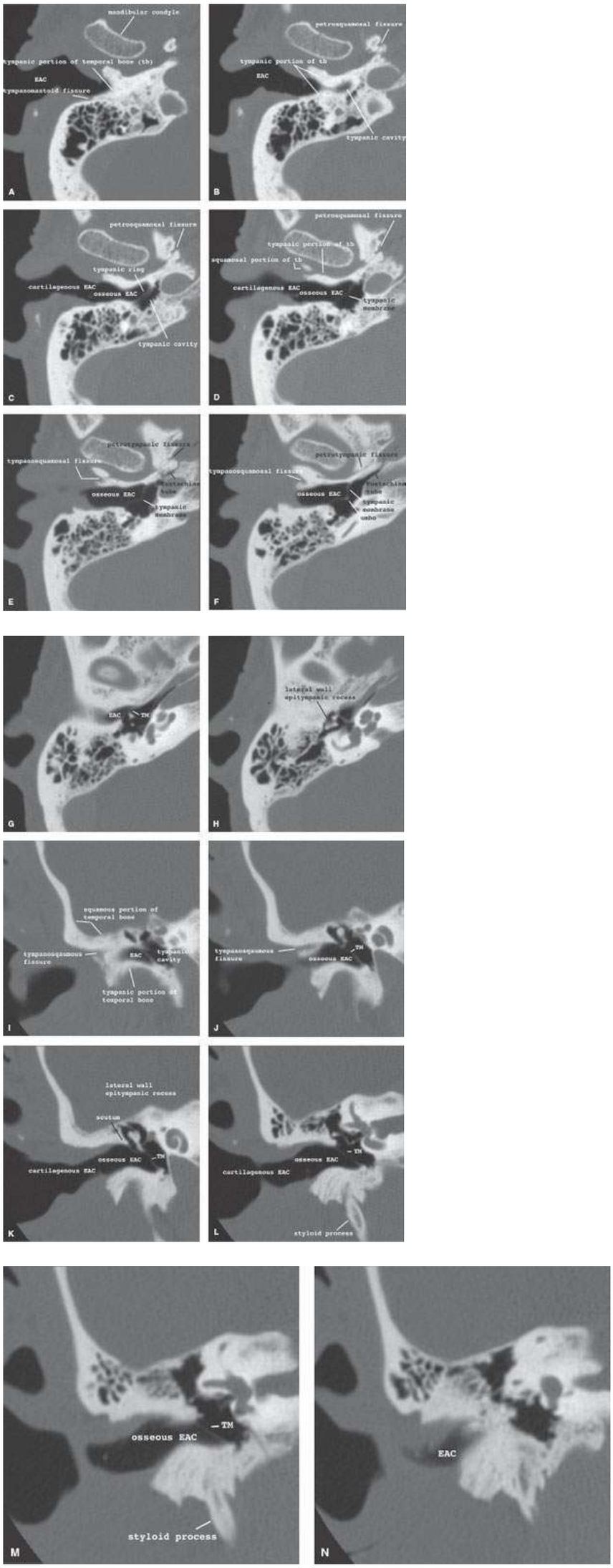

FIGURE 104.21. Normal anatomy of the external auditory canal on axial **(A–H)** and coronal **(I–N)** computed tomography images**.**

Hypotympanum

The hypotympanum lies inferior to the promontory below a horizontal plane drawn through the most inferior portion of the tympanic ring/annulus; its depth varies. The round window niche, sinus tympani, and facial recess open into the hypotympanum posteriorly and inferiorly (Fig. 104.33). The floor of the hypotympanum rests on the plate of bone covering the jugular bulb or roof of the jugular fossa. This bone may be thin or dehiscent. The floor may also be high posteriorly due to the common normal variant of a high jugular bulb. The jugular bulb is considered higher than usual when it is seen at the level of the round tympanic membrane (Fig. 104.18). Air cells anterior to the jugular bulb and posterior to the carotid artery may extend to the petrous apex and provide a minimally invasive surgical access to the petrous apex.

The hypotympanum also makes up that portion of the middle ear cavity leading to the bony auditory tube anteriorly. The term protympanum can be used to refer to the area inclusive of this anteroinferior extension of the middle ear cavity.

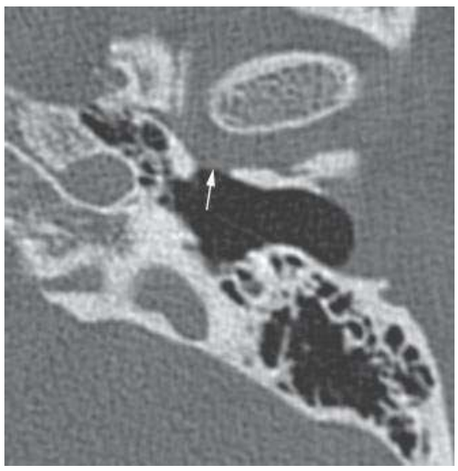

FIGURE 104.22. Foramen of Huschke. Dehiscence in the anterior wall of the external auditory canal.

Ossicles: Malleus, Incus, and Stapes

The three ossicles are located in the upper two divisions of the middle ear cavity. The head of the malleus and body of the incus lie in the epitympanum. The manubrium of the malleus, long process of the incus, and stapes superstructure are in the mesotympanum (Figs. 104.24, 104.25, and 104.36). The ossicles are suspended within the middle ear cavity by ligaments attaching the ossicular heads to the bony walls of the epitympanum22 (Fig. 104.37). The stronger of these ligaments sets the axis of rotation of the ossicles. The manubrium and anterior process of the malleus also attach to the tympanic membrane. Sound vibrations are mechanically transmitted via coordinated movement of the ossicles from their mallear attachments on the tympanic membrane to the body and then long process of the incus. The incus terminates at its lenticular process that articulates with the head of the stapes at the incudostapedial joint. The anterior and posterior crura of the stapes connect its head to the foot plate. The head and crura make up the suprastructure of the stapes. The anterior crus is often more delicate and straighter than the posterior crus (Fig. 104.38B,C). The stapes foot plate attaches to the oval window of the bony labyrinth and reproduces sound-induced vibrations of the tympanic membrane in the endolymphatic fluid of the cochlea. These vibrations are ultimately absorbed by motion of the round window membrane. The round window is located about 2 to 3 mm posterior and inferior to the oval window along the promontory.

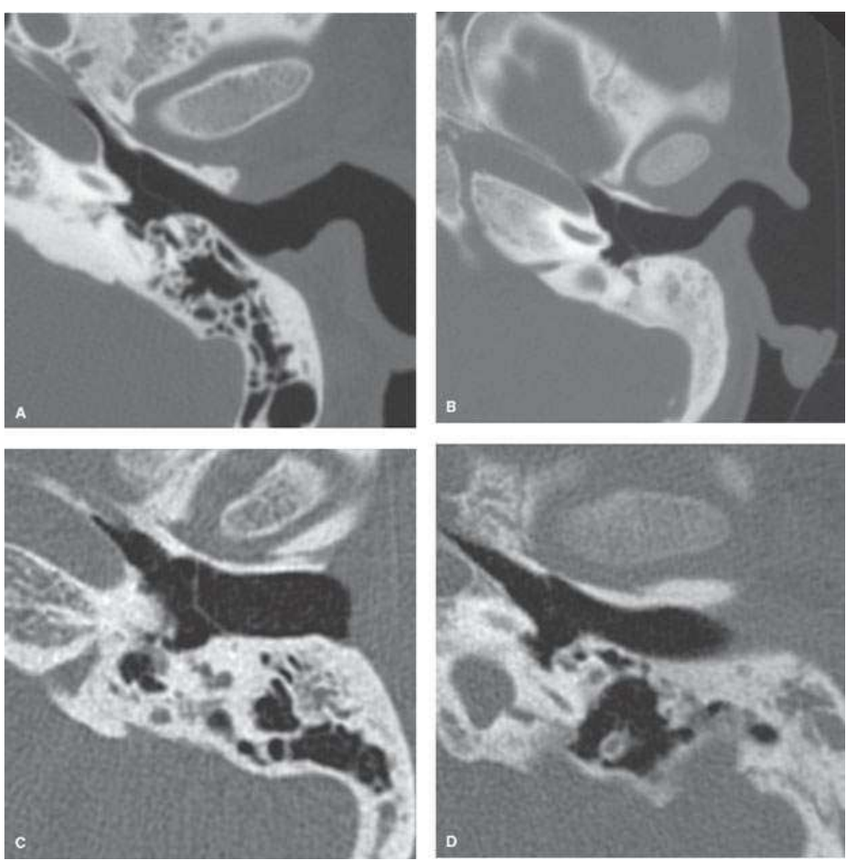

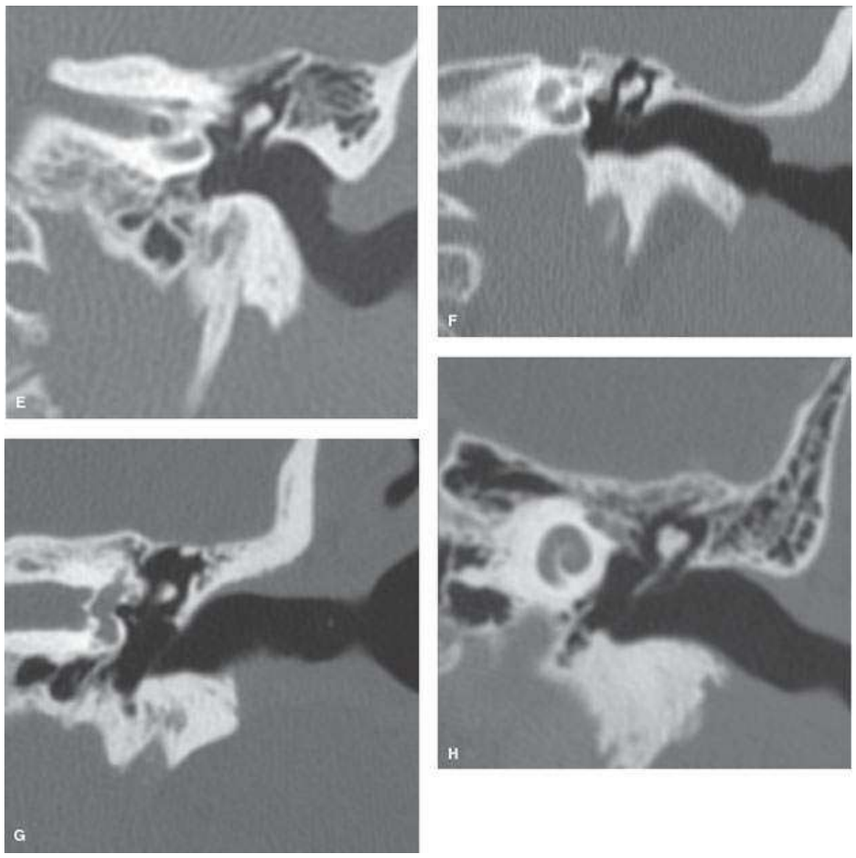

FIGURE 104.23. Normal variants of the external auditory canal regarding length, size, and slope on axial **(A–D)** and coronal **(E–H)** computed tomography images.

Ossicular motion is controlled by the tensor tympani and stapedius muscles (Fig. 104.38). The tensor tympani is located within a semicanal lying superior and lateral to both the auditory tube and the intrapetrous segment of the internal carotid artery. The muscle traverses the anterior mesotympanum just inferior to the facial nerve. At the cochleariform process, the tendon of the tensor tympani extends laterally and eventually attaches to the long process of the malleus. The stapedius muscle ascends from its origin within the pyramidal eminence to attach to the stapes; its specific point of attachment to the stapes varies (posterior crus or head). The stapedius muscle may be seen within the bone of the pyramidal eminence on CT and MRI; its tendon may not be seen. The course and appearance of the tensor tympani muscle as seen on MRI and CT is discussed in the Mesotympanum section.

Inner Ear

The inner ear includes the cochlea, vestibule, and semicircular canals and related aqueducts. For purposes of general orientation, the cochlea is located anterior in the temporal bone and related to the carotid canal, while the vestibular system is posterior and related to the jugular vein (Fig. 104.3). The functional part of the inner ear is the membranous labyrinth. The membranous labyrinth is encased in a bony labyrinth formed from the otic capsule. The bony labyrinth has an endosteal and periosteal layer encasing a middle layer of very dense intrachondral and enchondral bone.

The long axis of the bony labyrinth runs parallel to the posterior surface of the petrous pyramid (Fig. 104.39) and is about 20 mm in length along this axis.23

Cochlea

Although the cochlea is said to have spiraling basal, middle, and apical turns, it really has two and a half turns; the apical turn is incomplete. The vertical axis of the cochlea is oriented perpendicular to the posterior surface of the petrous portion of the temporal bone and therefore to the long axis of the bony labyrinth. The turns of the cochlea spiral around a central core of bone called the modiolus. The cochlea is about 5 mm in height.6 The osseous spiral lamina projects outward from the modiolus, and the cochlear division of CN VIII enters the cochlea at a depression in the base of the modiolus known as the cochlear cribrose area (Fig. 104.40). The turns of the cochlea should be routinely visible on temporal bone CT studies. The modiolus and even the osseous spiral lamina are routinely visible on #1 mm contiguous sections at fields of view <10 to 11 cm24 (Fig. 104.12). The cochlear fluid normally appears slightly hyperintense to CSF on T1-weighted images and obviously bright on T2-weighted images. T2-weighted images with slice thickness of 2 to 3 mm and a field of view of #14 to 16 cm will routinely demonstrate the fluid in each of the cochlear turns and the modiolus. This anatomy is better seen on steady state 3 DFT acquisitions. The normal cochlear membranous labyrinth does not enhance (Fig. 104.41).

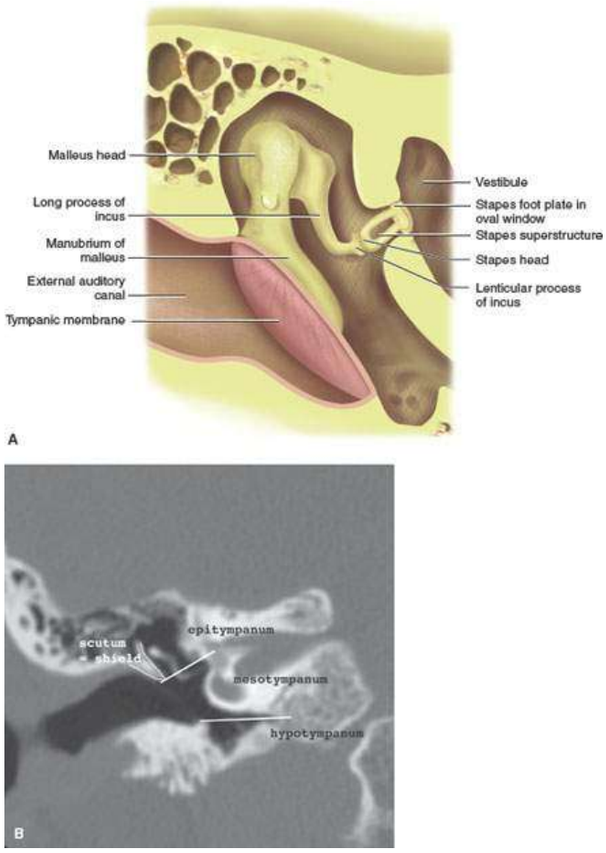

FIGURE 104.24. Anatomic drawing **(A)** and coronal computed tomography image **(B)** of the middle ear. The tympanic cavity is divided into three intercommunicating parts: the epitympanum, the mesotympanum, and the hypotympanum.

The cochlea communicates with the subarachnoid spaces via the cochlear aqueduct. The aqueduct opens into the posterior fossa just below the IAC and anterior to the jugular fossa on the inferior surface of the petrous pyramid. The aqueduct is 6 to 12 mm long and widest at its opening to the subarachnoid space near the glossopharyngeal nerve; its funnel-shaped cranial end tapers to <1 mm as it traverses the otic capsule to join the basal turn just inside the round window niche. The size of the aqueduct varies with age. Infantile aqueducts are larger than those in adults, the latter not obviously patent as seen on imaging near their point of entry to the cochlea although they remain microscopically patent. The position and other relationships of the round window were discussed in the Mesotympanum section. The cochlear aqueduct allows the perilymph to communicate with the CSF. Particulate matter can traverse the duct; thus, it is a potential source of inner ear infection. The role of the cochlear aqueduct in the spread of infection is supported by the observation that postmeningitic labyrinthitis usually shows ossification starting at the proximal part of the basal turn of the cochlea, close to the opening of the cochlear aqueduct (Fig. 104.42). Large cochlear aqueducts have been said to predispose a patient to perilymphatic oozing or fistula at the oval window. The size of the cochlear aqueduct is determined near its entry to the cochlea because its cranial end is highly variable in size (Fig. 104.43). However, enlargement of the cochlear aqueduct appears to be an exceedingly rare or perhaps even nonexistent malformation. It is important to recognize that even a radiographically normal cochlear aqueduct may be hyperpatent.25,26 The cochlear aqueduct is routinely visible on CT, although it may become imperceptible several millimeters prior to its entering the cochlea. The distal aqueduct is inconsistently visualized even on the highest-quality MR studies.

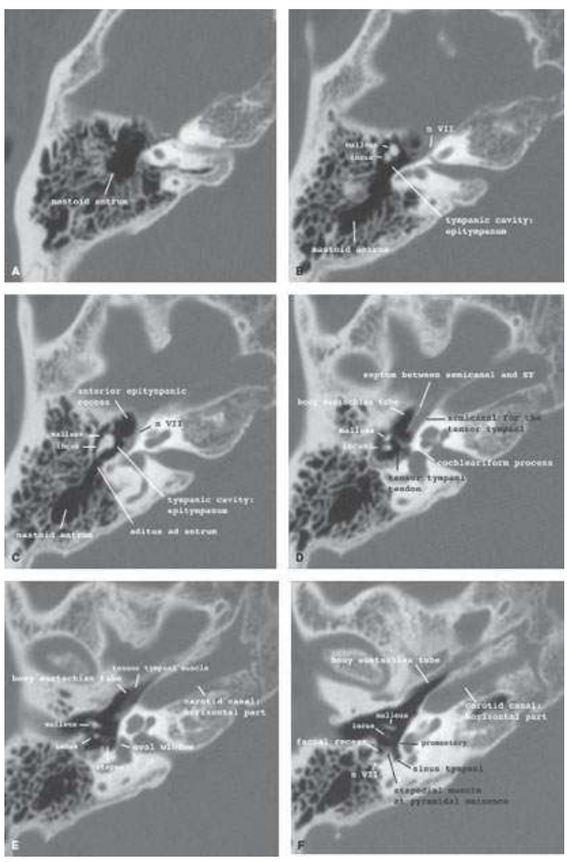

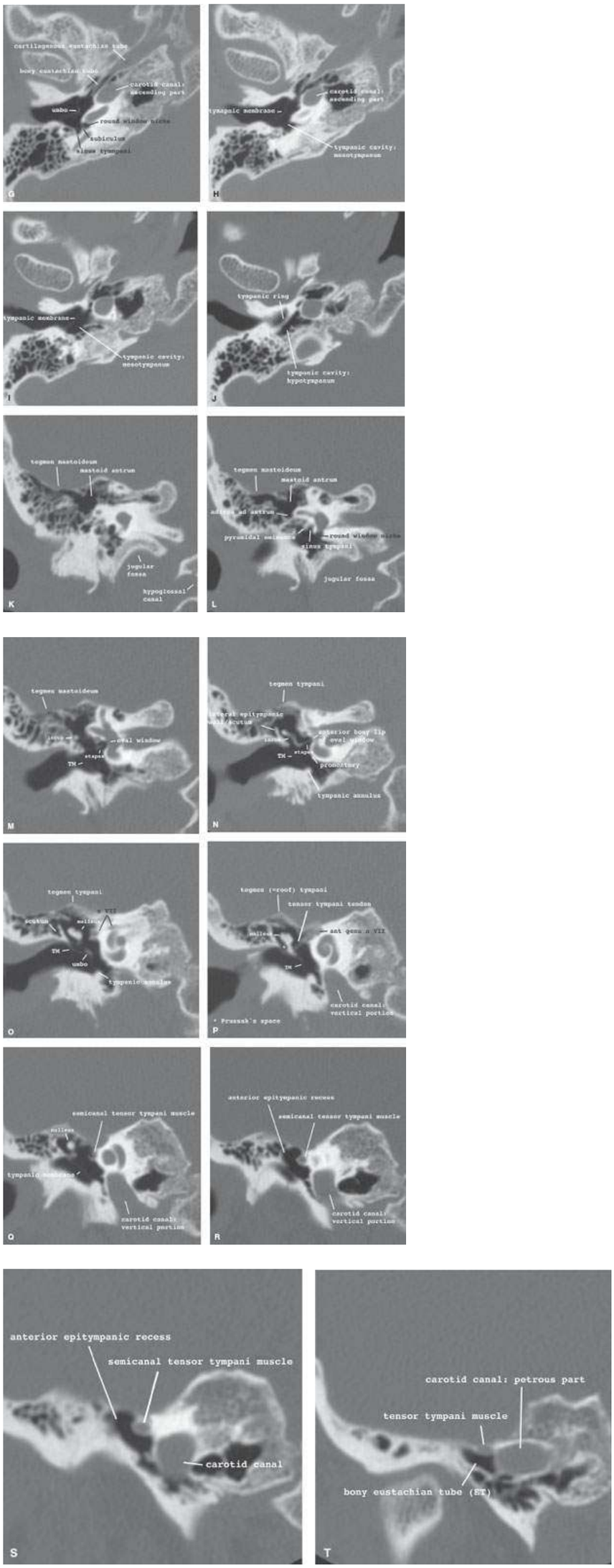

FIGURE 104.25. Normal anatomy of the middle ear. Axial **(A–J)** and coronal **(K–T)** computed tomography images.

Vestibular System

The superior, lateral or horizontal, and posterior semicircular canals house the respective vestibular ducts of the membranous labyrinth. The termination of the vestibular ducts within the saccule and utricle are housed within the vestibule. The vestibule is the central chamber of the bony labyrinth and its openings for the semicircular canals are located posteriorly, while the opening for the cochlea lies anteriorly. The oval window opens laterally into the mesotympanum (refer to the previous section), and the vestibular aqueduct joins the medial aspect of the vestibule before descending posteriorly and inferiorly (Fig. 104.44). The semicircular canals, normally 1 mm in diameter, enlarge to nearly double this size as they approach the vestibule; these are the ampullated ends of the semicircular canals. The nonampullated ends of the posterior and superior semicircular canal fuse forming the common crus. The nonampullated end of the LSCC remains independent. The canals are orthogonal to one another over and arc of 240 degrees (Figs. 104.12, 104.45, and 104.41). The superior semicircular canal is oriented perpendicular and the posterior semicircular canal parallel to the long axis of the temporal bone (Figs. 104.3D and 104.39). The bone over the semicircular canal is not visible on CT in about 7% of the population (Fig. 104.46). Such dehiscence suggests that there may be <0.1 mm of bone present, and that might be related to inner ear dysfunction. This is sometimes referred to as Tullio syndrome. The bone over the posterior semicircular canal may also be dehiscent but at a much lower frequency than that of the semicircular canal.

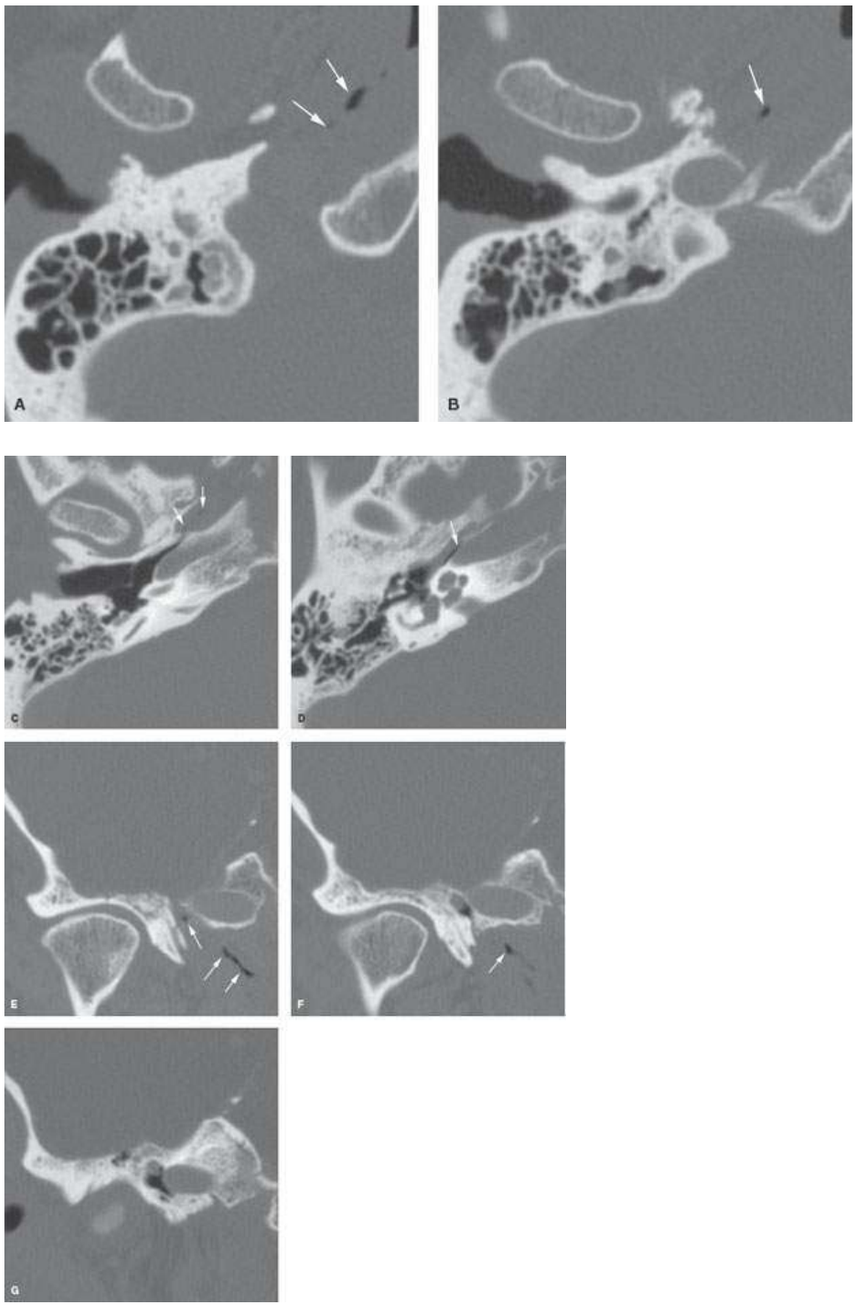

FIGURE 104.26. Axial **(A–D)** and Coronal **(E–G)** CT image of cartilaginous portion of the eustachian tube. The eustachian tube connects the middle ear to the nasopharynx. It contains a bony part, which can be seen anteriorly to the horizontal segment of the carotid artery, and a cartilaginous portion, which can occasionally be seen filled with air (*arrows*). It is very important to understand the anatomic relationships of the eustachian tube when evaluating a patient for unilateral middle ear disease.

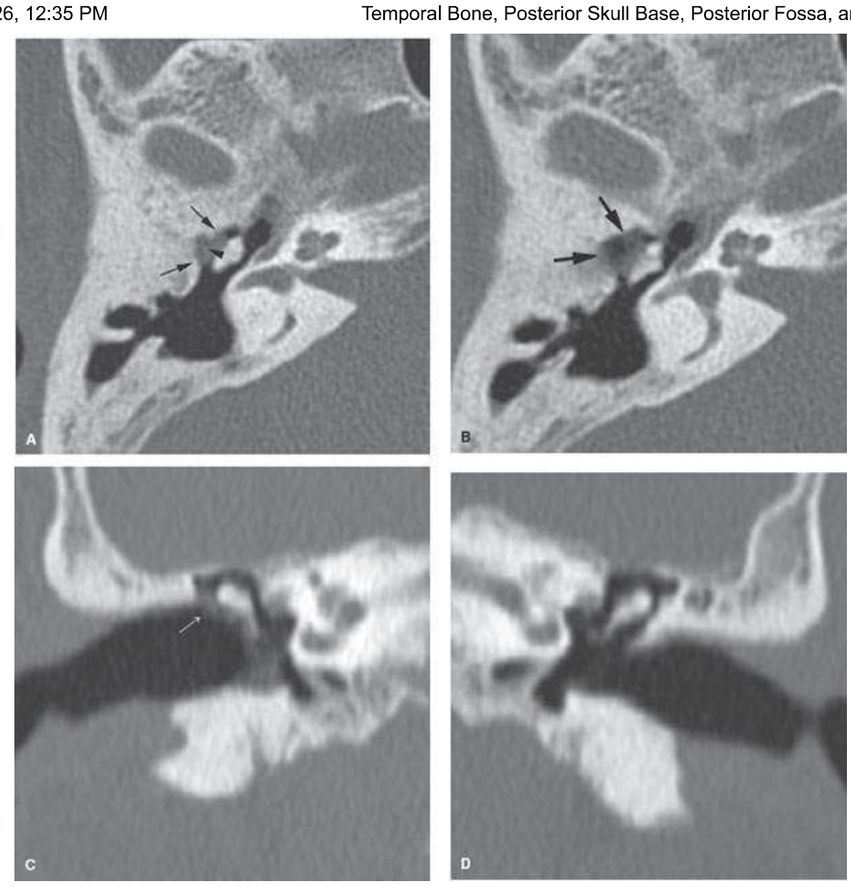

FIGURE 104.27. Pars flaccida cholesteatoma. On axial **(A, B)** and coronal **(C)** computed tomography (CT) images, a soft tissue mass (*arrowhead*) located in the Prussak space is seen. The mass has caused erosion of the scutum (*arrows*). In **(D)**, a normal coronal CT image of the left ear is shown.

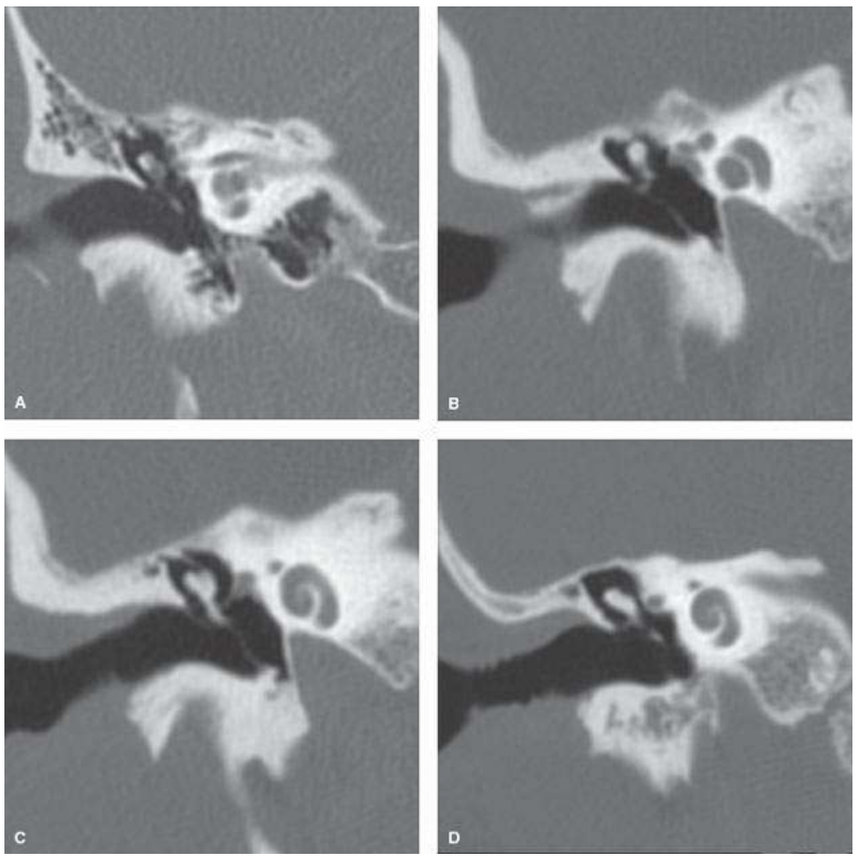

FIGURE 104.28. A–D: Anatomic variants of the scutum as seen on CT. The scutum differs in size and configuration but should always be pointed.

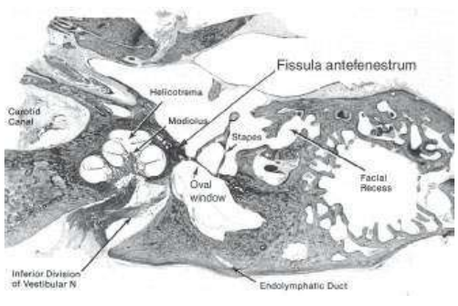

FIGURE 104.29. Microscopic image of the fissula ante fenestram.

The vestibular aqueduct is consistently found at its entrance to the posterior aspect of the vestibule parallel to the common crus. The course of the aqueduct becomes more variable through the remainder of the otic capsule and petrous portion of the temporal bone. The aqueduct runs a nearly straight course to the endolymphatic sac during early fetal development; however, because of disproportionate growth of the otic capsule and posterior fossa, it normally has a lateral and inferior curve. The course of the vestibular aqueduct can be even more profoundly altered by variations in temporal bone pneumatization and variations in the anatomy of the jugular vein–sigmoid sinus junction (Fig. 104.47). The duct tends to be 1 to 2 mm in diameter; ducts >1.5 mm in diameter are definitely abnormal. As a "screening" observation, the diameter should not exceed the diameter of the adjacent semicircular canal. The length is variable. The vestibular aqueduct of the bony labyrinth contains the endolymphatic duct of the membranous labyrinth; the duct terminates at the endolymphatic sac. The sac is typically located under a bony covering called the operculum, about 10 mm posterior to the opening of the IAC and about 10 mm inferior to the sulcus of the superior petrosal sinus.23 There is little question that an enlarged (.1.5 mm) vestibular aqueduct is an indicator of developmental abnormality of the membranous labyrinth. The predictive value of a small or not visualized labyrinth in both acquired and congenital disease manifest by possible endolymphatic hydrops is more controversial and will be discussed later in other chapters.

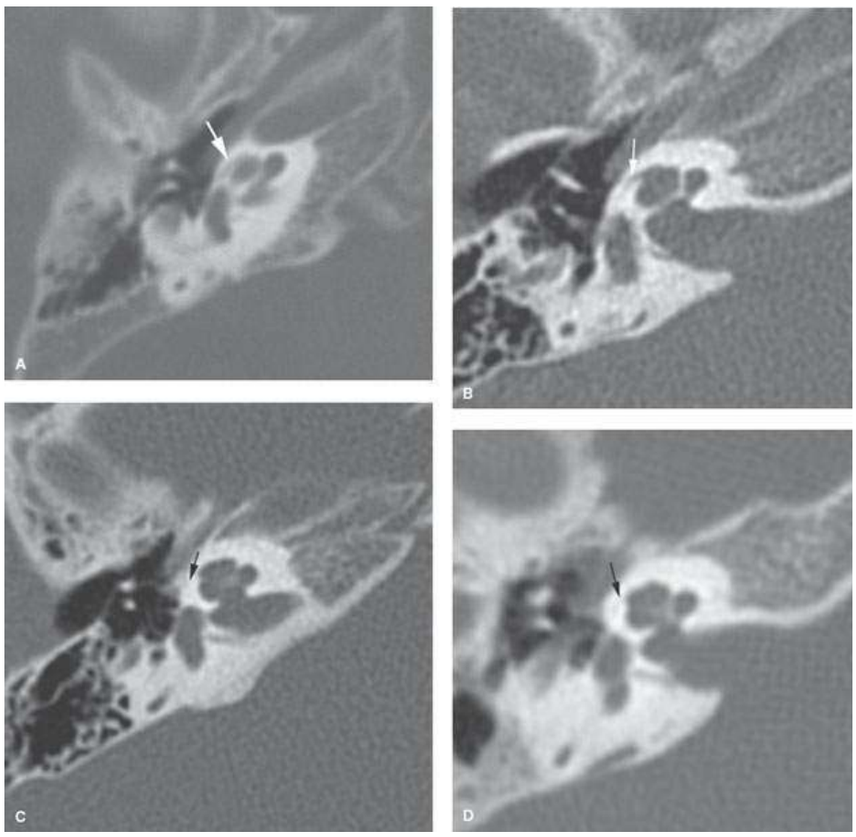

FIGURE 104.30. The fissula ante fenestram (*arrows*) can be identified consistently in children but become less clear with age. Shown are images of a 2-month-old baby **(A)**, a 4-year-old child **(B)**, an 8-year-old child **(C)**, and a 9-year-old child **(D)**. It can be seen into early adult years.

The normal vestibular aqueduct is consistently visualized on routine temporal bone CT studies. It can be demonstrated on T2-weighted high-resolution fast spin echo MR examinations but is much easier to see on 3DFT steady state images done with as small a field of view (#20 cm) as possible. Such high-resolution imaging is also making visualization of the macula possible.

Pneumatization of the Temporal Bone

The middle ear cleft and mastoid antrum are developed by extension of the auditory tube mucosa in utero and therefore prior to the stimulus for actual pneumatization (Fig. 104.48). The degree of aeration of the mastoid is variable but far less so than the development of air cells in the remainder of the temporal bone (Fig. 104.49). The patterns and extent of aeration can influence the surgical approach to the temporal bone; for example, narrow or sclerotic mastoid may preclude a posterior approach to the middle ear via the facial recess. The tracts of normal pneumatization can also be conduits for spread of pathology such as cholesteatoma, and normal air cells can be the substrate for developing pathology such as cholesterolosis or mucocele of the petrous apex. A basic understanding of the process of pneumatization is therefore more than an academic exercise.

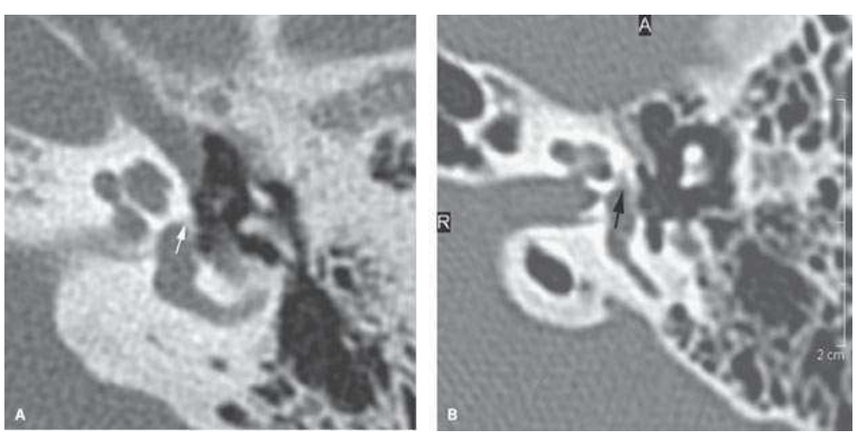

FIGURE 104.31. Two patients with a subtle osteolytic change (*arrow* in A) and more extensive lytic change (*arrow* in B) at the location of the fissula ante fenestrum, consistent with early otosclerosis.

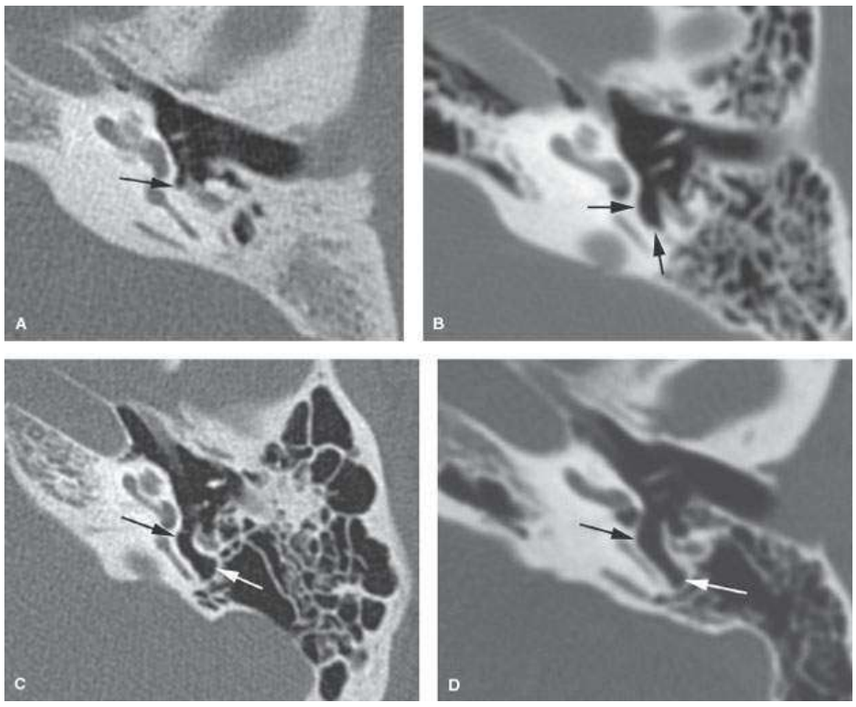

FIGURE 104.32. Variations in the dimensions of the tympanic sinus (*arrow*s in A–D)**.** A deep sinus may extend posterior to the pyramidal eminence and facial nerve canal **(C, D).**

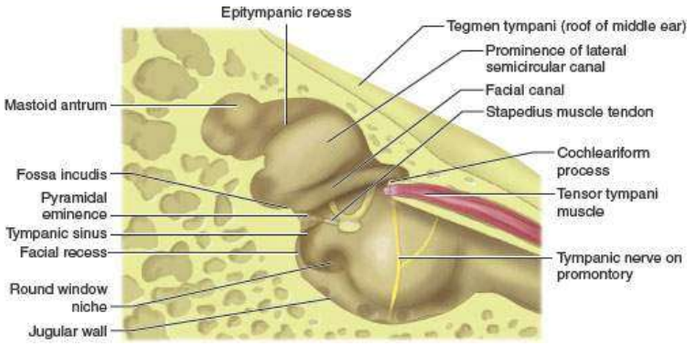

FIGURE 104.33. Anatomic drawing of the middle ear showing the ridges and depressions on the posterior mesotympanum wall: the sinus tympani, the pyramidal eminence, the facial recess, and the fossa incudis**.**

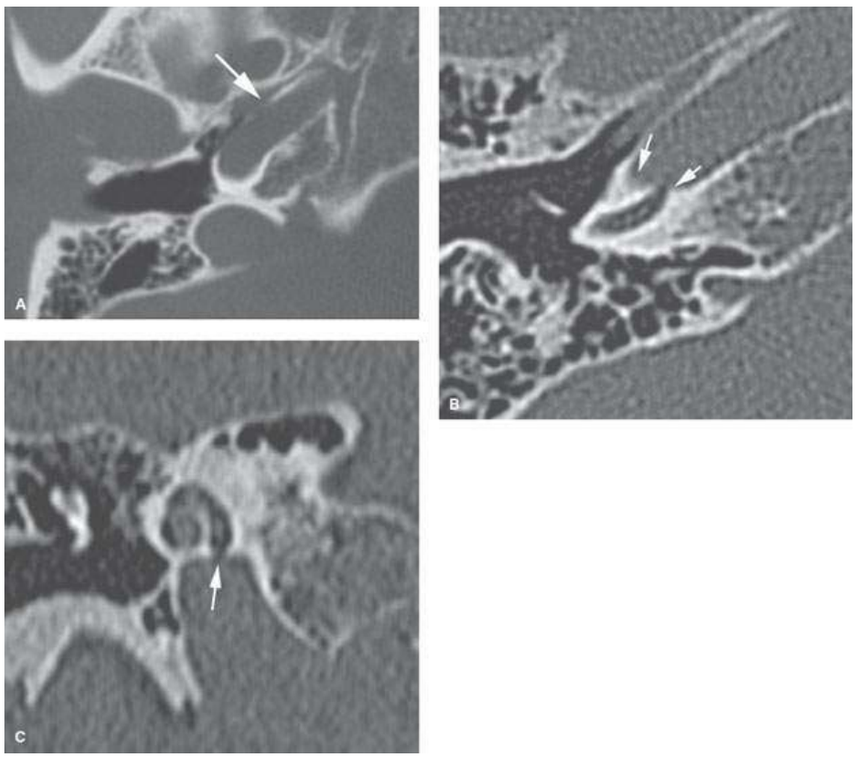

FIGURE 104.34. A: Anatomic variant of the carotid canal. Axial computed tomography image showing a focal dehiscence in the bony plate covering the carotid artery**. B, C:** Dehiscence between the carotid canal and cochlear basal turn that might be a cause of pulse synchronous tinnitus**.**

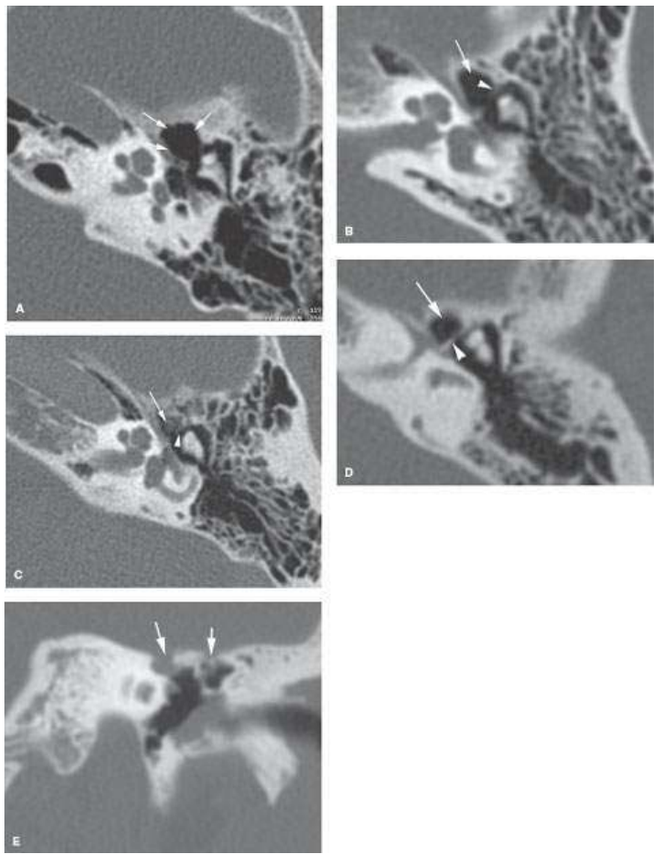

FIGURE 104.35. A–D: Anterior epitympanic recess (*arrows*). On axial computed tomography (CT) images, it is well seen that the recess differs in size. The recess may be separated from the epitympanum by a fibrous or bony septum (*arrowheads*). **E:** Dehiscence of the tegmen tympani (*arrows*) is common in the area of the anterior epitympanic recess and first genu of the facial nerve. The coronal CT image shows dehiscence of the tegmen in that area caused by arachnoid granulations.

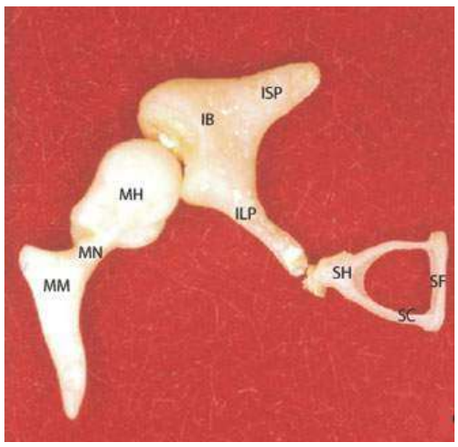

FIGURE 104.36. Photograph of an anatomic specimen showing the relationship between the three ossicles—the malleus head (MH), neck (MN), and manubrium (MM), respectively; the incus body (IB), short process (ISP), and long process (ILP), respectively; and the stapes head (SH), crus (SC), and foot plate (SF), respectively.

The petrous bone and part of the mastoid have an enchondral cartilaginous origin. The squamous portion of the temporal bone is of membranous origin and gives rise to the anterolateral portion of the mastoid. The internal junction between the two is called the petrosquamosal septum, also known as the Koerner septum. Externally, this junction is manifest by the petromastoid fissure that is obliterated in early adulthood. The Koerner septum is a bony plate of variable thickness and length oriented obliquely to the long axis of the temporal bone. It is usually easy to recognize on axial and coronal CT images. The septum may be absent in a well-pneumatized bone. Normally, it separates the mastoid antrum and mastoid air cells. Surgically, it can be mistaken for the medial wall of the antrum.

Air cell formation in the temporal bone begins with an aerated central (pneumatization) tract that first forms the mastoid antrum and then continues growing downward into the mastoid process. All other air cells develop as branches or extensions of this central tract. Those extending into the mastoid area include cells bordering the tegmen; those extending into the sinodural angle (posteriorly and superiorly); cells lying lateral, medial, and posterior to the sigmoid sinus; cells around the descending facial canal; and mastoid tip cells. Named groups of air cells in the petrous portion of the temporal bone include supralabyrinthine, infralabyrinthine, peritubal (i.e., along the auditory tube), and apical. Accessory cells may extend into the zygomatic (Fig. 104.50), squamous, occipital, and styloid regions.

Five main tracts of pneumatization are recognized by otologic surgeons, and all of them intercommunicate. These serve the otologic surgeon as routes to various portions of the temporal bone. They are also conduits for the spread of pathology. The tracts include the following:

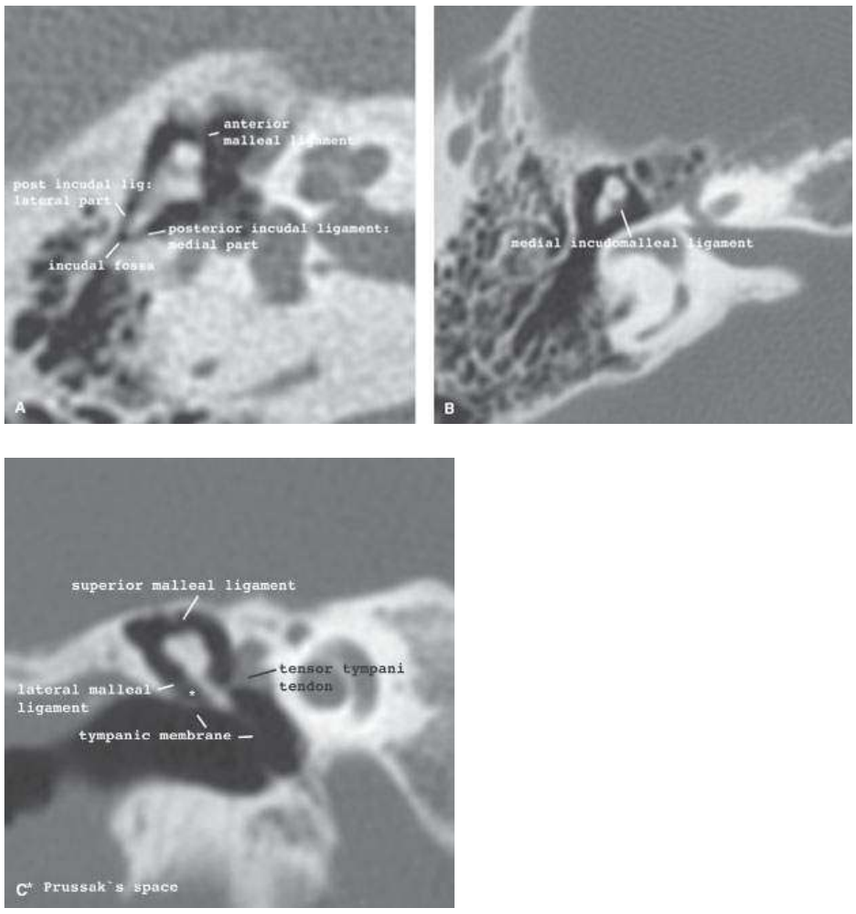

FIGURE 104.37. Normal anatomy and variable appearance of the ossicular ligaments. **A, B:** On axial images, the anterior malleal, medial incudomalleal, and posterior incudal ligament can be discerned. **C:** The superior and lateral malleal ligaments are best seen on coronal images.

- A posterosuperior tract extending to the sinodural angle and aerating the bone at the interface of the posterior and middle cranial fossae. This tract normally ends at the IAC but may reach the supralabyrinthine and apical cells.
- A posterior and medial tract that runs just inferior to the one just described, basically paralleling the posterior surface of the petrous bone. It can communicate with both the supralabyrinthine and infralabyrinthine cells.
- A subarcuate tract extending from the mastoid through the arc of the superior semicircular canal, potentially connecting with the apical region.
- Perilabyrinthine tracts originating in the epitympanum and hypotympanum.
- A peritubal tract arising from the auditory tube or anterior hypotympanum. These generally run anterior and lateral to the carotid and may reach the apical region.

All of these variations are easily recognized on CT and are difficult to distinguish on MRI. In fact, differences in mastoid and petrous aeration commonly account for missed and overdiagnosed pathologies on MRI (Fig. 104.16). The mucosa in the air cells is not normally visualized or enhanced on CT and MRI. Venous lakes and fatty marrow in the petrous apex are sometimes mistaken for disease air cells on MRI studies.

Facial Nerve

The facial nerve has a convoluted course from the brain stem to its exit from the skull base at the stylomastoid foramen. It is useful to consider the nerve in several segments, including (a) a cisternal segment from its root entry zone at the pontomedullary junction to the IAC, (b) a canalicular segment within the IAC, (c) the labyrinthine segment from the Bill bar to the anterior (first) genu (geniculate ganglion), (d) the anterior genu, (e) the tympanic (horizontal) segment running from the anterior to the posterior (second) genu, and (f) the mastoid (descending) portion from the second genu to the stylomastoid foramen (Figs. 104.3E, 104.8, and 104.51). The nerve passes through a fat pad below the stylomastoid foramen before turning anterior and laterally to enter the parotid gland. The course of the nerve beyond the stylomastoid foramen and through the parotid is discussed more fully with anatomy pathology related to the parotid gland and perineural spread of cutaneous malignancies.

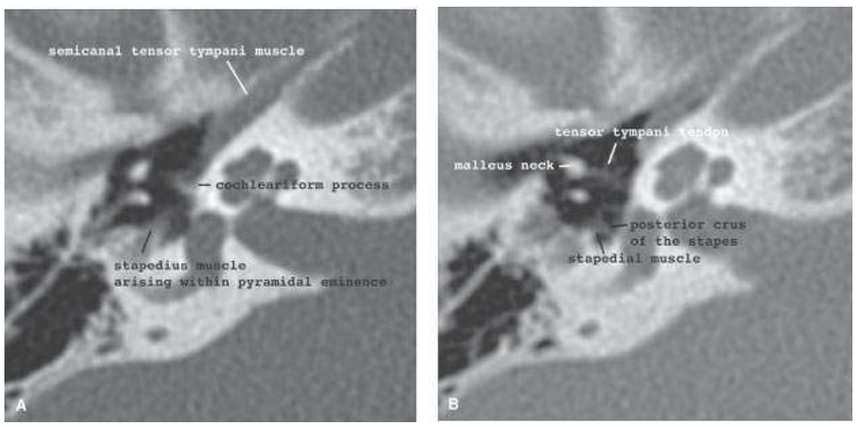

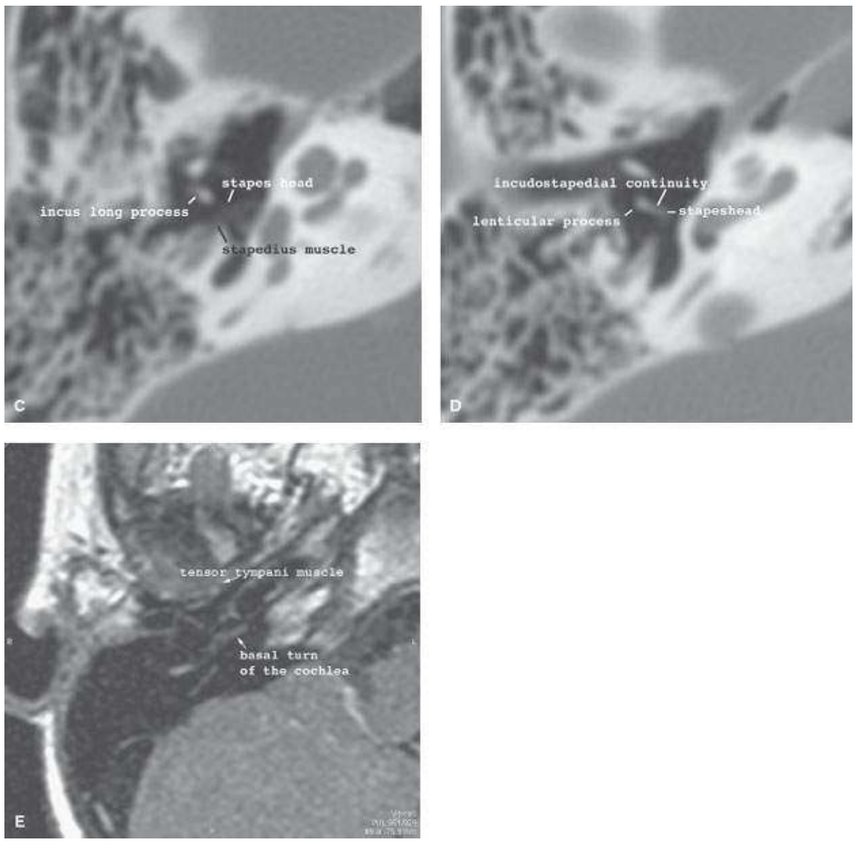

FIGURE 104.38. Normal appearance of the ossicular muscles. The tensor tympani muscle runs from the auditory tube to the long process of the malleus **(A, B).** The stapedial muscle originates at the pyramidal eminence and attaches to the stapes posterior crus **(A, B)** or head **(C, D).** The tensor tympani is consistently visible on magnetic resonance imaging **(E).**

The nucleus of the facial nerve is situated in the dorsal brain stem near the pontomedullary junction (Fig. 104.52 and 104.53). The nerve fibers loop medially around the CN VI nucleus, creating a "bump" in the floor of the fourth ventricle called the facial colliculus. The nerve roots exit the brain stem at the pontomedullary junction. The nerve travels superiorly and laterally to enter the anterosuperior aspect of the IAC. It exits the canal just anterior to the Bill bar. The labyrinthine segment, between this point of exit and the geniculate ganglion, is the narrowest portion of the facial canal. The nerve then does a hairpin turn at the anterior genu. Fibers for the greater superficial petrosal nerve are housed by the geniculate ganglion and exit at this point sometimes called the facial hiatus.

From the anterior genu to the stylomastoid foramen, the facial nerve is related to the middle ear; it first courses posteriorly in its own bony canal beneath the LSCC and above the oval window. Thus, on a coronal image, the tympanic segment of CN VII can easily be picked up just beneath the LSCC. Toward the posterior aspect of the tympanic cavity, the nerve turns inferiorly at nearly a right angle (posterior or second genu).

The mastoid or descending segment of the nerve descends from the second or posterior genu in a bony canal that is usually situated just posterior to the pyramidal eminence and facial recess (refer to the Mesotympanum section). The chorda tympani and nerve to the stapedius muscle usually originate from this descending mastoid segment.

There are some important variations of the anatomy just discussed (Fig. 104.54). The tympanic segment of the nerve may run anterior and inferior to the oval window or hang free within the upper mesotympanum. Dehiscence of the bony canal is common along the tympanic and mastoid segments. Multiple (branching) descending canals may make up the mastoid segment. The horizontal semicircular canal is used as a surgical landmark to define the course of the mastoid segment of the facial nerve. Normally, the mastoid segment is located inferior and medial to the level of the semicircular canal. The size of the facial hiatus (point of exit of the greater superficial petrosal nerve from the geniculate ganglion) is high variable.

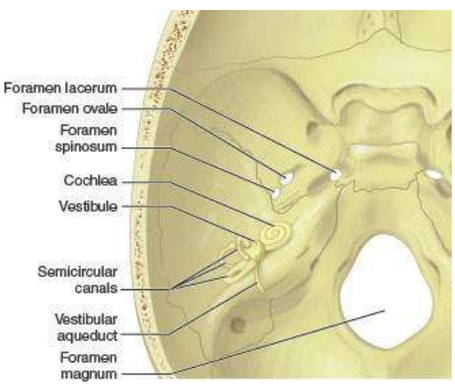

FIGURE 104.39. Anatomic drawing showing the orientation of the inner ear within the temporal bone.

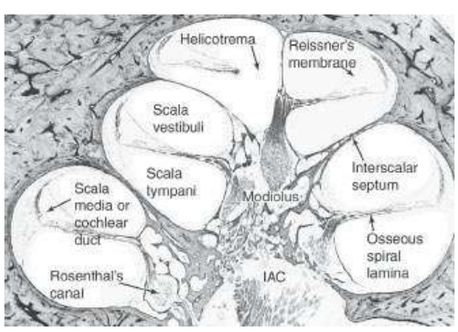

FIGURE 104.40. Mid modiolar cross section of the cochlea. The cochlea has 21/2 turns spiraling around the modiolus. The cochlear lumen is divided into the scala tympani and scala vestibuli by the osseous spiral lamina. Laterally, the Reissner membrane divides the scala media from the scala vestibuli.

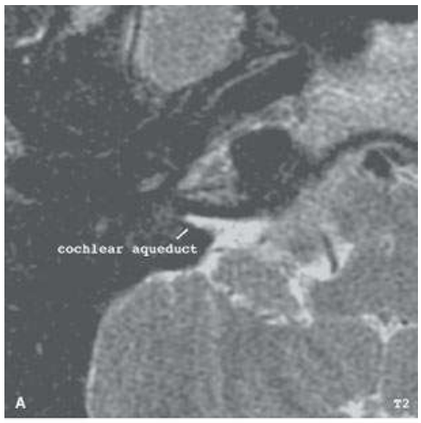

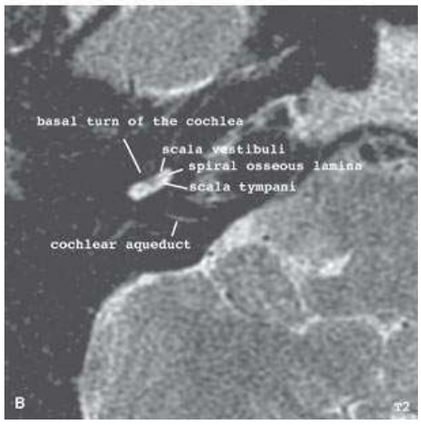

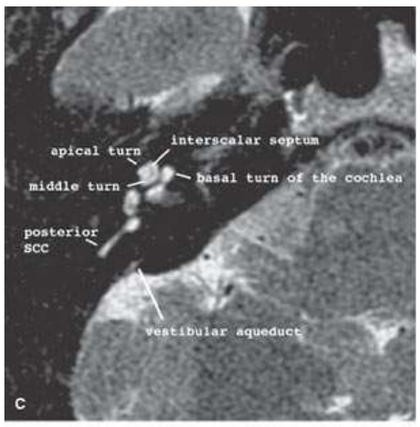

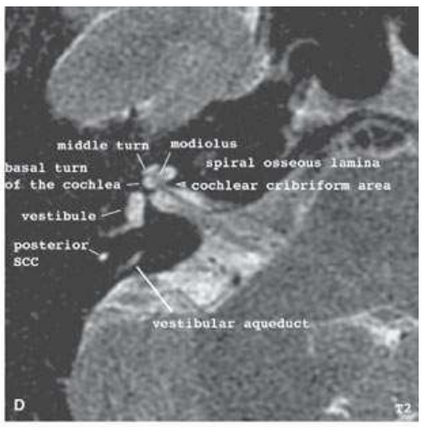

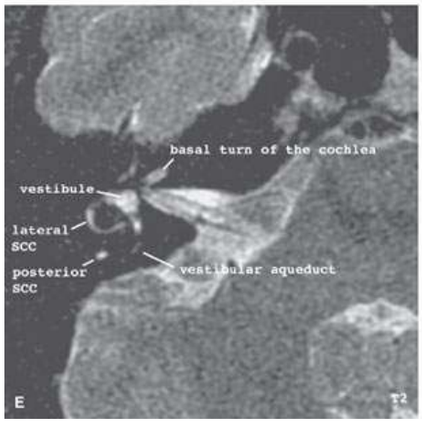

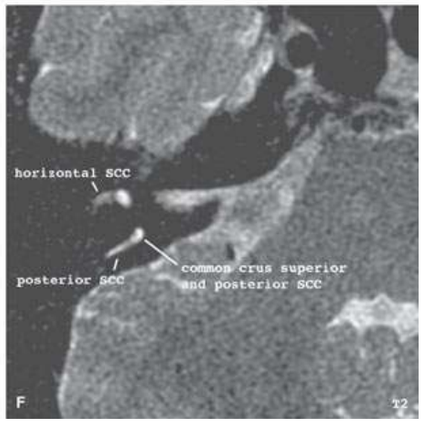

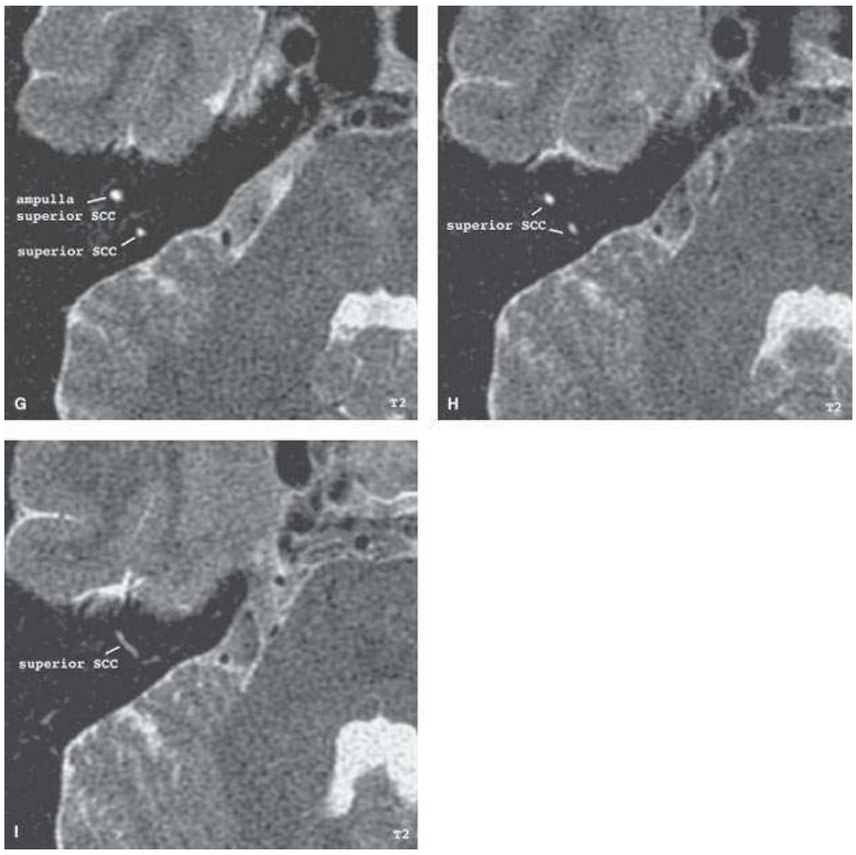

FIGURE 104.41. A–E: Axial T2-weighted magnetic resonance images of the normal anatomy of the inner ear.

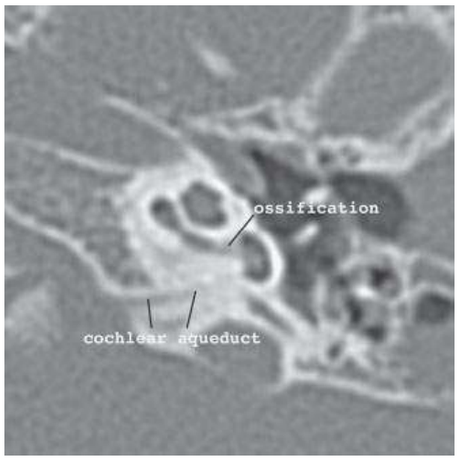

FIGURE 104.42. Ossifying labyrinthitis. In postmeningitic labyrinthitis, cochlear ossification often starts at the proximal basal turn of the cochlea, which is in close relationship with the cochlear aqueduct.

As with other CNs, a perineural vascular plexus accompanies CN VII. This tends to be most prominent at the anterior genu but is also present at the second genu and in the mastoid segment (Fig. 104.52E–L). Enhancement of this vascular plexus is a common normal variant seen on gadolinium-enhanced MRI. Such enhancement is usually symmetric; however, some asymmetry is not uncommon, and only some segments of this perineural plexus may enhance.

Vestibulocochlear Nerve

The vestibular and cochlear nuclei are found in the brain stem at the pontomedullary junction. The cochlear nuclei are located lateral to the inferior cerebellar peduncle. The vestibular nuclei are located medial to the inferior cerebellar peduncle as they lie just below the more lateral aspect of the floor of the fourth ventricle (Figs. 104.13 and 104.52). The vestibulocochlear nerve exits the brain stem anterior and laterally, its root entry zone being just posterior to that of the facial nerve, and angles slightly cephalad as it travels through the lower CPA cistern to reach the porus acusticus (meatus) of the IAC. The specific arrangement of CNs VII and VIII in the IAC and their course to their “end organs” is described in the prior Petrous Bone and Inner Ear sections.

The vestibulocochlear and facial nerves are routinely visible on MRI from their root entry zones at the pontomedullary junction to the fundus of the IAC. On T1-weighted images, they appear as strands of tissue isointense to brain within the darker CSF of the CPA and IAC. An adjacent petrosal vein, or looping AICA, is occasionally visible on T1-weighted images, especially those done with gadolinium enhancement. Fast spin echo images done with sections #3 mm in thickness and a field of view of 14 to 16 cm routinely show these nerves as thin, low-intensity bands within the bright CSF. These high-resolution T2-weighted images also show the normal AICA, AICA loops in the IAC or the petrosal vein, and the point of entry of the cochlear and vestibular nerves to their respective end organs more frequently than T1-weighted images (Fig. 104.2). The cisternal and IAC segments of the facial and vestibulocochlear nerves do not enhance. The preferred MRI sequence for showing the nerves anatomically is a 3DFT steady state image with #1 mm section thickness. The nerves can then be studied in any plane, with the best being the sagittal or oblique sagittal relative to the IAC and axial. The normal cochlear nerve as seen on these images measures 1.21/20.2 mm in the mid to distal IAC and 1.8 1/2 0.2 mm at the porus acusticus. The normal vestibular and facial nerves measure 1.5 1/2 0.2 mm and 1.1 1/2 0.2 mm, respectively. Normative measurements do not differ significantly in the adult and pediatric age ranges[27,28] (Figs. 104.13).

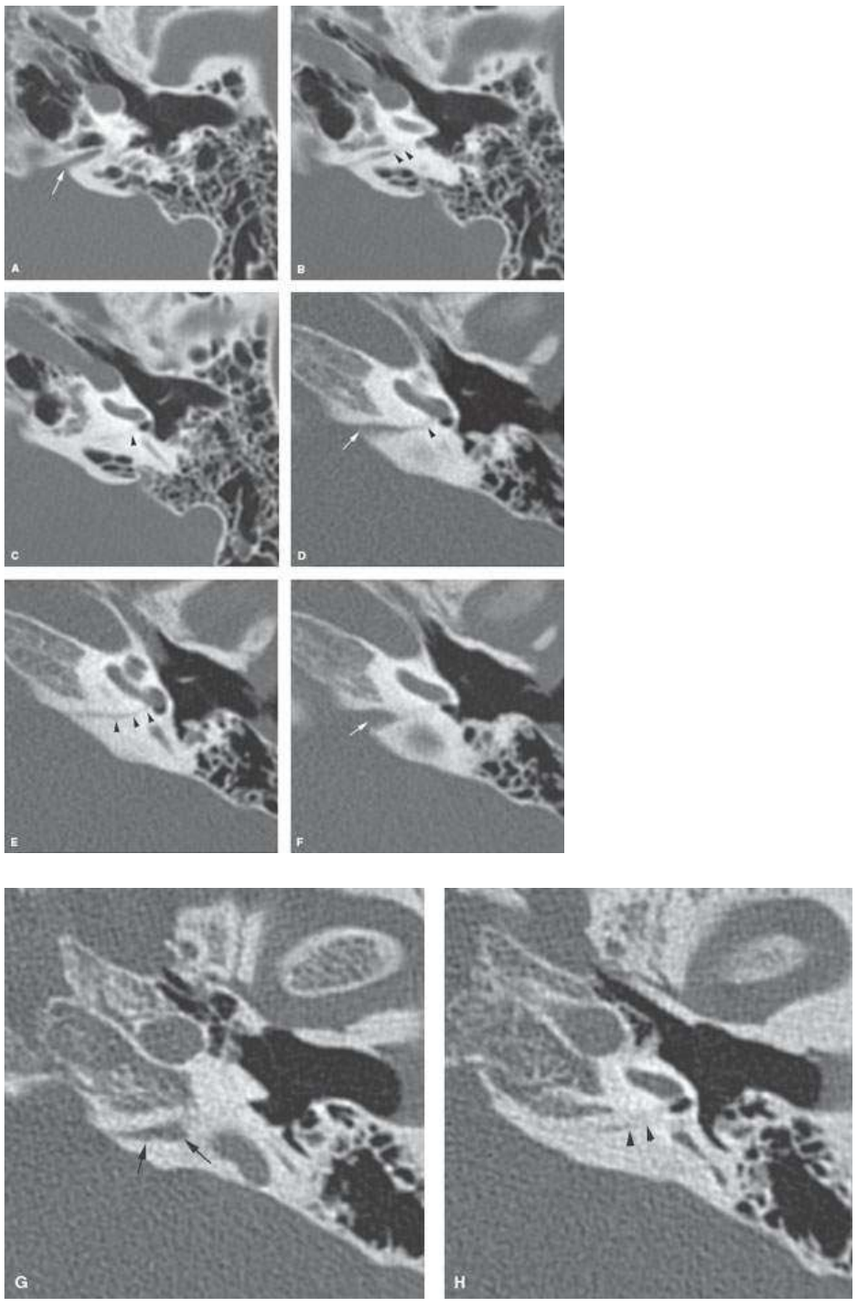

FIGURE 104.43. Variable appearance of the cochlear aqueduct**. A–H:** The size and shape of the more cranial end (*arrows*) of the cochlear aqueduct can be small **(A)** or wider (D and F) and funnel shaped or tubular **(G).** Therefore, the size has to be determined near its entry to the cochlear, and the duct almost tapers to invisible in the vast majority of patients (*arrowheads*) as it approaches its cochlear end; shows it as visibly patent as it will be seen and not be considered enlarged (which is quite rare)**.**

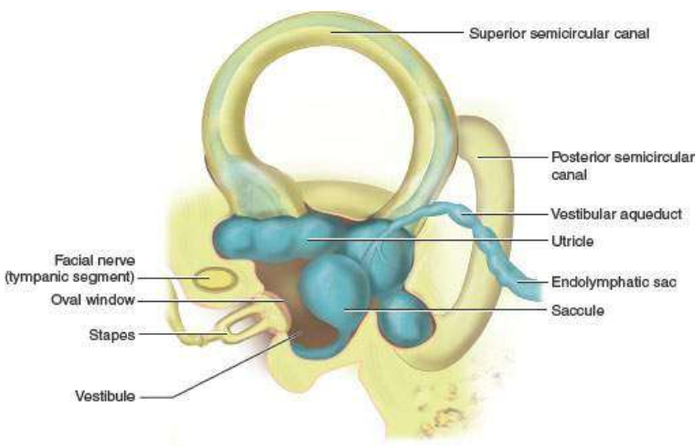

FIGURE 104.44. Anatomic drawing of the vestibular system**.** The horizontal, posterior, and superior semicircular canals terminate in the vestibule**.** The vestibule contains the utricle and saccule and is connected to the vestibular aqueduct, the middle ear (by the oval window), and the cochlea**.**

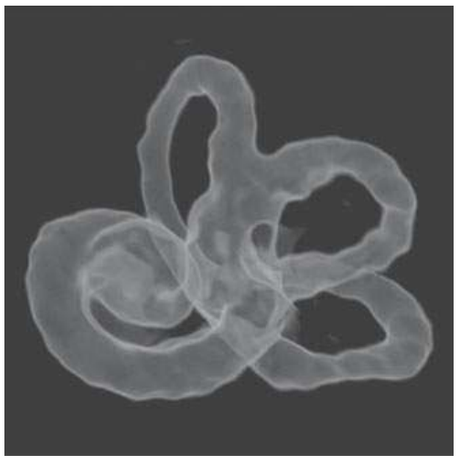

FIGURE 104.45. Three-dimensional computed tomography reconstruction of the cochleovestibular system. The semicircular canals are positioned orthogonal to one another and show enlargement at their entrance into the vestibule (ampullary ends).

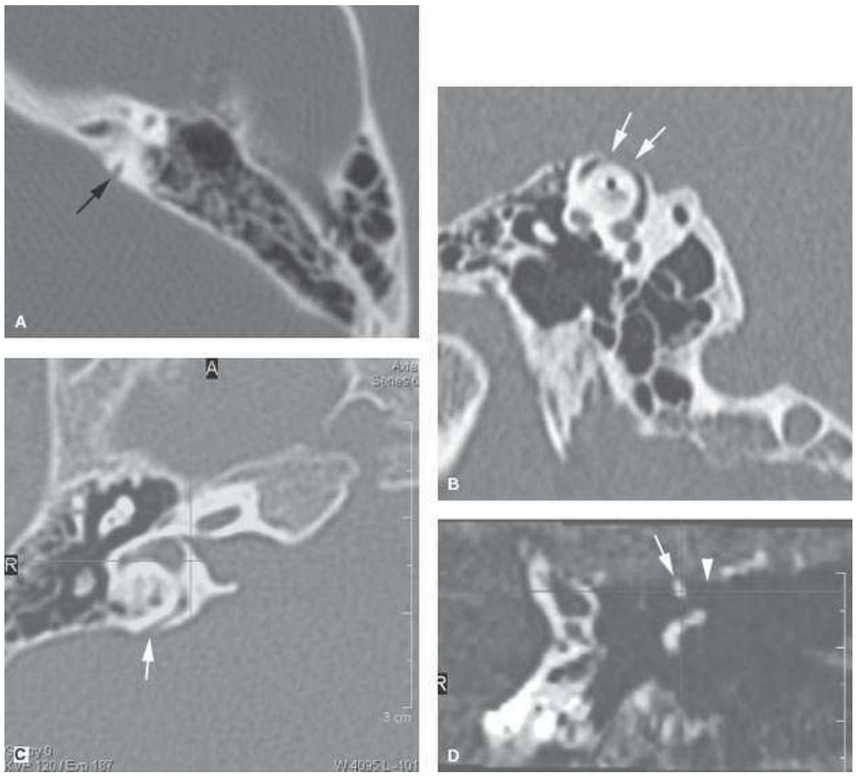

FIGURE 104.46. Images in four patients with dehiscent semicircular canals (*arrows*) that might be the cause of inner ear dysfunction. **A:** Axial section of a dehiscent superior semicircular canal (SSCC). **B:** Oblique reformatted computed tomography (CT) image showing dehiscence of the SSCC. **C:** CT of a dehiscent posterior semicircular canal. **D:** Magnetic resonance imaging in the coronal plane. The arrowhead indicates the roof of the temporal bone.

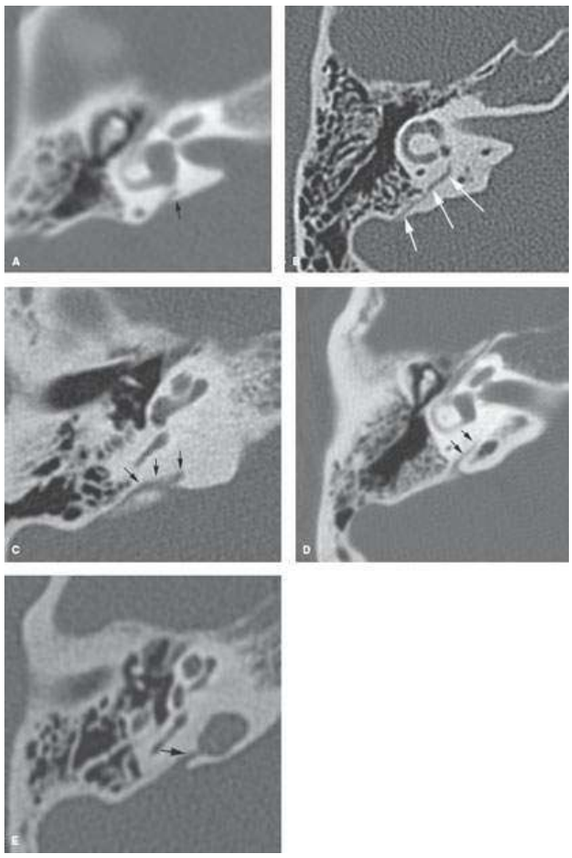

FIGURE 104.47. Normal variants of the vestibular aqueduct**.** The course and width of the vestibular aqueduct is variable. It can be short and narrow **(A)**, long and straight **(B)**, long and curved **(C)**, or altered by variations of mastoid pneumatization **(D)** or the jugular vein **(E).**

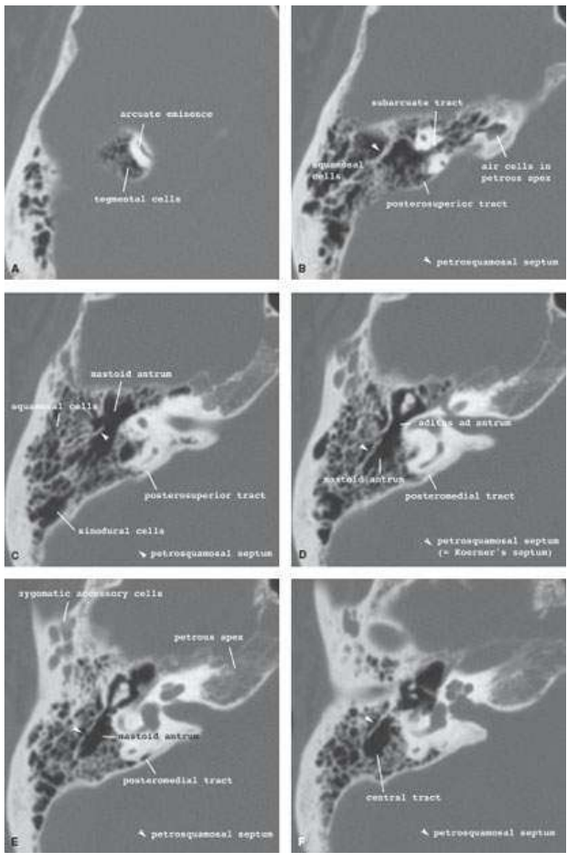

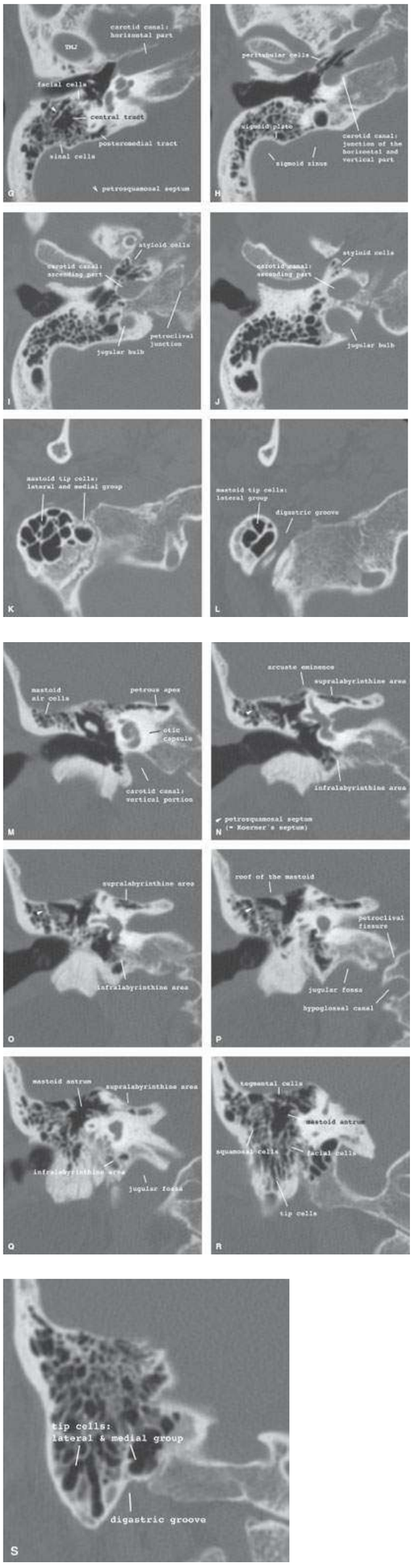

FIGURE 104.48. Normal anatomy of the mastoid pneumatization on axial **(A–G)** and coronal (M-S) CT Sections. Several pneumatization tracts extend from the central mastoid antrum.

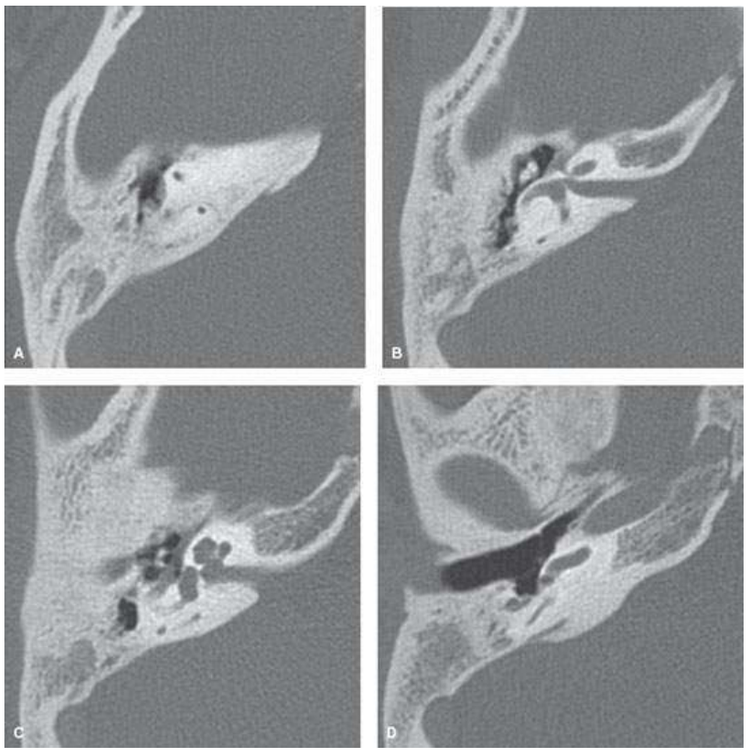

FIGURE 104.49. The degree of aeration of the mastoid is variable. In this underdeveloped mastoid **(A–D)**, only the antrum and upper central tract is developed. A well-pneumatized mastoid shows all pneumatization tracts as in Figure 104.48.

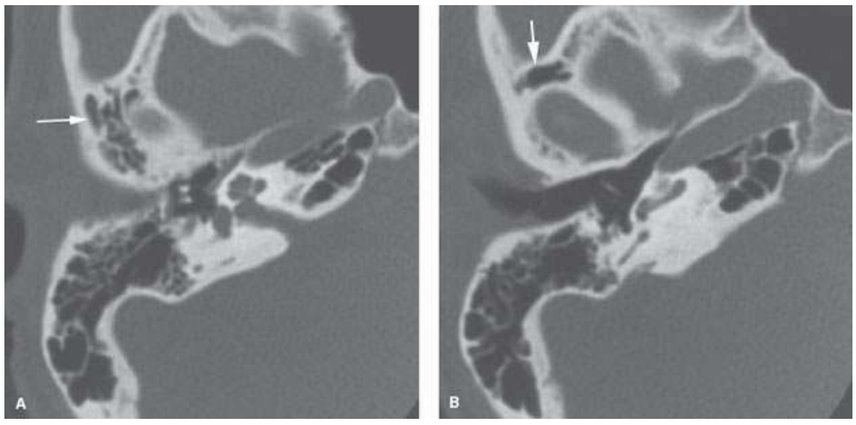

FIGURE 104.50. Mastoid aeration variations. Accessory air cells can be seen in the zygomatic root **(A, B)**.

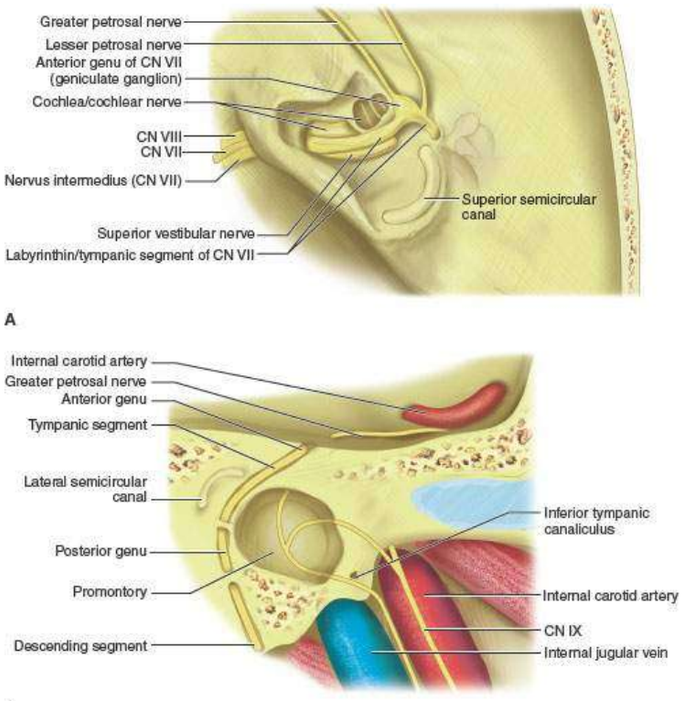

FIGURE 104.51. Anatomic drawing of facial nerve in its course through the temporal bone. **A**: The nerve entering the temporal bone in the internal auditory canal, where it is called the canalicular segment. At the level of the Bill bar, it becomes the labyrinthine segment running to the anterior ganglion. From the anterior genu, fibers for the greater superficial petrosal nerve exit. At this point, the nerve takes a sharp turn posteriorly to form the tympanic segment. **B**: The tympanic segment shows a horizontal course through the middle ear cavity and runs to the posterior genu. At this point, the nerve makes a second sharp turn to descend vertically through the mastoid.

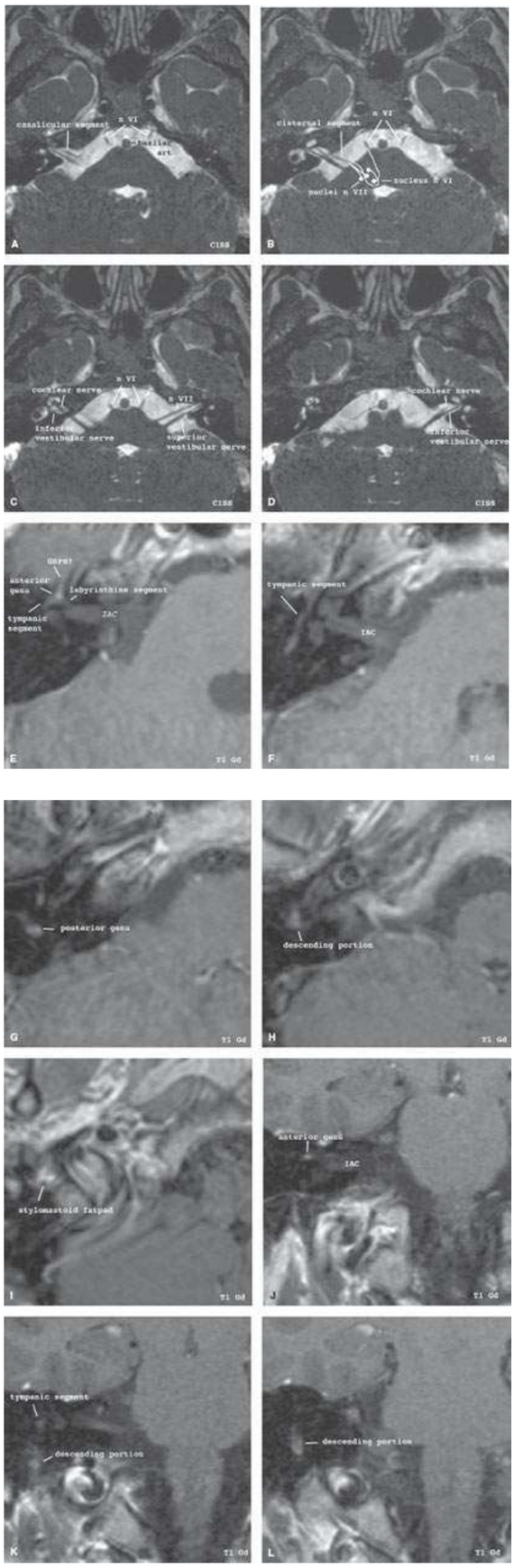

FIGURE 104.52. Normal anatomy of the facial nerve on magnetic resonance imaging. **A–D**: The facial nerve originates in the dorsal brain stem near the pontomedullary junction. The cisternal and canalicular segments are well seen on thin slice volume T2-weighted images (e.g., CISS, FIESTA, and three-dimensional turbo spin echo). **E–L**: The tympanic and labyrinthine segment of the facial nerve can be seen on axial and coronal T1-weighted images. Enhancement at the anterior genu and in the mastoid and descending segments is due to an accompanying vascular plexus.

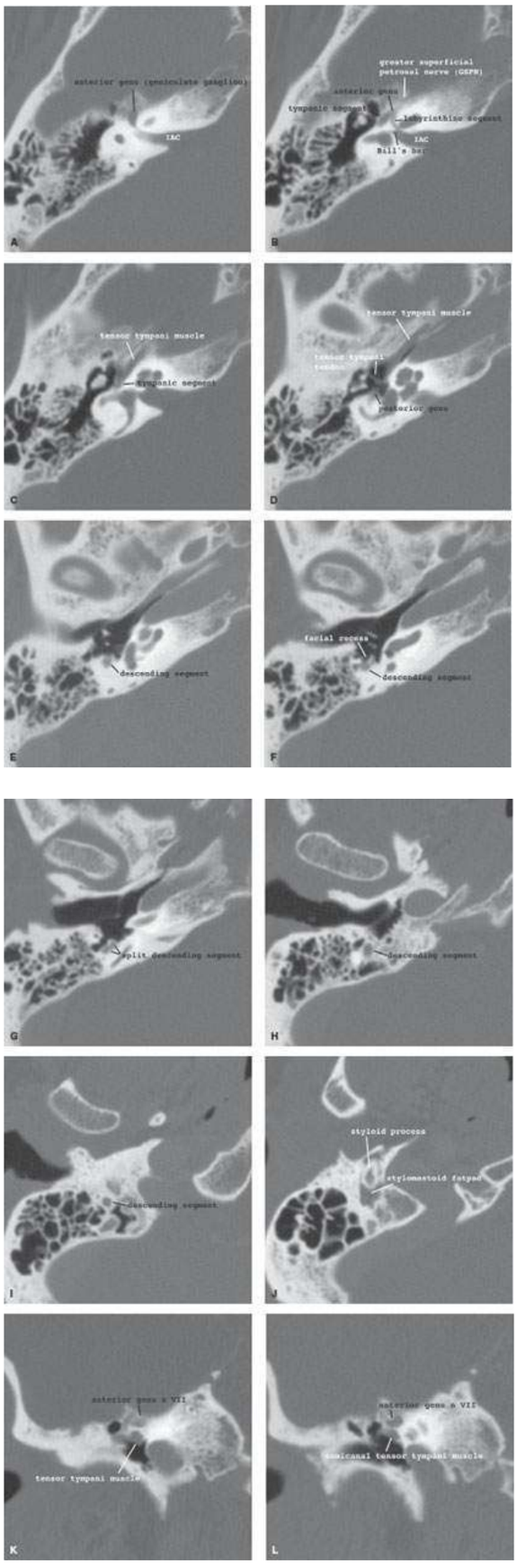
anterior genu (geniculate ganglion)
IAC
A
greater superficial petrosal nerve (GSPN)
anterior genu
tympanic segment
labyrinthine segment
IAC
Bill's bar
B
tensor tympani muscle
tympanic segment
C
tensor tympani muscle
tensor tympani tendon
posterior genu
D
descending segment
E
facial recess
descending segment
F
split descending segment
G
descending segment
H
descending segment
I
styloid process
stylomastoid foramen
J
anterior genu & VII
tensor tympani muscle
K
anterior genu & VII
musculotubal canal
tensor tympani muscle
L

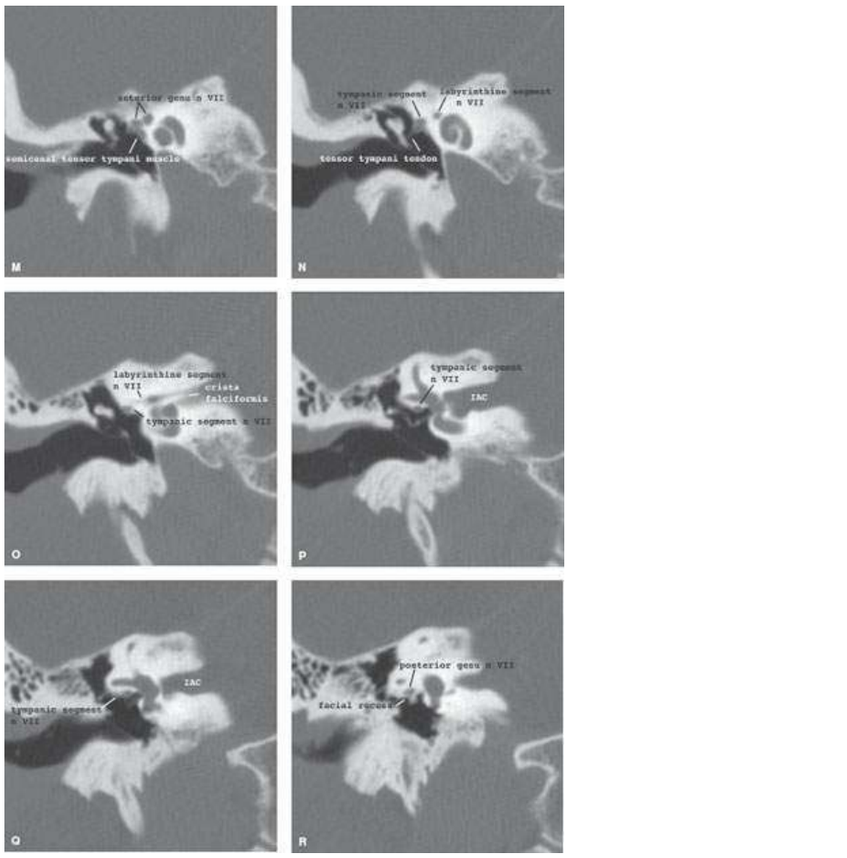

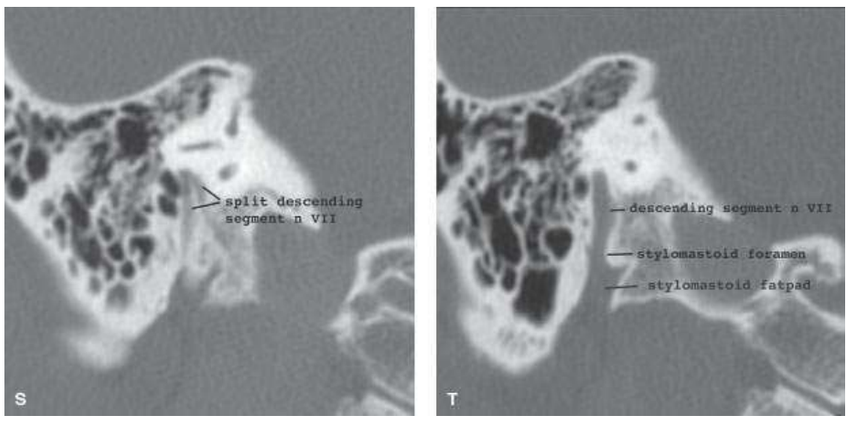

FIGURE 104.53. Normal anatomy of course of the facial nerve through the temporal bone on axial **(A–J)** and coronal **(K–T)** computed tomography images**.**

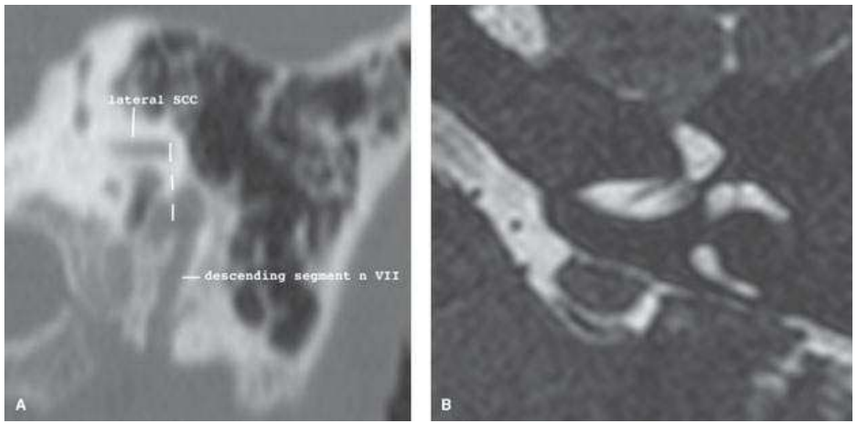

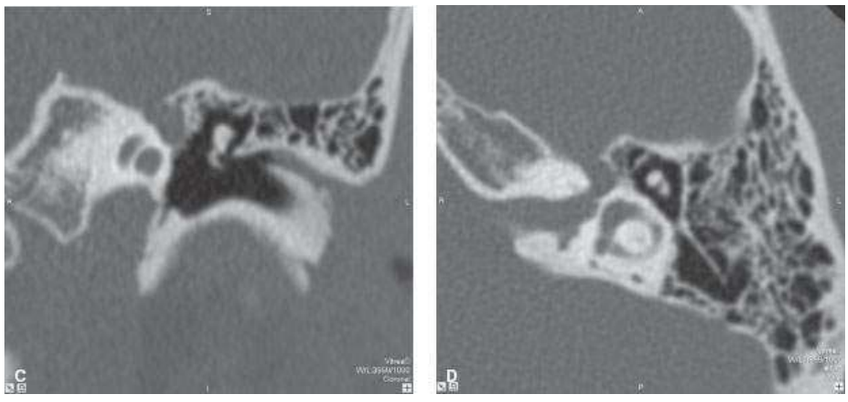

FIGURE 104.54. Normal variants of the facial nerve**.** Dehiscence of the bony canal of cranial nerve VII is most common in the tympanic segment (Fig. 104.21L,M) but can be seen in other segments, including the labyrinthine, descending segments and at the anterior (Fig. 104.25P) and posterior genus**. A:** A

dehiscence just beyond the posterior genu and a more lateral course of the distal tympanic and descending segments posing a potential risk during surgery; the dashed lines show the facial canal's usual position. In its descending or mastoid segment, the facial nerve can also divide into more than one branch show descending canal (Fig. 104.53G). **B–D:** Normal variations and dehiscence that can mimic pathology are relatively common at the anterior genu as well. The size of the facial hiatus is variable, contributing to this as seen in the magnetic resonance imaging in **(B)** and computed tomography in **(C)** and **(D)** as examples of a patulous facial canal/hiatus. Arachnoid granulations are a common cause of the variability in bony integrity seen in this region.

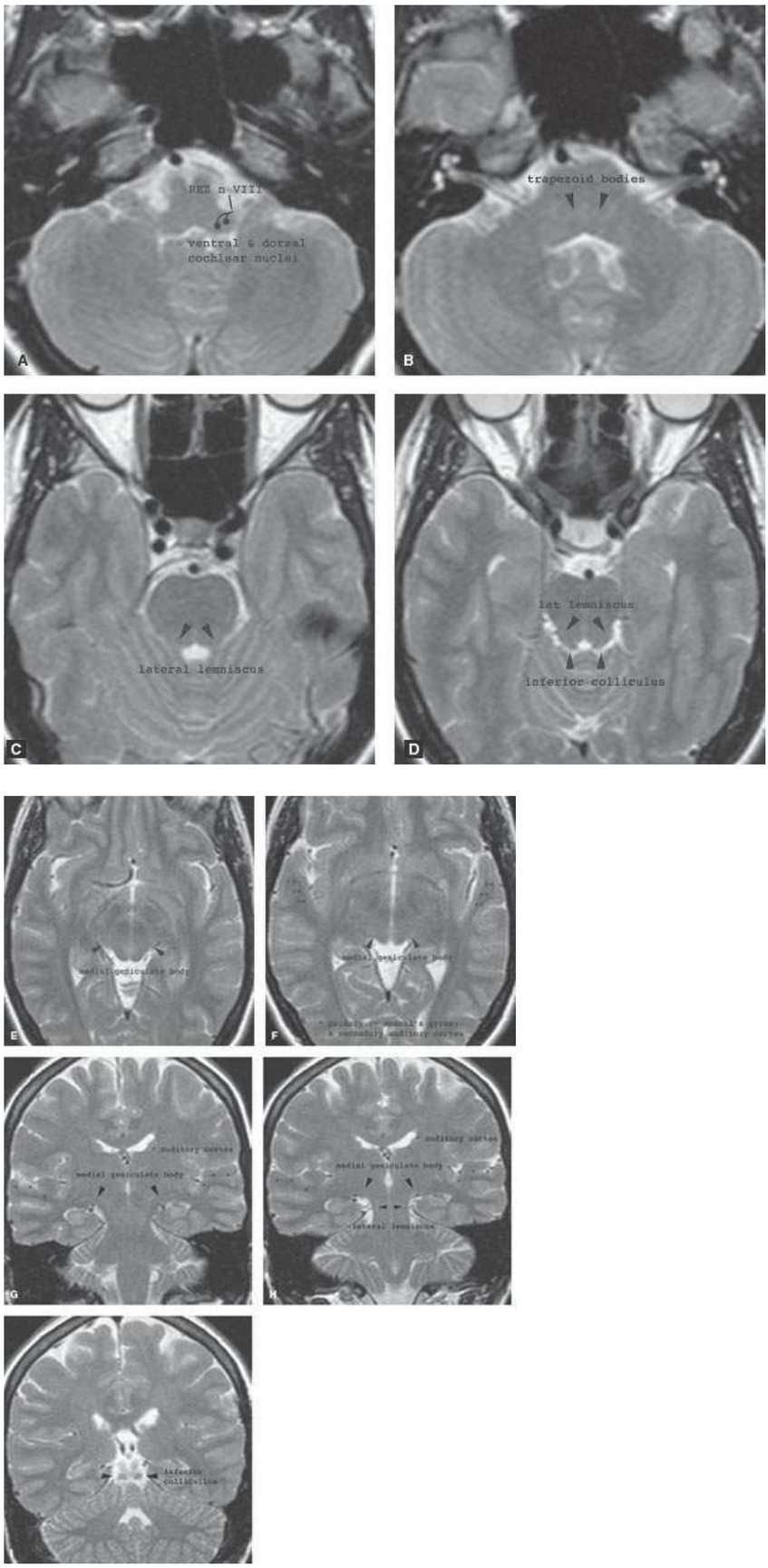

FIGURE 104.55. Normal anatomy of the central auditory pathway shown on axial **(A–F)** and coronal **(G–I)** T2W MR images. Afferent pathways of the central auditory system involve the cochlear nuclei, olivary nuclei, lateral lemniscus, inferior colliculus, medial geniculate body, and auditory cortex.

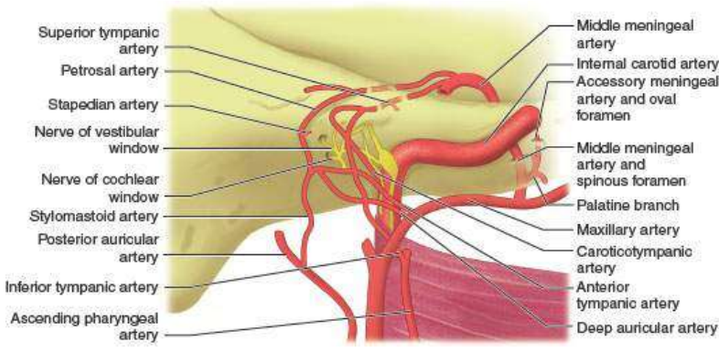

FIGURE 104.56. Normal anatomy of the vascular supply to the temporal bone.

Central Auditory Pathway

The cochlear nucleus is divided into three regions based on the morphology of the cells they contain: the anterior ventral cochlear nucleus, the posterior ventral cochlear nucleus, and the dorsal cochlear nucleus. The auditory nerve connects to the ipsilateral cochlear nucleus, which processes time and frequency information of auditory signals and distributes the auditory information to several bilaterally ascending tracts. The anterior ventral cochlear nucleus is the entryway to the binaural pathway. This pathway contains connections to the bilateral superior olivary nuclei via the trapezoid body. At this level, comparisons of interaural time delays and intensity differences are made on behalf of spatial localization. Signals are transmitted through the lateral lemniscus to the inferior colliculus. The monaural contralateral pathway begins at the dorsal cochlear nucleus and directly relays spectral information (differences in frequency) to the contralateral lateral lemniscus and inferior colliculus. The inferior colliculus is the major auditory processing center in the brain stem and has afferents to the medial geniculate bodies bilaterally. The medial geniculate bodies project to the auditory cortex, located on the superior temporal lobe (Heschl gyrus, transverse gyrus). This gyrus roughly corresponds to the primary auditory cortex (Brodmann area 41). The secondary auditory cortex largely contains the planum temporale (Brodmann area 42). Part of the superior temporal gyrus comprises auditory association and possibly language areas (Fig. 104.55).

Vascular Supply

Blood supply to the outer ear is by external carotid branches (superficial temporal, posterior auricular, and occipital arteries). Blood supply to the middle ear is by the anterior tympanic branch of the maxillary artery, which enters the middle ear through the petrotympanic fissure. Blood supply to the posterior tympanic cavity is by the stylomastoid branch of the posterior auricular or occipital arteries. Other blood supply comes from the ascending pharyngeal artery, the artery of the pterygoid canal, the caroticotympanic branches of the petrous portion of the carotid artery, and the middle meningeal artery. These vessels supply the temporal bone, the tympanic cavity mucosa, and the facial nerve. The latter becomes an important consideration during embolotherapy for hypervascular masses of the temporal bone or temporal region dura.

The inner ear is supplied by the labyrinthine artery, which arises from the AICA or directly from the basilar artery (Fig. 104.56).

Innervation

Innervation of the temporal bone can be broken into categories dealing with special sensation, general sensation, and motor efferents. The vestibular and cochlear nerves conduct afferent special sensation of balance and hearing from the membranous labyrinth to the brain stem. General sensation has multiple sources since the temporal bone anlage is derived from the first, second, and a portion of the third branchial arches.

Afferent sensory fibers from the external ear follow CNs V (auriculotemporal), VII, IX, and X. Afferent innervation from the middle ear is mainly by CNs VII and IX. Sensory innervation of the auditory tube is via CN IX. The glossopharyngeal branch to the middle ear mucosa is called the tympanic nerve or Jacobson nerve. It enters the tympanic cavity through the inferior tympanic canaliculus and ascends in a groove, canal, or the submucosa on the medial wall of the middle ear, usually on the cochlear promontory. It is joined by sensory fibers from CN VII and pericarotid sympathetic fibers (caroticotympanic nerves) to form a neural plexus over the promontory. Chromaffin cells (glomus bodies) accompany the tympanic nerve and plexus and can give rise to glomus tympanicum tumors. The tympanic plexus supplies the mucous membrane of the tympanic cavity, mastoid cells, and eustachian tube (Fig. 104.57). The inferior tympanic canaliculus, which transmits the tympanic nerve and inferior tympanic artery, lies in the bony ridge between the jugular foramen and the petrous carotid canal. The canal is only occasionally identified on high-resolution CT. Enlargement of the inferior tympanic canal can be seen in glomus tympanicum tumors or neurogenic tumors (Fig. 104.58) or as a sign of an aberrant carotid artery (Fig. 104.59). An aberrant carotid artery is the result of a disturbed differentiation of the third branchial artery. The cervical segment of the internal carotid artery is underdeveloped or has been regressed during embryogenesis. Consequently, an enlarged inferior tympanic artery anastomoses with the horizontal part of the internal carotid artery and gives rise to an enlarged inferior tympanic canaliculus.

Ear pain (otalgia) can be referred along a number of CN pathways. Sources of such ear pain can be local from remote sites such as the tongue base by way of the glossopharyngeal nerve, the pyriform sinus by way of the Arnold nerve of the vagus nerve, or areas as close as the deep lobe of the parotid via the auriculotemporal nerve.

Motor innervation to the tensor tympani muscle is from the mandibular division of the trigeminal nerve, while that of the stapedius muscle is from the facial nerve.

Temporal Bone Lymphatic Drainage

The lymphatic drainage of the EAC is directed to the periauricular and parotid lymph nodes. Lymphatic drainage of the petrous bone, middle ear, inner portion of the external canal, and mastoid air cells can be either superficial to periauricular and parotid nodes or deep to the retropharyngeal lymph nodes. Mastoid disease may drain to occipital and mastoid nodes. All of these groups tend to drain to both the internal jugular and spinal accessory groups.

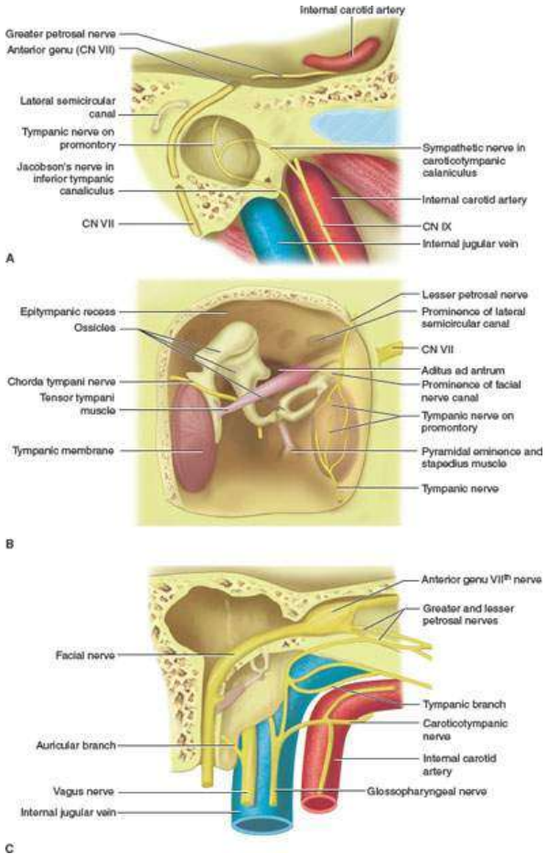

FIGURE 104.57. A–C: Anatomic drawings of the normal anatomy of the tympanic nerve. The tympanic nerve is a branch of the glossopharyngeal nerve, which enters the middle ear cavity through the inferior tympanic canaliculus and forms a neural plexus over the promontory with caroticotympanic branches of cranial nerve VII.

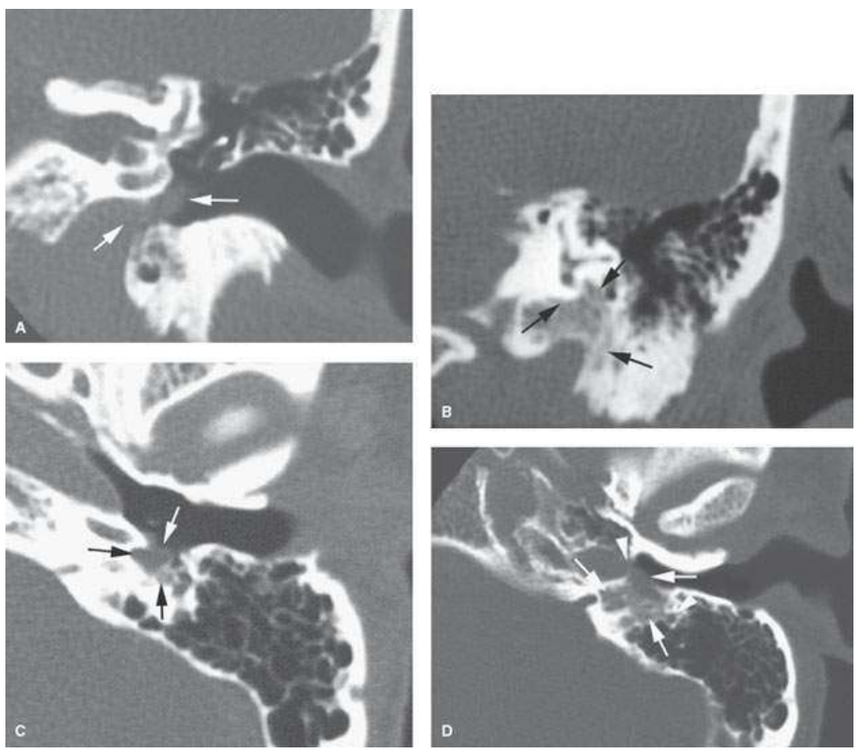

FIGURE 104.58. A tumor originally believed to be a glomus tympanicum confined to the middle ear is actually shown (*arrow*s in A–C) to be arising in the inferior tympanic canaliculus and/or tympanicocarotid canal, extending into the hypotympanum and eroding the bone above the dome of the jugular fossa including the carotid and facial canals (*arrow*heads in D). Understanding the anatomy in this region will help avoid such misdiagnosis. Such findings significantly alter the surgical approach to this tumor.

Posterior Skull Base

The posterior skull base (Fig. 104.60) is formed, to a large extent, by the occipital bone. The foramen magnum, through which the cranial cavity communicates with the spinal canal, is located within the occipital bone and divides it into the paired squama, the lateral parts and the basiocciput. The basiocciput is the part of the occipital bone that lies anterior to the foramen magnum and joins with the body of the sphenoid bone. The basiocciput is embryologically derived from four primary cranial vertebrae and forms the inferior two thirds of the clivus. The superior one third of the clivus is formed by the basisphenoid. The basisphenoid and basiocciput are separated by the spheno-occipital synchondrosis/fissure. Between the ages of 18 and 25 years, this cartilage plate becomes ossified, and the occipital and sphenoid bone are united. This synchondrosis is a predilection place for chordoma, which arises from notochordal remnants. Other intrinsic lesions that can involve the clivus are metastasis, lymphoma, plasmacytoma, or fibrous dysplasia. Extrinsic lesions such as nasopharyngeal carcinoma, sphenoid sinus carcinoma, and meningioma can invade the clivus. The lateral margins of the basiocciput form the petro-occipital or petroclival fissures. In this location, chondrosarcoma appears.

The occipital squama is situated above and behind the foramen magnum. At the sides of the foramen magnum, the lateral parts of the occipital bone are found. On their undersurfaces are the condyles. Each condyle is tunneled at the base by the hypoglossal canal. Through this canal, the hypoglossal nerve (CN XII)

exits the skull, whereas the meningeal branch of the ascending pharyngeal artery enters the skull. Lateral to the posterior half of the condyle is the jugular process, which forms the posterior part of the jugular foramen. At their undersurfaces, the condyles articulate with the atlas.

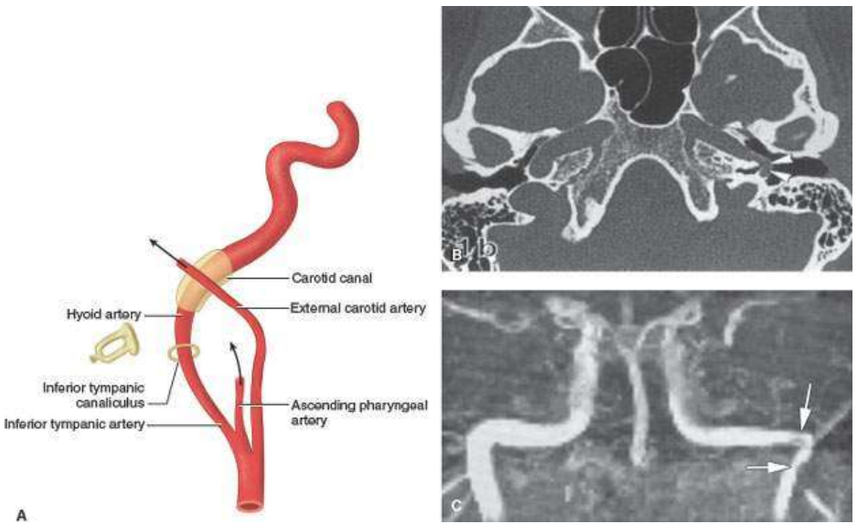

FIGURE 104.59. Aberrant carotid artery development. **A:** Schematic drawing showing that since the cervical segment of the carotid artery is missing, the blood flow runs through an enlarged inferior tympanic artery and hyoid artery that anastomoses to the horizontal segment of the carotid artery through a dehiscence in the carotid plate. **B:** The aberrant carotid showing a laterally displaced course of the anastomotic artery on computed tomography projecting well into the middle ear (*arrowheads*). **C:** Magnetic resonance angiography.

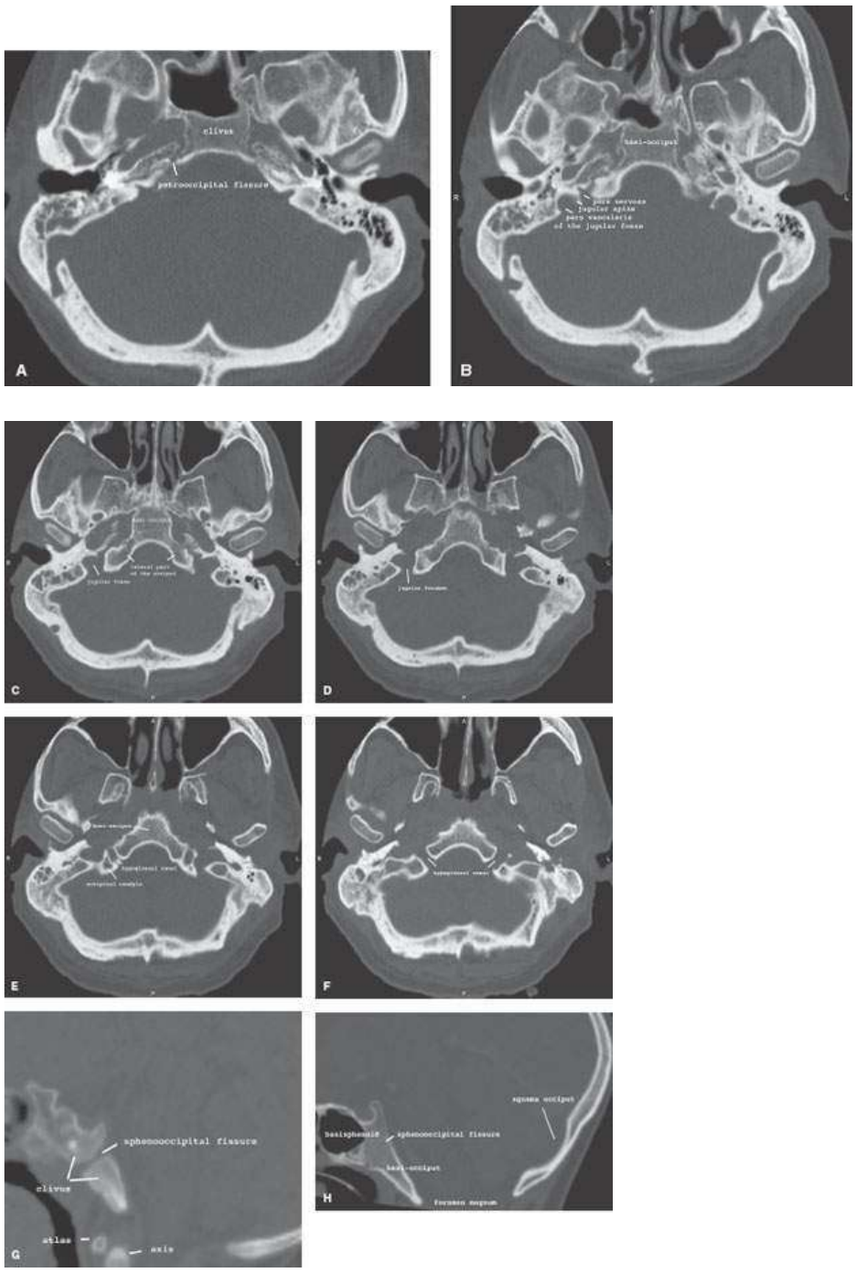

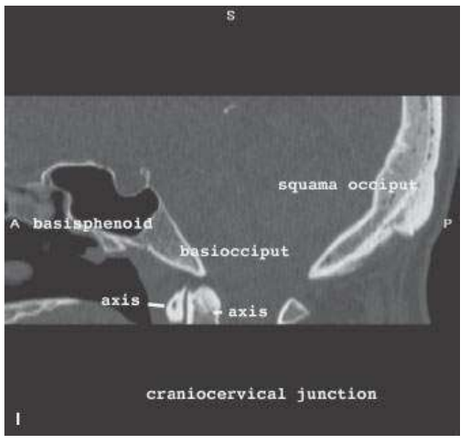

FIGURE 104.60. Posterior skull base. **A–F**: Normal anatomy of the posterior skull base is shown on consecutive axial computed tomography images. **G–I**: The clivus is formed by the basisphenoid and basiocciput, as shown on these sagittal images. The spheno-occipital fissure or synchondrosis is well seen in children, as in the 4 year old in **(G)** and the teenager in **(H)**, but will be ossified in adults **(I)**.

The posterior skull base, atlas, and axis form the craniocervical junction. Attention should be paid to this region by the head and neck radiologist since many symptoms associated with pathology of the craniocervical junction lead to referral to an otolaryngologist.

Jugular Foramen and Cranial Nerves IX, X, and XI

The jugular foramen is situated between the more anterior and lateral petrous bone and the occipital bone situated more posterior and medial. The jugular foramen (fossa) actually has two parts separated incompletely by a fibrous or osseous jugular bridge (or jugular spine). The more medial and smaller of the two compartments (pars nervosa) contains the terminus of the inferior petrosal sinus and the glossopharyngeal nerve (CN IX). The more lateral of the two (pars vascularis) is larger and contains the jugular bulb, vagus nerve (CN X), and spinal accessory nerve (CN XI) (Fig. 104.10A–C). The inferior petrosal sinus drains the cavernous sinus and courses inferiorly within the petro-occipital fissure to enter the jugular foramen in the pars nervosa and join the internal jugular vein.

CNs IX through XI share nuclei of the medulla. Motor fibers of all three nerves originate in the nucleus ambiguus dorsal to the inferior olivary nucleus. Additional motor fibers of CN XI originate in the spinal accessory nucleus in the lateral anterior gray column of the cervical cord at level C5. Sensory fibers of CN IX and X enter between the medullary olives and the inferior cerebellar peduncle. The fibers course in the tractus solitarius and end in the nucleus solitarius. Parasympathetic fibers that innervate the parotid gland originate in the inferior olivary nucleus and course in the deep lesser petrosal nerve (CN IX). Vagal parasympathetic fibers to the visceral ganglia originate from the dorsal motor nucleus along the fourth ventricle and central canal of the cord. Once they leave the lateral medulla, all roots, including the spinal roots of CN XI, traverse the basal cistern conjoined. As the CN complex enters the jugular fossa, CN IX diverges alone into the pars nervosa and will give off the tympanic nerve (Jacobson nerve), supplying sensory fibers to the tympanic plexus. CN X and XI run through the pars vascularis. Within the jugular foramen, CN X gives off the auricular branch (Arnold nerve), supplying sensory fibers to the external ear, EAC, and inferior tympanic membrane. CNs IX through XI share their extracranial course in the nasopharyngeal segment of the carotid sheath. CN XI diverges quickly posterior and lateral to descend along the medial aspect of the sternocleidomastoid muscle. The vagus nerve courses within the carotid sheath to the thoracic inlet while giving off peripheral branches such as superior laryngeal branches and the recurrent laryngeal branch. The glossopharyngeal nerve (CN IX) follows the carotid sheath to the level of the hyoid, where it curves upward and forward to terminate in the posterior sublingual space at the floor of the mouth. On its way, motor and sensory peripheral branches to the pharynx and posterior third of the tongue are given off.

BASIC NORMAL FUNCTION AND PHYSIOLOGY

Conductive Hearing

Conductive hearing describes the processing of sound waves in the surrounding air into vibrations of the fluid in the inner ear through the outer and middle ear. Sound waves are caught by the pinna; its complex structure helps to determine the direction of the sound. The auricle and external ear canal amplify and guide the sound waves to the tympanic membrane. Thanks to contraction of the tensor tympani muscle and equalization of the air pressure in the auditory canal and in the middle ear by the eustachian tube, the tympanic membrane is kept tense for optimal vibration. The frequency of the sound determines how fast the tympanic membrane vibrates. The sound waves are directed toward the oval window through the ossicular chain (malleus, incus, stapes). The ossicles amplify the sound waves by the size difference between the tympanic membrane and the foot plate of the stapes, a primarily hydraulic phenomenon, on the one hand and to a lesser extent by a lever mechanism on the other hand. The round window is protected from sound waves by the tympanic membrane and the round window niche. To protect the inner ear from loud noises, reflex contraction of the tensor tympani and stapes muscle can occur.

When the conduction of sound through the outer or middle ear is impaired, conductive hearing loss occurs. Generally, with pure conductive hearing loss, the quality of hearing (speech discrimination) is good as long as the sound is amplified loud enough to be easily heard. Conductive hearing loss can also be related to a fistula (dehiscence) of the superior semicircular canal; the conductive loss is due to dissipation of sound energy at the site of the bony dehiscence/fistula.

Sensorineural Hearing

Sensorineural hearing involves transformation of sound energy into nerve impulses. Movements of the stapes foot plate at the level of the oval window cause waves in cochlear fluid; the wave starts in the perilymph of the scala vestibuli and continues through the helicotrema in the perilymph of the scala tympani to end at the round window. The third scala is the cochlear duct or scala media that contains the basilar membrane on which the organ of Corti with the cilia of its hair cells attach to the tectorial membrane. The incoming pressure waves cause motion of the basilar membrane and shearing of the cilia, resulting in hair cell depolarization and nerve impulses. High frequencies activate hair cells close to the oval window, and lower frequencies do the same at the apex of the cochlea. These impulses are processed by the central auditory pathways, resulting in the auditory perception of pitch, loudness, and location of sound. Hearing loss due to insensitivity of the inner ear, usually at the level of the hair cells, or caused by pathology along the central auditory pathway is categorized as SNHL. This can cause total deafness.

Balance and Coordination

The vestibular system, which is situated in the inner ear, provides all information necessary to keep our balance. To monitor motion, one must be able to detect rotation as well as linear translation. The vestibular system consists of three semicircular canals and the otolithic organs housed in the vestibule. The three orthogonally oriented semicircular canals are maximally sensitive to rotations in their plane. The semicircular canals of the right and the left ear are oriented in such a way that they almost parallel each other, and when one side is stimulated the other side will be inhibited. In this way, rotational movements in any plane can be detected. The semicircular canals send signals to the eye muscles, ensuring compensation for head movements (vestibulo-ocular reflex). Signals are also sent to the cerebellum to maintain the vestibulo-ocular reflex and posture. Within the osseous vestibule, two membranous sacs—the utricle and the saccule—are found. They contain otoliths, which transduce linear acceleration. The utricle and saccule send signals to control eye movements and posture, respectively. When balance is impaired, individuals will experience vertigo and instability, often accompanied with nausea, visual blurring, or disorientation. When the vestibulo-ocular reflex is provoked, the patient may show nystagmus (compensatory eye movements in the absence of head motion) or inability to fixate a point during head movement. Possible causes for balance disorders are peripheral vestibular (e.g., labyrinthitis), central vestibular, systemic, or vascular.

Facial Nerve

CN VII supplies motor function to the muscles of facial expression, buccinator, platysma, occipitalis, stapedius, stylohyoid, and posterior belly of the digastric muscles. Sensory innervation includes cutaneous sensation from the ear and taste sensation from the anterior two thirds of the tongue. Parasympathetic supply is provided to the submandibular, sublingual, and lacrimal glands.

Cochleovestibular Nerve

CN VIII is a sensory nerve that consists of two distinct nerves: the cochlear nerve and the vestibular nerve. The cochlear nerve transmits auditory information. The vestibular nerve serves balance. It gathers information from the utricle, anterior and superior semicircular canal (superior vestibular root), and the saccule and posterior semicircular canal (inferior vestibular root). Fibers from the vestibular nuclear complex connect with the nuclei of CNs III, IV, and VI to provide gaze and conjugate eye reflexes.

Glossopharyngeal Nerve

CN IX has a motor branch to the stylopharyngeus, superior pharyngeal constrictor (with branches of CN X), and styloglossus muscle. Several branches supply sensation to the middle ear and bony eustachian tube and the posterior oropharynx and soft palate and sensation and taste to the posterior third of the tongue. Parasympathetic function is supplied to the parotid gland, and the sinus nerve supplies the pressor and chemoreceptors at the carotid artery. Isolated glossopharyngeal nerve injury is rare. Pathologic processes usually involve the CN IX, X, and XI complex. Isolated injury causes otalgia, dysphagia, throat pain, loss of cough or gag reflex, loss of taste of the posterior one third of the tongue, dry mouth hypotension, and tachycardia or bradycardia.

Vagus Nerve

CN X supplies motor fibers to the soft palate, pharynx (superior and middle constrictor muscles), and larynx (inferior constrictor, cricothyroid, and endolaryngeal muscles). Sensory innervation is supplied to the soft palate, part of the base of the tongue, hypopharynx, and larynx above the true vocal cords. Parasympathetic functions include the cardiovascular system and thoracoabdominal organs. Proximal injury to the vagus nerve may also involve the CN IX, X, and XI complex as well as CN XII, causing complex vagal neuropathy with oropharyngeal signs and symptoms and hoarseness. Distal injury will create isolated vagus nerve symptoms manifesting as hoarseness and aspiration secondary to vocal cord dysfunction.

Spinal Accessory Nerve

The course of CN XI is intimately associated with the vagus nerve and therefore distributes partly to the pharynx and larynx. The other part forms motor innervation to the sternocleidomastoid and trapezius muscles. The most common cause of isolated injury to the spinal accessory nerve is radical neck dissection. This clinically manifests with shoulder drop and inability to use the arm. Usually, injury involves the CN IX, X, and XI complex.

Hypoglossal Nerve

CN XII is the motor nerve of the tongue. It supplies the all-intrinsic (longitudinal, transverse, and vertical) and almost all-extrinsic (genioglossus, geniohyoid, hyoglossus, styloglossus) tongue muscles. Isolated injury causes fasciculation of the tongue or atrophy, deviation of the protruded tongue toward the side of the lesion, and dysarthria.

Suggested Readings

Purcell DD, Fischbein NJ, Patel A, et al. Two temporal bone computed tomography measurements increase recognition of malformations and predict SNHL. *Laryngoscope*. 2006;116(8):1439–1446.

Shuknecht HF, Gulya AJ. *Anatomy of the temporal bone with surgical implications*. Philadelphia, Pa: Lea & Febiger; 1986.

References

1. Krishnan A, Mattox DE, Fountain AJ, et al. CT arteriography and venography in pulsatile tinnitus: Preliminary results. *AJNR Am J Neuroradiol.* 2006;27(8):1635–1638.

2. Marsot-Dupuche K. Cochlear implant assessment: Imaging issues. *Eur J Radiol*. 2001;40:119–132.

3. Parry DA, Booth T, Roland PS. Advantages of MRI over CT in preoperative evaluation of pediatric CI candidates. Otol Neurotol. 2005;26(5): 976–982.

4. Arriaga MA, Carrier D. MRI and clinical decisions in cochlear implantation. Am J Otol. 1996;17(4):547–553.

5. Held P, Fellner F, Seitz J, et al. Correlation of 3D MR and clinical findings in patients with sensorineural hearing loss and/or vertigo. Clin Imaging. 1998;22:309-322.

6. Purcell DD, Fischbein NJ, Patel A, et al. Two temporal bone computed tomography measurements increase recognition of malformations and predict SNHL. Laryngoscope. 2006;116(8):1439–1446.

7. Fitzek C, Mewes T, Fitzek S, et al. Diffusion-weighted imaging MRI of cholesteatomas of the petrous bone. J Magn Reson Imaging. 2002;15(6): 636–641.

8. Ayache D, Williams MT, Lejeune D, et al. Usefulness of delayed postcontrast MRI in the detection of residual cholesteatoma after canal wall-up tympanoplasty. Laryngoscope. 2005;115(4):607–610.

9. Dubrulle F, Souillard R, Chechin D, et al. Diffusion-weighted MR imaging sequence in the detection of postoperative recurrent cholesteatoma. Radiology. 2006;238(2):604–610.

10. Stasolla A, Magliulo G, Parrotto D, et al. Detection of postoperative relapsing/residual cholesteatoma with diffusion-weighted echo-planar magnetic resonance imaging. Otol Neurotol. 2004;25(6):879–884.

11. Aikele P, Kittner T, Offergeld C, et al. Diffusion-weighted MR imaging of cholesteatoma in pediatric and adult patients who have undergone middle ear surgery. AJR Am J Roentgenol. 2003;181(1):261–265.

12. Reisser C, Schuknecht HF. The anterior inferior cerebellar artery in the internal auditory canal. Laryngoscope. 1991;101:761–766.

13. Makins AE, Nikolopoulos TP, Ludman C, et al. Is there a correlation between vascular loops and unilateral symptoms? Laryngoscope. 1998; 108(11 Pt 1):1739–1742.

14. Okomura T, Kurokawa Y, Ikeda N, et al. Microvascular decompression for cochlear symptoms. J Neurosurg. 2000;93(3):421–426.

15. Lenarz T, Schackert G, Schwarz D. Vascular loop. A contributing factor to vascular cerebellopontine syndrome. Laryngol Rhinol Otol (Stuttg). 1984; 63(10):524–528.

16. McDermott AL, Dutt SN, Irving RM, et al. Anterior inferior cerebellar artery syndrome: Fact or fiction. Clin Otolaryngol Allied Sci. 2003;28(2): 75–80.

17. Kress B, Griesbeck F, Stippich C, et al. Bell palsy: Quantitative analysis of MRI data as a method of predicting outcome. Radiology. 2004;230(2): 504–509.

18. Engstrom M, Abdsaleh S, Ahlström H, et al. Serial gadolinium enhanced MRI and assessment of facial nerve function in Bell's palsy. Otolaryngol Head Neck Surg. 1997;117(5):559–566.

19. Gilden DH. Bell's palsy N Engl J Med. 2004;31(13):1323–1331.

20. Overton SB, Ritter FN. A high placed jugular bulb in the middle ear: A clinical and temporal bone study. Laryngoscope. 1973:83(12):1986– 1993.

21. Lacout A, Marsot-Dupuch K, Smoker WR, et al. Foramen tympanicum, or foramen of Huschke: Pathologic cases and anatomic CT study. AJNR Am J Neuroradiol. 2005;26:1317–1323.

22. Lemmerling MM, Stambuk HE, Mancuso AA, et al. CT of the normal suspensory ligaments of the ossicles in the middle ear. AJNR Am J Neuroradiol. 1997;18(3):471–477.

23. Shuknecht HF, Gulya AJ. Anatomy of the temporal bone with surgical implications. Philadelphia, Pa: Lea & Febiger; 1986.

24. Lemmerling MM, Mancuso AA, Antonelli PJ, et al. Normal modiolus: CT appearance in patients with a large vestibular aqueduct. Radiology. 1997;204(1):213–219.

25. Jackler RK, Hwang PH. Enlargement of the cochlear agueduct: fact or fiction? Otolaryngol Head Neck Surg 1993; 109(1):14-25.

26. McFadden MD, Wilmouth JG, Mancuso AA, et al. Preoperative computed tomography may fail to detect patients at risk for perilymph gusher. Ear Nose Throat J. 2005;84(12):770, 772–774.

27. Naito Y, Honjo I, Takahashi H, et al. Surface-coil magnetic resonance imaging of the internal auditory canal and the inner ear: Preliminary report. Ann Otol Rhinol Laryngol. 1995;104(10 Pt 1):776–782.

28. Nadol JB Jr, Xu WZ. Diameter of the cochlear nerve in deaf humans: Implications for cochlear implantation. Ann Otol Rhinol Laryngol. 1992; 101(12):988–993.

29. Virapongse C, Sarwar M, Bhimani S, Sasaki C, Shapiro R. Computed tomography of temporal bone pneumatization: 1. Normal pattern and morphology. AJR Am J Roentgenol. 1985;145(3):473–81.

30. Virapongse C, Sarwar M, Bhimani S, Sasaki C, Shapiro R. Computed tomography of temporal bone pneumatization: 2. Petrosquamosal suture and septum. *AJNR Am J Neuroradiol*. 1985;6(4):561–8.

May 14, 2017 | Posted by admin in HEAD & NECK IMAGING | Comments Off